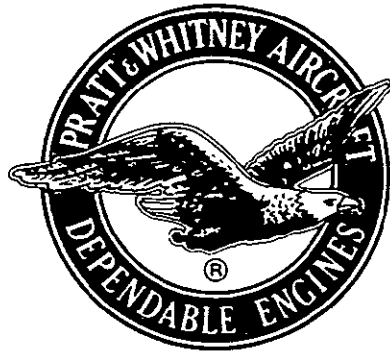


# TANK HEAD IDLE OXYGEN HEAT EXCHANGER DEVELOPMENT FOR TUG ENGINE

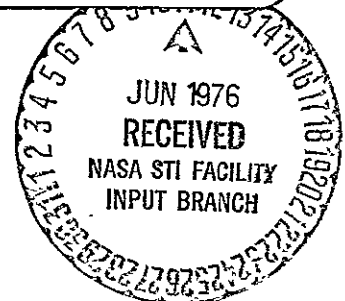
## FINAL REPORT



Prepared for  
Contract NAS8-31151

George C. Marshall Space Flight Center  
Marshall Space Flight Center, Alabama 35812

(NASA-CR-144313) TANK HEAD IDLE OXYGEN HEAT N76-24352  
EXCHANGER DEVELOPMENT FOR TUG ENGINE Final  
Report (Pratt and Whitney Aircraft) 88 p HC  
\$5.00 CSCL 21H Unclas  
G3/20 - 28260 -



# PRATT & WHITNEY AIRCRAFT



P. O. Box 2691 - West Palm Beach, Florida 33402

# PRATT & WHITNEY AIRCRAFT GROUP

GOVERNMENT PRODUCTS DIVISION

P. O. Box 2691  
West Palm Beach, Florida 33402

21 May 1976

In reply please refer to:  
MFS:AFK:lsf:Cont. Adm.

National Aeronautics and Space Administration  
George C. Marshall Space Flight Center  
Marshall Space Flight Center, Alabama 35812

Attention: Mr. Ray Weems, AP13-F  
Contract Manager


Reference: Letter from Mr. Ray Weems, dated 22 April 1976,  
"Contract NAS8-31151 - Approval of Final Draft."

Dear Mr. Weems:

As required under Section III(C) of Exhibit A - Scope of Work of Contract NAS8-31151 (Tank Head Idle Oxygen Heat Exchanger Development for Tug Engine Program), Mod. 1, and, in accordance with the referenced letter, we herewith distribute the approved final report, FR-7498.

Very truly yours,

UNITED TECHNOLOGIES CORPORATION  
Pratt & Whitney Aircraft Group



M. F. Samples  
Senior Contract Administrator  
Government Products Division

cc: With FR-7498 enclosed

National Aeronautics and Space Administration  
George C. Marshall Space Flight Center  
Marshall Space Flight Center, Alabama 35812  
Attention: AT01/Aubrey Smith (1 copy)  
AS21D (5 copies)  
EM34-11/Jim Venus (1 copy)  
EP43/J. H. Pratt (5 copies)  
EP43/T. H. Winstead (1 copy)



National Aeronautics and Space Administration  
George C. Marshall Space Flight Center  
Marshall Space Flight Center, Alabama 35812

-2-

Without FR-7498 enclosed

Naval Plant Branch Representative Officer  
Pratt & Whitney Aircraft Group  
Government Products Division  
West Palm Beach, Florida 33402

1 Report No.	2 Government Accession No	3 Recipient's Catalog No	
4. Title and Subtitle Tank Head Idle Oxygen Heat Exchanger Development for Tug Engine - Final Report		5. Report Date 21 May 1976	6. Performing Organization Code
		8 Performing Organization Report No FR-7498	10. Work Unit No.
7. Author(s) P. S. Thompson T. C. Mayes C. D. Limerick		11 Contract or Grant No. NAS8-31151	
		13. Type of Report and Period Covered Contractor's Final Report	
9 Performing Organization Name and Address Pratt & Whitney Aircraft Division of United Technologies P. O. Box 2691 West Palm Beach, Florida 33402		14. Sponsoring Agency Code	
		12 * Sponsoring Agency Name and Address George C. Marshall Space Flight Center Marshall Space Flight Center, Alabama 35812	
15 Supplementary Notes			
16 Abstract This report covers the design, fabrication, and test for a breadboard oxygen heat exchanger, which is the preliminary step in the design, fabrication, and testing of a flight oxygen heat exchanger. This assembly will be used for the tank head idle mode operation of the RL10 Derivative II Space Tug main engine. The Space Tug is the upper stage to be used with the Space Shuttle Vehicle.			
17 Key Works (Suggested by Author(s) RL10 Oxygen Heat Exchanger Space Tug		18. Distribution Statement Unclassified - Unlimited	
19 Security Classif (of this report) Unclassified	20 Security Classif. (of this page) Unclassified	21 No of Pages 90	22. Price *

\*For sale by the National Technical Information Service, Springfield, Virginia 22151

**FOREWORD**

This technical report presents the results of the "Breadboard" oxygen heat exchanger design, fabrication, and test program, performed by the Pratt & Whitney Aircraft Division of United Technologies for the National Aeronautics and Space Administration, George C. Marshall Space Flight Center, under Contract NAS8-31151. This program was initiated in April 1975, and the technical effort was completed in January 1976. The program was completed with the delivery of the final report in May 1976.

The technical effort was conducted under the direction of Mr. J. H. Pratt, Contracting Officer Representative of the Marshall Space Flight Center. This effort was conducted by Pratt & Whitney Aircraft at their Florida Research and Development Center under the direction of Mr. W. C. Shubert, Advanced Rockets Program Manager. Others who contributed to this report were Messrs. P. S. Thompson, T. C. Mayes, C. D. Limerick, C. C. Thompson, A. A. Palgon, and M. J. Blanchard.

## CONTENTS

<i>SECTION</i>	<i>PAGE</i>
ILLUSTRATIONS.....	vi
TABLES.....	ix
SYMBOLS.....	x
I INTRODUCTION.....	I-1
II DESIGN REQUIREMENTS.....	II-1
III DESIGN.....	III-1
A. Breadboard Heat Exchanger Fluid/Thermal Analysis.....	III-1
B. Mechanical and Structural Design.....	III-27
IV FABRICATION.....	IV-1
A. Basic Fabrication.....	IV-1
B. Assembly.....	IV-1
V FACILITIES.....	V-1
A. General.....	V-1
B. Facilities Design.....	V-1
C. Modifications.....	V-3
D. Insulation.....	V-3
E. Checkout.....	V-4
VI TEST.....	VI-1
A. General.....	VI-1
B. Checkout Tests (Test 1.01).....	VI-1
C. Second Test (Test 2.01).....	VI-5
D. Third Test (Test 3.01).....	VI-5
VII ANALYSIS.....	VII-1
A. Checkout Test (Test No. 1.01).....	VII-1
B. Test With 30% Dense Feltmetal Insulation (Test No. 2.01).....	VII-1
C. Test With Powdered Aluminum Between the Panels (Test No. 3.01).....	VII-12
D. Overall Test Results.....	VII-20
VIII CONCLUSIONS AND RECOMMENDATIONS.....	VIII-1
A. Conclusions.....	VIII-1
B. Recommendations.....	VIII-1
IX REFERENCES.....	IX-1

**ILLUSTRATIONS**

<i>FIGURE</i>		<i>PAGE</i>
I-1	RL10 Derivative IIB Tank Head Idle Mode.....	I-2
III-1	Breadboard Hydrogen/Oxygen Heat Exchanger.....	III-3
III-2	Estimated Performance at Constant Heat Fluxes.....	III-5
III-3	Breadboard Hydrogen/Oxygen Heat Exchanger Oxygen-Side Core $\Delta P$ vs Heat Flux $\dot{w}_{O_2}=0.32 \text{ lb}_m/\text{sec}$ .....	III-5
III-4	Breadboard Heat Exchanger Critical Heat Flux vs Oxygen Quality Design-Point Operation.....	III-6
III-5	Breadboard Hydrogen/Oxygen Heat Exchanger Insulation Conductance Requirements.....	III-6
III-6	Breadboard Hydrogen/Oxygen Heat Exchanger Potential Insulating Materials.....	III-7
III-7	Potential of 347 Stainless Steel Feltmetal as Thermal Insulation.....	III-8
III-8	Stainless Steel 347 Feltmetal Thermal Conductivity vs Density.....	III-10
III-9	Hydrogen/Oxygen Breadboard Heat Exchanger Potential Heat Transfer Increases Possible Using Variable Density Insulation.....	III-11
III-10	Heat Transfer and Friction Data for Heat Exchanger Core (Reference 8).....	III-14
III-11	Hydrogen-Forced Convection Film Coefficients $10 < P < 20 \text{ psia}$ ( $68,948 < P < 137,895 \text{ N/m}_2$ ).....	III-15
III-12	Oxygen-Forced Convection Film Coefficients ( $P \approx 15 \text{ psia}$ [ $103,421 \text{ N/m}_2$ ])...	III-15
III-13	Boiling Heat Transfer to $20 \text{ psia}$ ( $137,895 \text{ N/m}_2$ ) Saturated Oxygen.....	III-16
III-14	Area-Weighted Effectiveness of Copper Fins.....	III-16
III-15	Gaseous Hydrogen Pressure Losses Through Heat Exchanger Plate.....	III-17
III-16	Two-Phase Frictional Pressure Gradients for Atmospheric Boiling Oxygen Flowing Through Heat Exchanger Plates (Martinelli-Lockhart Separated Flow Model).....	III-19
III-17	Two-Phase Momentum $\Delta P$ Atmospheric Boiling Oxygen Flowing Through Heat Exchanger Panels (Martinelli-Lockhart Separated Flow Model, Reference 12).....	III-20
III-18	Critical Heat Flux for Stable Boiling of Oxygen at $1 \text{ atm}$ ( $51.01 \text{ N/m}_2$ ).....	III-22
III-19	Instrumentation Requirements for Fluid Supply/Discharge Lines.....	III-23
III-20	Instrumentation Requirements for Center Hydrogen Panel.....	III-23
III-21	Instrumentation Requirements for One Outer Hydrogen Panel.....	III-24
III-22	Instrumentation Requirements for One Oxygen Panel (No Requirements for Other Panel).....	III-24
III-23	Breadboard Heat Exchanger Heat Flux Variation for Constant Conductance Insulation Configuration.....	III-27
III-24	Manifold End Cap Stresses.....	III-29
III-25	Typical Heat Exchanger Panel.....	III-30
III-26	Typical Manifold Cross Section.....	III-30
III-27	Oxygen Panel and Manifold.....	III-31
III-28	Hydrogen-Panel and Manifolds.....	III-31
IV-1	Fabrication Flow Chart.....	IV-2
IV-2	Hand-Formed Copper Sheet - Basic Extended Shape ( $\frac{3}{4}$ Plan View).....	IV-3
IV-3	Hand-Formed Copper Sheet - Basic Extended Shape (End View).....	IV-3
IV-4	Fabricated Hydrogen Panel Assembly.....	IV-4
IV-5	Breadboard Heat Exchanger Rig Assembly.....	IV-4

**ILLUSTRATIONS (Continued)**

<i>FIGURE</i>		<i>PAGE</i>
V-1	Breadboard Heat Exchanger Test Configuration.....	V-2
V-2	Engine and Test Rig Installation.....	V-5
V-3	Modified Test Configuration.....	V-6
V-4	Quality Meters.....	V-7
VI-1	GOX Heat Exchanger Rig Schematic of Configuration Used for Checkout Test .....	VI-4
VI-2	GOX Heat Exchanger Rig Schematic of Configuration Used for Tests 2.01 and 3.01.....	VI-6
VII-1	Measured Oxygen Data Characteristics of Breadboard Heat Exchanger Checkout Test.....	VII-2
VII-2	Measured and Calculated Oxygen Data Characteristics of Breadboard Heat Exchanger Checkout Test.....	VII-3
VII-3	Measured and Calculated Hydrogen Data Characteristics of Breadboard Heat Exchanger Checkout Test.....	VII-4
VII-4	Hydrogen Pressure Loss Characteristics from Breadboard Heat Exchanger Tests.....	VII-4
VII-5	Gaseous Oxygen Pressure Loss Characteristics from Breadboard Heat Ex- changer Run 1.01 Checkout Test.....	VII-5
VII-6	30% Dense Feltmetal Insulation Data Characteristics for Breadboard Heat Exchanger Test No. 2.01.....	VII-6
VII-7	30% Dense Feltmetal Insulation Data Characteristics for Breadboard Heat Exchanger Test No. 2.01.....	VII-6
VII-8	30% Dense Feltmetal Insulation Data Characteristics for Breadboard Heat Exchanger Test No. 2.01.....	VII-7
VII-9	30% Dense Feltmetal Insulation Data Characteristics for Breadboard Heat Exchanger Test No. 2.01.....	VII-7
VII-10	30% Dense Feltmetal Insulation Data Characteristics for Breadboard Heat Exchanger Test No. 2.01.....	VII-8
VII-11	Estimated Performance at Constant Heat Fluxes for Breadboard Hydrogen/Oxygen Heat Exchanger.....	VII-9
VII-12	Insulation Conductance Requirements of Breadboard Hydrogen/Oxygen Heat Exchanger.....	VII-9
VII-13	Fuel Flow Effects on Heat Transfer of Breadboard Heat Exchanger.....	VII-10
VII-14	Oxygen Core Pressure Loss for Breadboard Heat Exchanger Test No. 2.01....	VII-11
VII-15	Exit Quality Flowrate for Breadboard Heat Exchanger Test No. 2.01.....	VII-11
VII-16	Steady-State Instability Characteristics of 30% Dense Feltmetal Insultion for GOX Heat Exchanger Test No. 2.01.....	VII-12
VII-17	Data Characteristics of Breadboard Heat Exchanger Test No. 3.01.....	VII-13
VII-18	Data Characteristics of Breadboard Heat Exchanger Test No. 3.01.....	VII-14
VII-19	Data Characteristics of Breadboard Heat Exchanger Test No. 3.01.....	VII-15
VII-20	Oxygen Core Pressue Loss from GOX Heat Exchanger Test No. 3.01.....	VII-16
VII-21	Steady-State Instability Characteristics of Powdered Aluminum Between Panels for GOX Heat Exchanger Test No. 3.01.....	VII-16



**ILLUSTRATIONS (Continued)**

<i>FIGURE</i>		<i>PAGE</i>
VII-22	Second Cooldown Transient Characteristics from Breadboard Heat Exchanger Test No. 3.01.....	VII-17
VII-23	Third Cooldown Transient Characteristics of Breadboard Heat Exchanger Test No. 3.01.....	VII-18
VII-24	Second Transient Instability Characteristics of GOX Heat Exchanger Test No. 3.01.....	VII-19
VII-25	Third Transient Instability Characteristics of GOX Heat Exchanger Test No. 3.01.....	VII-20
VII-26	Oscillation Amplitude Characteristics of Breadboard GOX Heat Exchanger Tests No. 2.01 an 3.01.....	VII-21
VIII-1	Compact Hydrogen/Oxygen Heat Exchanger - RL10 Derivative II.....	VIII-3

**TABLES**

<i>TABLES</i>		<i>PAGE</i>
III-1	Heat Exchanger Geometry and Design-Point Performance.....	III-4
III-2	Breadboard Heat Exchanger Possible Test Conditions.....	III-9
VI-1	Breadboard Heat Exchanger Rig Instrumentation.....	VI-2

**SYMBOLS**

A	=	Area
$C_p$	=	Specific heat at constant pressure
$\epsilon$	=	Heat exchanger effectiveness
f	=	Friction factor
G	=	Mass flux ( $G=W/A$ )
h	=	Film coefficient
k	=	Thermal conductivity
L	=	Length
$\eta_o$	=	Area-weighted fin effectiveness
P	=	Pressure
Q	=	Heat transfer rate (heat picked up)
$\rho$	=	Density
$r_h$	=	Hydraulic radius
T	=	Temperature
U	=	Overall Heat transfer coefficient
W	=	Flowrate
X	=	Vapor quality
$\lambda$	=	Heat of vaporization
$\sigma$	=	Free-flow area/frontal area
C	=	Coolant, cold (oxygen) side
H	=	Heat transfer, hot (hydrogen) side
W	=	Wall
HT	=	Heat transfer
$H_2$	=	Hydrogen
$O_2$	=	Oxygen

## SECTION I INTRODUCTION

Vehicle system studies have shown that pressure-fed tank head idle (THI) mode operation of the Space Tug main engine is very desirable for thermal conditioning, propellant settling, and low  $\Delta V$  maneuvers. RL10 derivative engine design studies and evaluation of RL10 engine THI test data have shown that reliable THI operation without the need for an active control system should be practical if a heat exchanger is incorporated in the oxygen system upstream of the injector. This heat exchanger, which obtains its energy from the hydrogen used to cool the engine thrust chamber, ensures that the oxygen supplied to the thrust chamber injector in THI operation is always superheated. As a result, good injector stability and uniform flow distribution are obtained and no sudden increases in thrust chamber mixture ratio can occur (due to oxidizer in the injector going to liquid phase). In addition, because the oxygen is heated by the hydrogen, which is used to cool the thrust chamber, a degree of negative feedback is built into the system to reduce thrust chamber mixture ratio variations. Though the purpose of this heat exchanger is to enable an RL10 derivative engine to operate satisfactorily in THI, it also gives the engine the capability for oxygen autogeneous pressurization when operating at full thrust and for autogeneous prepressurization when operating in the pumped idle mode (25% full thrust). A propellant flow schematic of the RL10 Derivative IIB engine in the tank head idle mode is illustrated in figure I-1 to show how the oxygen heat exchanger will operate in this mode.

The low-pressure and low-pressure drop requirements for the heat exchanger could result in self-induced pressure oscillations in the oxidizer side as the oxidizer inlet quality decrease during engine thermal conditioning. By using insulation between the hydrogen and oxygen elements of the heat exchanger, the magnitude of the pressure oscillations can be reduced at the expense of an increase in heat exchanger size. To empirically optimize the heat exchanger design, a "breadboard" heat exchanger, capable of having its configuration changed to vary the insulation between the oxygen and hydrogen elements, was tested and the results are presented in this report.

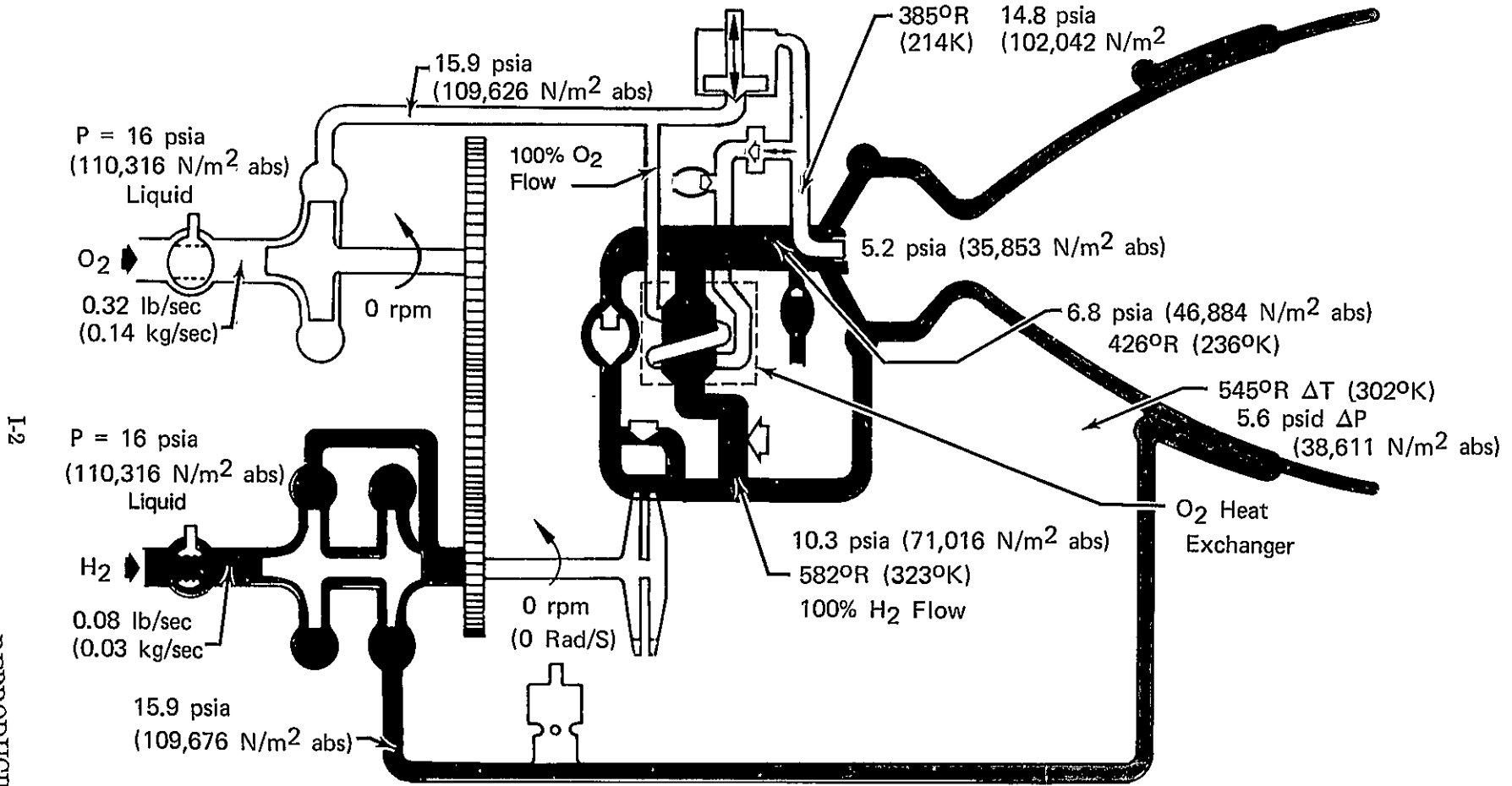


Figure I-1. RL10 Derivative IIB Tank Head Idle Mode

REPRODUCIBILITY OF THE ORIGINAL PAGE IS POOR

I-2

## SECTION II DESIGN REQUIREMENTS

The breadboard oxygen heat exchanger design requirements were established using tank head idle cooldown data generated during a previous contract (Design Study of RL10 Derivatives, Contract NAS8-28989). An extensive amount of data directly applicable to the design of the heat exchanger were available from this study. Estimates of flowrates, propellant temperatures, and pressures at the heat exchanger inlets during a tank head idle cooldown were used to establish worst case conditions for each requirement in terms of overall engine operation.

The selected design requirements for the breadboard heat exchanger were as follows:

1. Flow Oscillation - It was determined that a mixture ratio oscillation of  $\pm 0.5$  in the engine chamber would be acceptable without being detrimental to the engine. This is equivalent to an allowable  $\pm 12.5\%$  oxidizer flow oscillation through the engine injector. The worst case condition was determined to occur at the end of cooldown, when saturated liquid oxygen is present at the heat exchanger inlet. This is the condition at which the largest change in density across the heat exchanger is available, making the existence of large pressure (flow) oscillations possible.
2. Pressure Loss - The maximum allowable pressure loss for the fuel side was initially set at 2 psid (13,789 N/m<sup>2</sup> diff). This requirement was later changed to 10 psid (68,747 N/m<sup>2</sup> diff) to make fabrication and testing easier. The highest fuel pressure loss would be expected to occur at the end of cooldown, where fuel flow is at its highest value of 0.08 lb/sec (0.03 kg/sec). On the oxidizer side, the maximum allowable pressure loss was set at 1 psid (6,894 N/m<sup>2</sup> diff). There are two possible worst case conditions in which this requirement must be satisfied: (1) at the end of cooldown, where oxidizer flowrate (0.32 lb/sec [0.14 kg/sec]) is highest, but density is also greatest (saturated liquid), (2) at the start of cooldown, where flowrate is lower (0.18 lb/sec [0.08 kg/sec]) but density is also lower (500°R [278°K] temperature gas). These allowable pressure losses were set for the heat exchanger core only since the manifolds used for the breadboard heat exchanger will be different than those used for the engine heat exchanger.
3. Strength - Because the plate design is to be used for both the breadboard and engine heat exchangers, the burst pressure limits for the heat exchanger core plates were set by the full thrust maximum expected pressures of the engine (900-psia [6,205,230-N/m<sup>2</sup> abs] fuel at 400°R [222°K] and 700 psia [4,826,332 N/m<sup>2</sup> abs] oxidizer at 170°R [94°K]). Since different manifolds will be used for the engine heat exchangers, it is only necessary that the manifolds withstand the maximum pressures expected during breadboard heat exchanger tests (40-psia [275,790-N/m<sup>2</sup> abs] fuel, 30-psia [206,843-N/m<sup>2</sup> abs] oxidizer).
4. Heat Transfer - Heat transfer requirements were set to maintain a high quality (near gaseous) or gaseous oxygen at the heat exchanger exit during the worst case condition of saturated liquid oxygen at the heat exchanger inlet.

### SECTION III DESIGN

#### A. BREADBOARD HEAT EXCHANGER FLUID/THERMAL ANALYSIS

The prime objective of this analysis was to confirm the heat exchanger geometry and thermal/fluid characteristics as defined under preliminary IR&D efforts (Reference 3). Additional requirements were to select the insulating material, specify needed fluid/thermal instrumentation and instrumentation locations, and to provide working curves to define the heat exchanger operating characteristics at THI conditions.

The breadboard heat exchanger, figure III-1, consists of two 20-in. (0.51-m) flow width by 10-in. (0.25-m) flow length oxygen plate-fin panels sandwiched between three 10-in. (0.25-m) flow width by 20-in. (0.51-m) flow length hydrogen panels. All panels have identical cross-sections. Four 10- by 20- by 0.125-in. (0.25- by 0.51 by 0.003-m) sheets of SS 347 feltmetal (sintered metal fiber) sandwiched between the plates, provide the means for controlling the heat transfer rate from the ambient temperature (530°R [294°K]) hydrogen to the cryogenic saturated LOX at 168°R [93°K]).

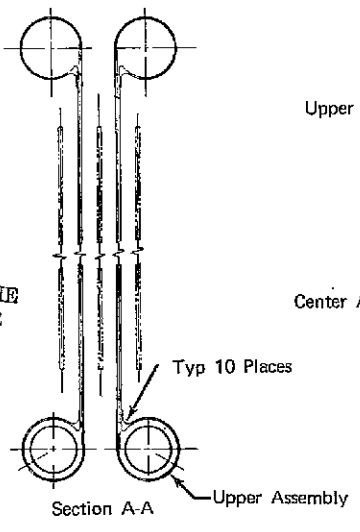
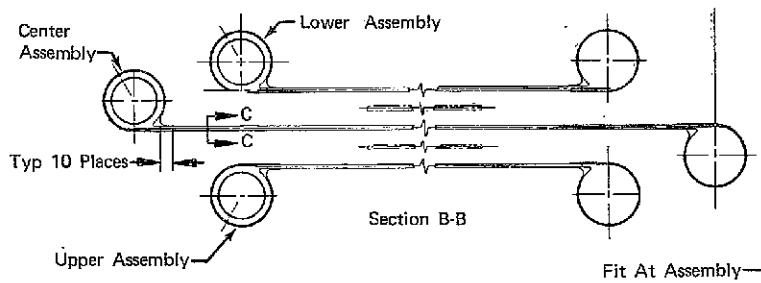
Performance predictions indicated that the breadboard heat exchanger should be able to produce a range of oxygen discharge conditions from saturated liquid (no heat transfer) to superheated vapor (maximum heat transfer) with oxygen pressure losses  $\leq 2$  psia (13,789 N/m<sup>2</sup> abs) in the heat exchanger. Hydrogen pressure losses are expected to be approximately 10 psia (68,947 N/m<sup>2</sup> abs).

Fluid and thermal test results obtained from the breadboard heat exchanger will be used to establish Liquid Oxygen (LOX) boiling stability limits for THI conditions and will provide the necessary parameters for the design of the flight-weight hydrogen/oxygen heat exchanger.

##### 1. Breadboard Heat Exchanger Geometry and Performance

The breadboard heat exchanger presented in figure III-1 is exactly the same in concept as the heat exchanger configuration proposed in Reference 3 except that the oxygen flow area has been increased from 1.59 in.<sup>2</sup> (0.0010 m<sup>2</sup>) to 3.05 in.<sup>2</sup> (0.0019 m<sup>2</sup>) and the oxygen flow length has been reduced from 23 in. (0.58 m) to 10 in. (0.25 m). These changes were required to ensure that the desired oxygen flowrate could be successfully passed by the heat exchanger in spite of relatively high pressure losses associated with two-phase (boiling) flow.

Due to the nature of cross-flow heat exchangers (nearly equal size plates), the resulting hydrogen flow area was reduced from 6.08 in.<sup>2</sup> (0.004 m<sup>2</sup>) to 2.29 in.<sup>2</sup> (0.0015 m<sup>2</sup>) and the hydrogen flow length was increased from 9 in. (0.23 m) to 20 in. (0.51 m). The predicted hydrogen core  $\Delta P$  of 10 psid (68,947 N/m<sup>2</sup> diff), is considerably higher than that allowed in actual RL10 THI operation ( $\approx 2$  psia [13,789 N/m<sup>2</sup> abs], Reference 4), because the heat exchanger was designed with fewer hydrogen panels (smaller effective flow area) than an engine heat exchanger design to make fabrication and testing easier. Repackaging the breadboard heat exchanger for flight operation would result in hydrogen  $\Delta P$ 's that meet THI cycle requirements. Table III-1 summarizes the breadboard heat exchanger geometry and design-point performance predictions.



REPRODUCIBILITY OF THE ORIGINAL PAGE IS POOR

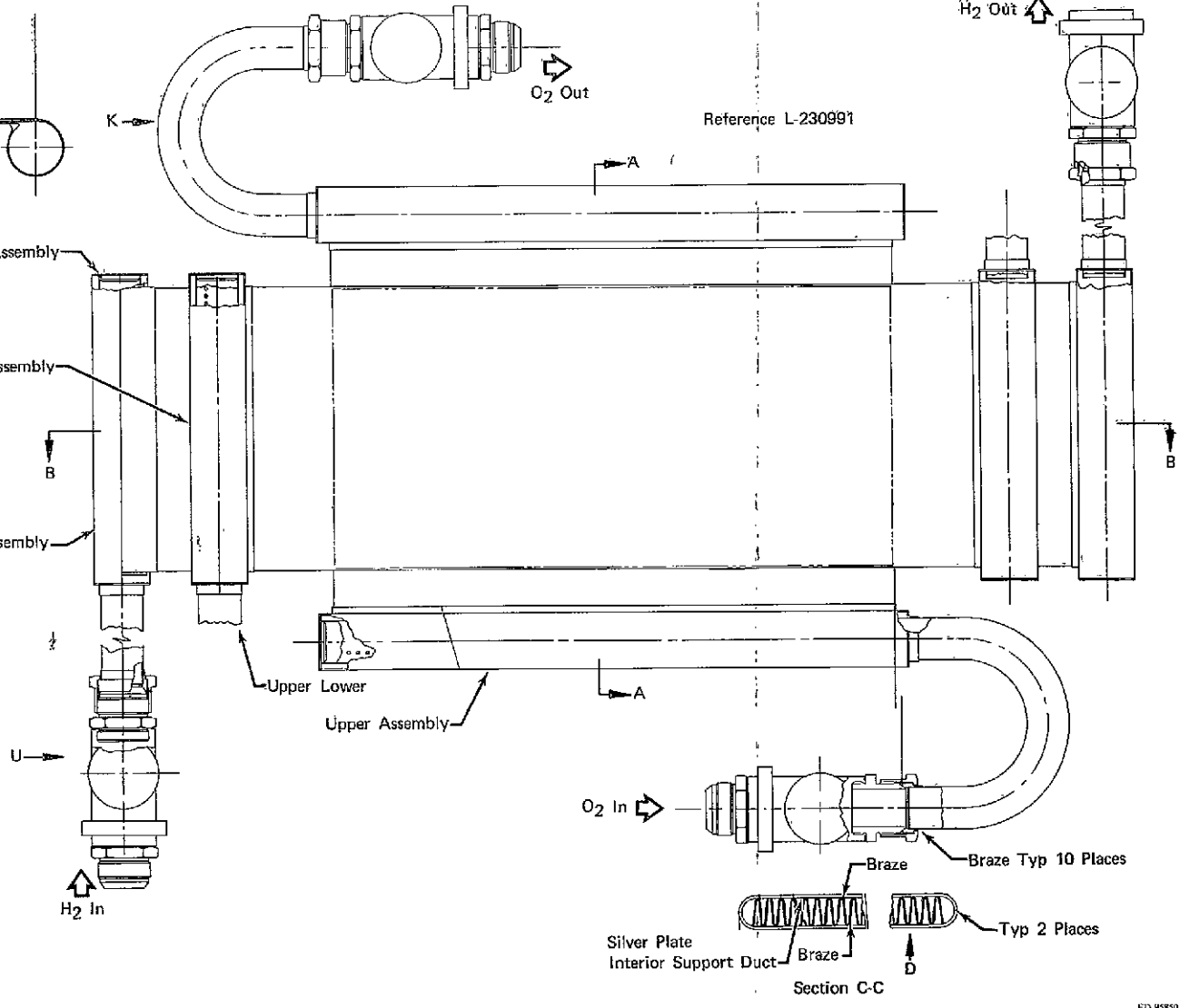


Figure III-1. Breadboard Hydrogen/Oxygen Heat Exchanger



Table III-1. Heat Exchanger Geometry and Design-Point\* Performance

Parameter	Hydrogen-Side	Oxygen-Side
No. of panels	8	2
Minimum panel width, in.	10 (0.25 m)	20 (0.51 m)
Minimum panel length, in.	20 (0.51 m)	10 (0.25 m)
Panel thickness, in.	0.120 (0.003 m)	0.120 (0.003 m)
$A_c$ , in. <sup>2</sup>	2.29 (0.0015 m <sup>2</sup> )	3.05 (0.0019 m <sup>2</sup> )
$\dot{w}_c$ , lb <sub>m</sub> /sec	0.080 (0.04 kg/sec)	0.320 (0.14 kg/sec)
Fluid $\Delta T$ , °R	-13.1 (-7.27°K)	0 (0°K)
Core $\Delta P$ , psia	10 (68,947 N/m <sup>2</sup> abs)	0.125 (862 N/m <sup>2</sup> abs)
Fluid exit quality	1 (All Gas)	0.134
Q, Btu/sec	3.76 (3,964 w)	3.76 (3,964 w)
$A_{heat transfer}$ , ft <sup>2</sup>	30.84 (2.87 m <sup>2</sup> )	30.84 (2.87 m <sup>2</sup> )

\*Fluid inlet conditions from Reference 4; overall heat flux equal to predicted critical heat flux for stable boiling of LOX (0.122 Btu/ft<sup>2</sup>-sec [1384.6 w/m<sup>2</sup>]).

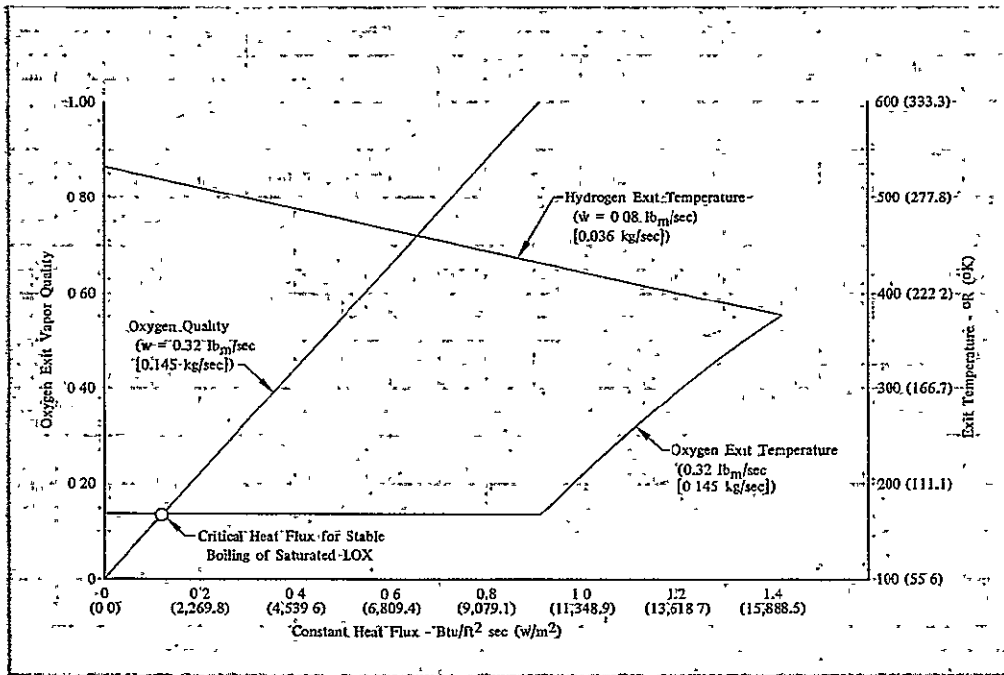
Figures III-2 and III-3 present predicted breadboard heat exchanger performance at design-point hydrogen and oxygen flowrates at various heat flux levels (controlled by the insulation conductance selected) ranging from zero heat transfer to maximum heat transfer (all plates in contact, no insulation). The critical heat flux for stable boiling of saturated LOX, (Reference 5), is 0.122 Btu/ft<sup>2</sup>-sec (1384.6 w/m<sup>2</sup>). Test plans call for stability testing at heat flux levels higher and lower than this predicted critical heat flux.

Figure III-4 shows the effect of oxygen quality on critical heat flux. The maximum heat flux of the breadboard heat exchanger is 1.42 Btu/ft<sup>2</sup>-sec (16,115.481 w/m<sup>2</sup>); thus, no boiling instabilities should be encountered for qualities greater than approximately 15%.

Insulation conductance requirements are presented as a function of desired heat flux in figure III-5. These requirements were determined using a one-dimensional steady-state heat balance between the hydrogen and oxygen panels and did not include the effects of contact resistance at the insulation/coverplate interfaces. Figure III-5 presents the maximum possible heat transfer rate for a given insulation conductance.

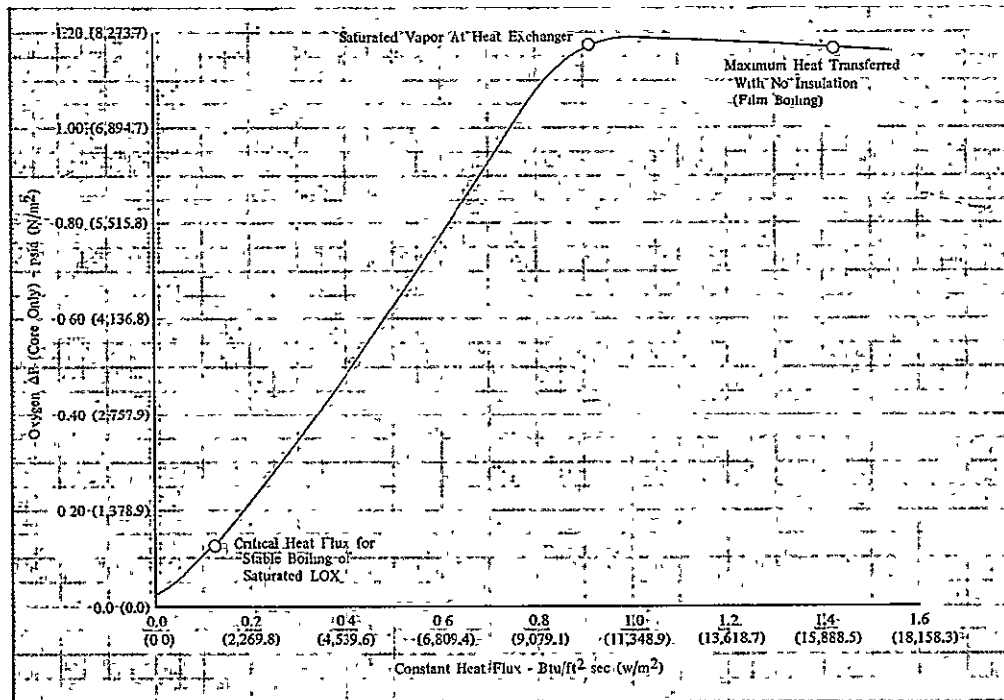
## 2. Insulation Selection

Various types of insulations and insulation thicknesses were investigated. The calculated thermal conductances of these insulations are plotted as functions of insulation thicknesses in figure III-6. Thicknesses up to 0.5 in. (0.013 m) (the maximum possible between-panel thickness) and thermal conductances up to 100 Btu/ft<sup>2</sup>-hr-°R (537,446 w/m<sup>2</sup>-°K) are included. An insulation conductance of 7 Btu/ft<sup>2</sup>-hr-°R (39,721 w/m<sup>2</sup>-°K) is required to produce the predicted critical heat flux (0.122 Btu/ft<sup>2</sup>-sec [1384,569 w/m<sup>2</sup>]). Note that materials such as glass, ceramics, and plastics are poorly suited for this application, as excessively thick layers are required to produce the low conductances needed. Teflon and styrofoam have too low a conductance for this application, since extremely thin layers are required. The materials indicated by the numbers are feltmetal (sintered metallic) fiber metal sheets (Reference 6). Wide conductance ranges are possible with reasonable sheet thicknesses (0.06 to 0.25 in. [0.0015 to 0.0064 m]).



DF 101968

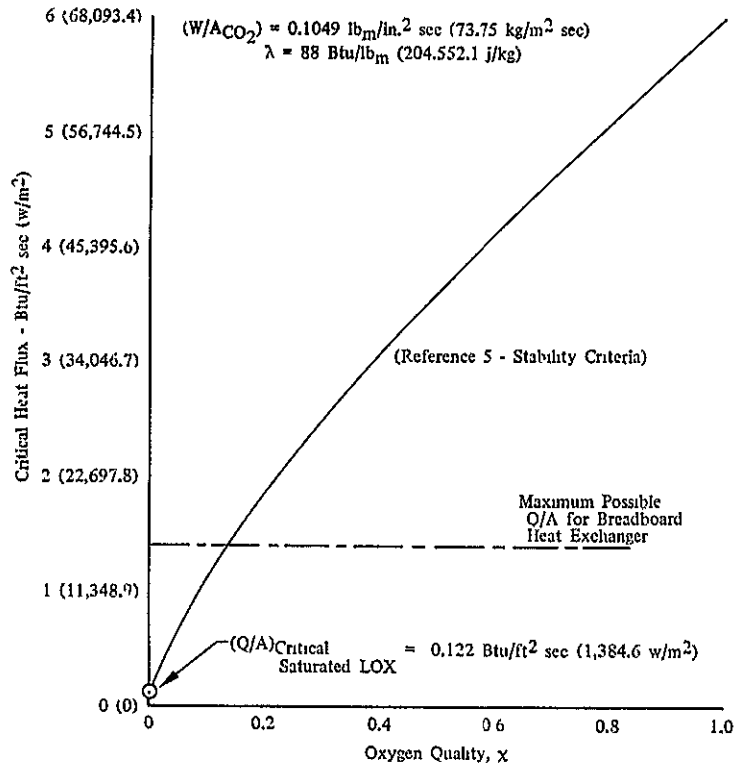
Figure III-2. Estimated Performance at Constant Heat Fluxes



DF 101969

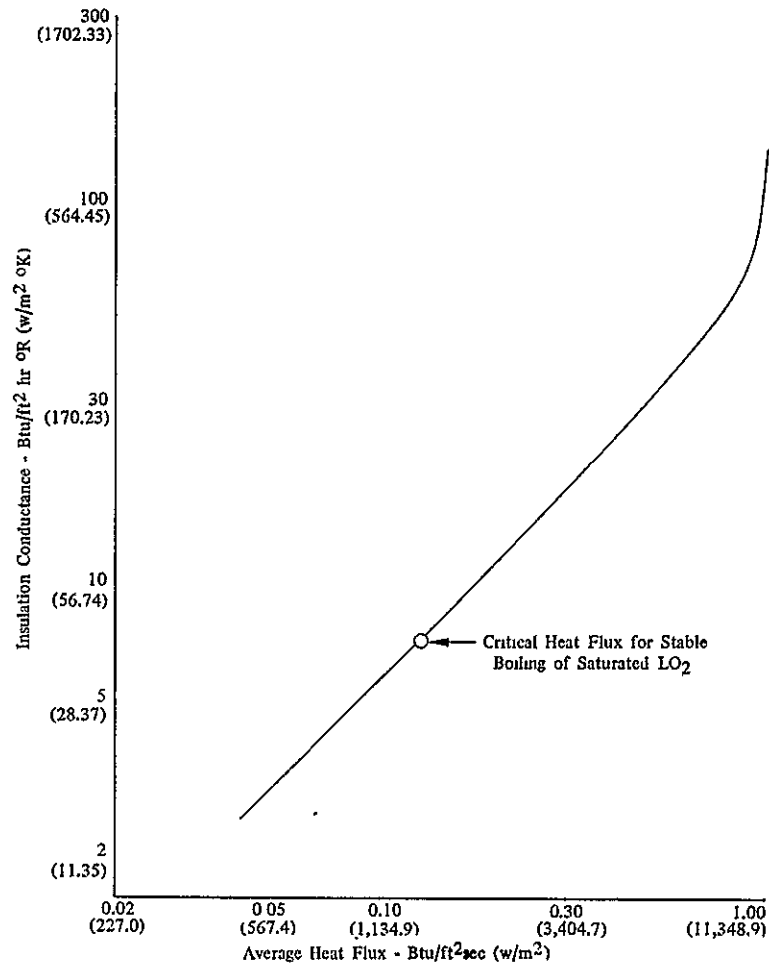
Figure III-3. Breadboard Hydrogen/Oxygen Heat Exchanger Oxygen-Side Core ΔP vs Heat Flux w<sub>O<sub>2</sub></sub> = 0.32 lbm/sec

III-6



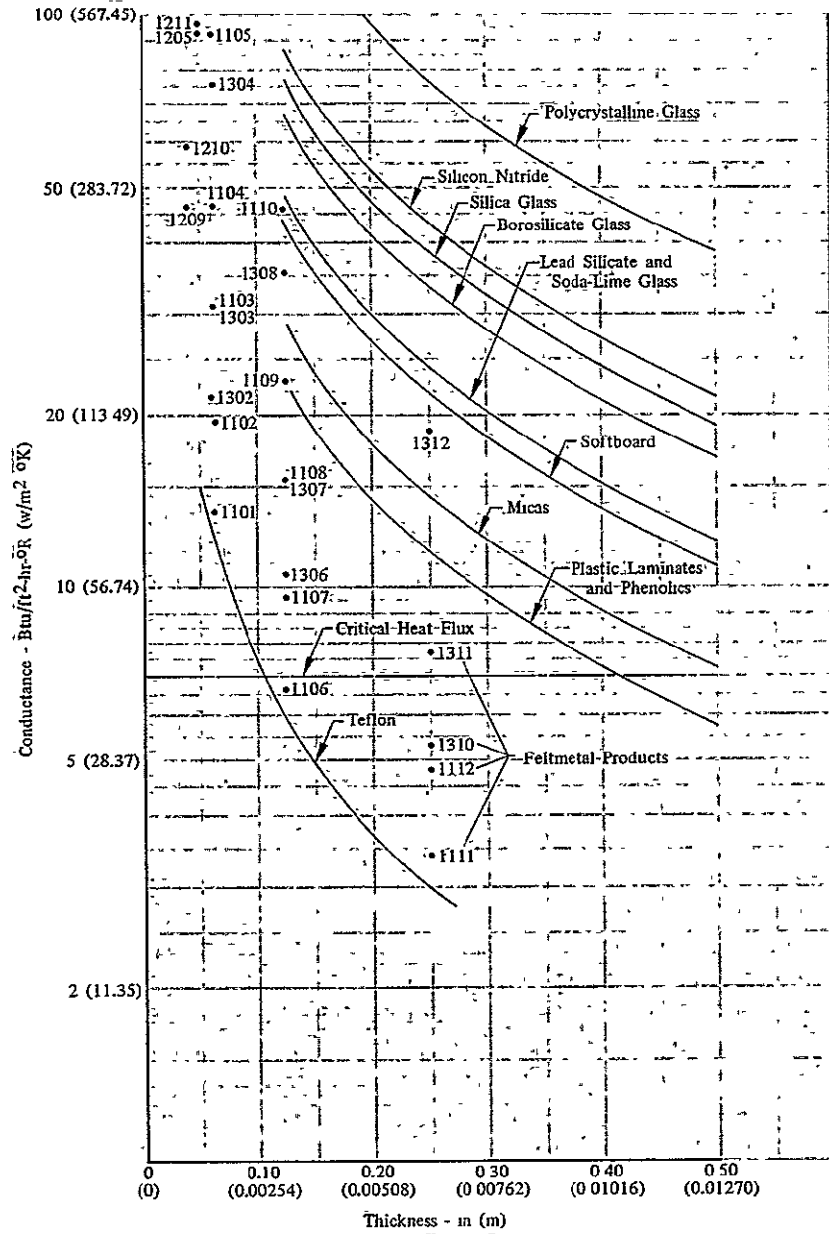
DF 101970

Figure III-4. Breadboard Heat Exchanger Critical Heat Flux vs Oxygen Quality Design-Point Operation



DF 101953

Figure III-5. Breadboard Hydrogen/Oxygen Heat Exchanger Insulation Conductance Requirements



DF 101971

Figure III-6. Breadboard Hydrogen/Oxygen Heat Exchanger Potential Insulating Materials

Figure III-7 shows the insulating potential offered by feltmetal sheets constructed of stainless steel (347). This feltmetal product appears well-suited for the breadboard heat exchanger application because of its thermal compatibility with the plate-fin panels (also SS 347), and because it could be successfully brazed to the panels should it be used in the final flight-weight heat exchanger design. Furthermore, it might be well suited for absorbing thermal strains induced by different thermal growths of the hydrogen and oxygen panels (due to its fibrous nature), and it offers a high potential for increasing heat exchanger performance by increasing its thermal conductance (through squashing) in regions where increased heat transfer rates are not detrimental to flow stability.

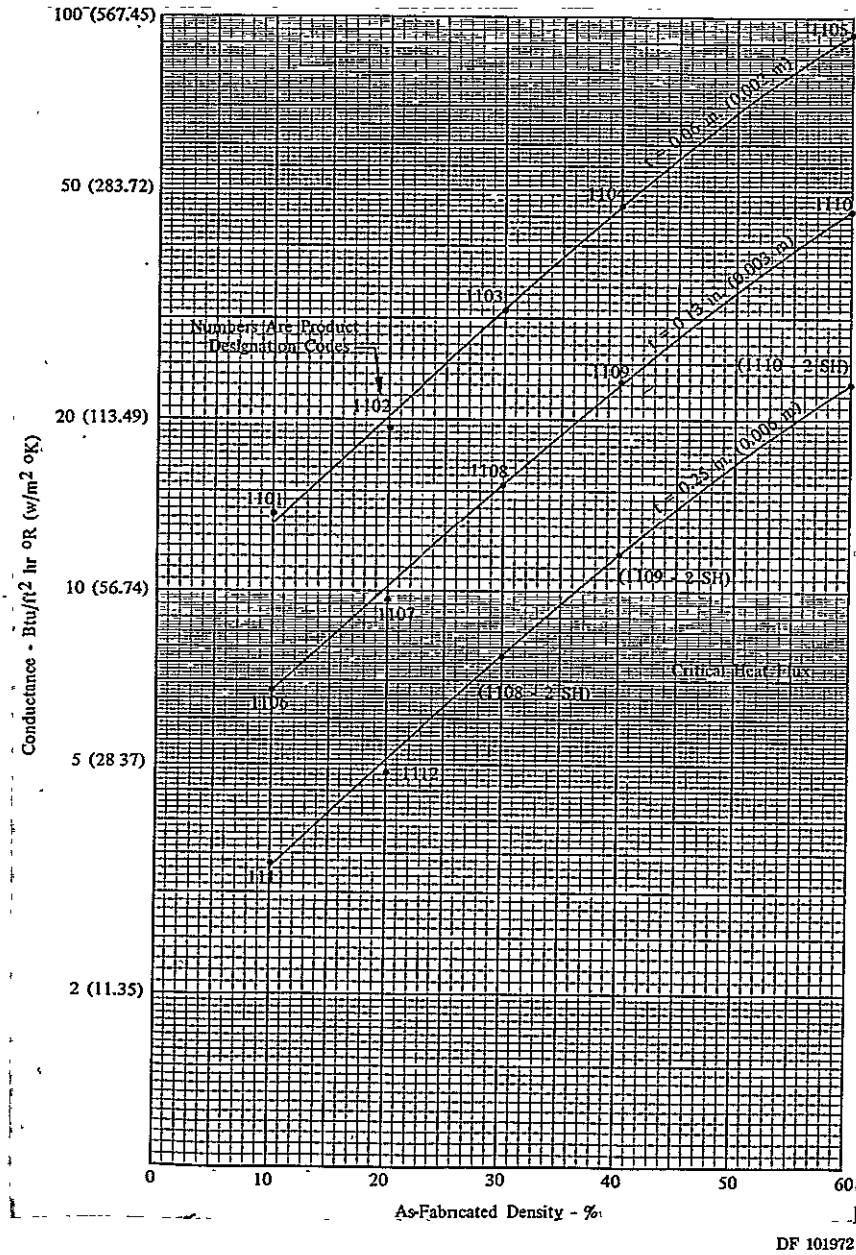


Figure III-7. Potential of 347 Stainless Steel Feltmetal as Thermal Insulation

A cost-effectiveness trade study was undertaken using the thermal conductance predictions of figure III-7 (from Reference 6), and vendor-quoted prices for available SS 347 feltmetal sheets (Reference 13). Basically, the intent was to determine the number of and type of SS 347 feltmetal sheets that should be purchased to maximize the potential results per dollar.

Four sheets of 10% dense feltmetal, FM 1106 (12 by 24 by 0.125 in. [0.305 by 0.610 by 0.0032 m]), and three sheets of 30% dense feltmetal, FM 1108 (14 by 28 by 0.125 in. [0.356 by 0.711 by 0.0032 m]), were selected to be purchased. This amount of material enabled the construction of four 10 by 20 in. (0.254 by 0.508 m) sheets of FM 1106 and four 10 by 20 in. (0.254 by 0.508 m) sheets of FM 1108. Table III-2 is a summary of potential test points that could be run with these insulation sheets.

Table III-2. Breadboard Heat Exchanger Possible Test Conditions

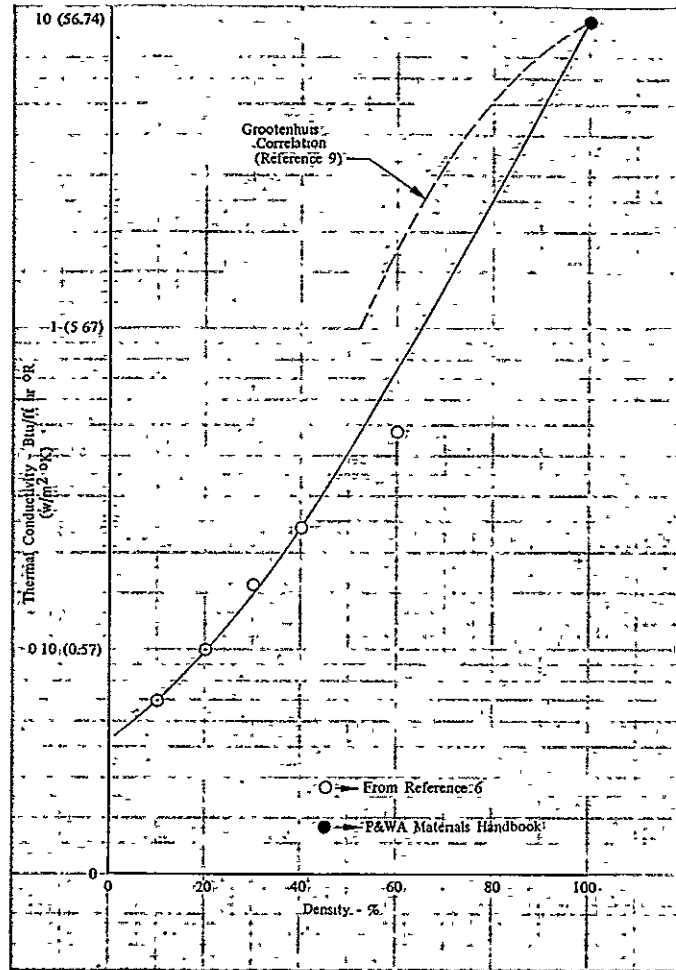
Test No.	Insulation	Maximum Insulation Conductance,* Btu/ft-hr-°R (w/m-°K)	Maximum Heat Flux,* Btu/ft-sec (w/m)
1	None	0	1.42 (16,115.48)
2	FM 1106	6.72 (38.13)	0.119 ( 1,350.52)
3	FM 1108	15.36 (87.16)	0.265 ( 3,007.47)
4	FM 1106 + FM 1108 (Two Sheets Together)	4.67 (24.50)	0.082 ( 930.61)

\* The thermal resistance at interfaces between the insulation and the panels has not been included. The result would be an actual heat flux somewhat lower than that given in this table.

Figure III-4 shows predicted critical heat flux as a function of oxygen quality. Low heat fluxes are only required in low quality regions. Consequently, heat exchanger tests with low density feltmetal (FM 1106) near the oxygen inlet and medium density feltmetal (FM 1108) in the remaining heat transfer zone (sheets butted together) would be possibilities for additional tests.

Figure III-8 shows the increases in SS 347 feltmetal thermal conductivity with density. Feltmetal sheets of increased density (up to 60%) could be either purchased from the vendor or produced in-house by compressing (squashing) the sheets (10% and 30%) already purchased. In this way, testing at heat flux levels from 0.082 Btu/ft<sup>2</sup>-sec (930.61 w/m<sup>2</sup>) (Test No. 4) all the way to 1.42 Btu/ft<sup>2</sup>-sec (16,115.48 w/m<sup>2</sup>) (Test No. 1) would be theoretically possible at no additional cost.

Figure III-9 shows the tremendous potential for increasing heat transfer rates (gradually so as to always be less than critical) that can be realized by compressing various geometry wedges of 10% dense feltmetal into a constant 0.125 in. (0.0032 m) sheet. An order of magnitude increase in oxygen exit quality is theoretically possible. This potential made feltmetal and the obvious choice for the flight-type heat exchanger, as well as for the breadboard configuration.



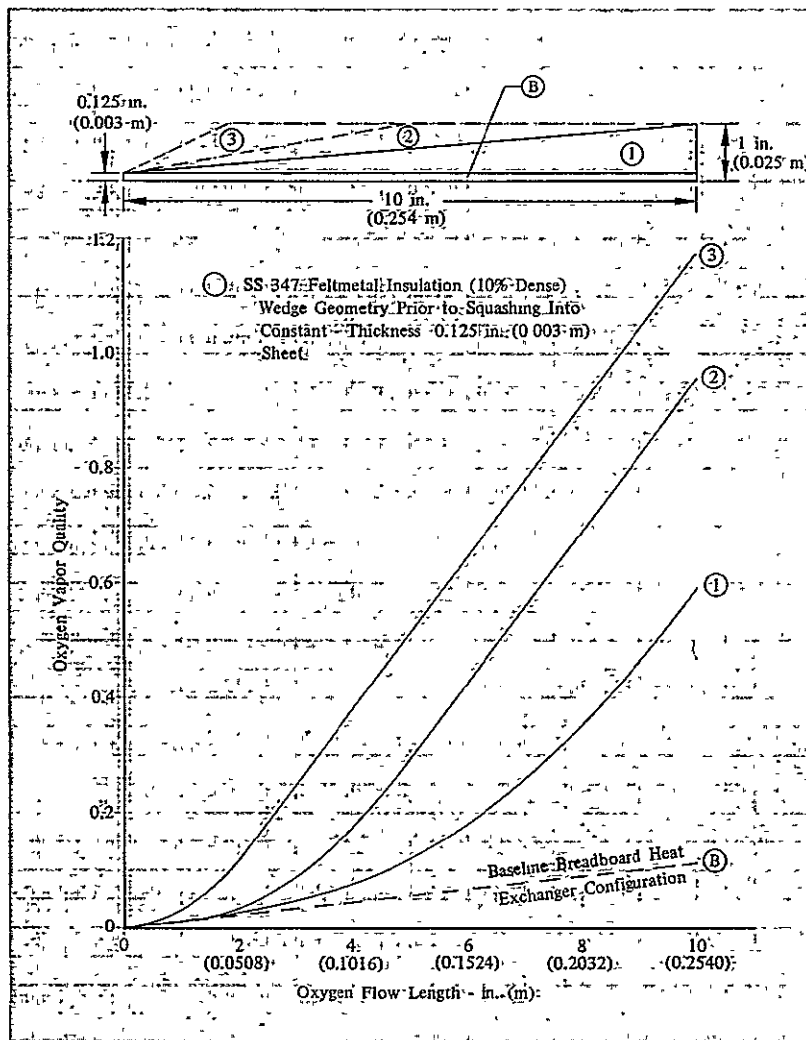
DF 101973

Figure III-8. Stainless Steel 347 Feltmetal Thermal Conductivity vs Density

### 3. Fluid and Thermal Analysis

#### a. Thermal Analysis

The breadboard heat exchanger design-point performance and insulation requirements were determined by assuming a heat flux level, calculating the overall heat exchanger performance parameters (fluid  $\Delta T$ 's,  $\Delta P$ 's,  $T_H$ , and  $T_C$ ), and then calculating the required insulation thermal conductance needed to produce the assumed heat flux (using a one-dimensional heat balance). As is shown below, this method is straightforward for fixed heat exchanger geometry. The heat exchanger hydrogen and oxygen panel dimensions and flow areas are set primarily by fluid flow considerations.



DF 101974

Figure III-9. Hydrogen/Oxygen Breadboard Heat Exchanger Potential Heat Transfer Increases Possible Using Variable Density Insulation

For each assumed average heat flow ( $Q/A$ ), the overall heat exchanger effectiveness ( $\epsilon$ ) and overall heat transfer coefficient ( $U$ ) can be calculated:

$$Q = (Q/A) \times A_{HT} \quad (1)$$

Where  $A_{HT}$  is heat exchanger heat transfer area and  $Q/A$  is the assumed heat flux. Furthermore,

$$\epsilon = Q/Q_{\max} = Q/\dot{w}_{H_2} C_{pH_2} (T_{H_2} - T_{O_2})_{IN} \quad (2)$$

from Reference 8.

$$(T_{IN} - T_{EX})_{H_2} = Q/\dot{w}_{H_2} C_{pH_2} \quad (3)$$

$$(\chi_{EX} - \chi_{IN})_{O_2} = Q/\dot{w}_{O_2} \quad (4)$$



Now for a gas heat exchanger with

$$(\dot{w}Cp)_{IG}/(\dot{w}Cp)_{gas} \ll 1$$

from Reference 8.

$$\epsilon = 1 - e^{-N_{TU}}$$

or

$$N_{TU} = -\ln(1 - \epsilon) \quad (5)$$

From the definition of  $N_{TU}$  (number of transfer units) the overall heat transfer coefficient between the hot and cold fluids can be found to be

$$U = N_{TU} \dot{w}_{H_2} C_{p_{H_2}} / A_{HT} \quad (6)$$

A one-dimensional heat balance is used to relate the thermal resistance across the warm and cold fluid films, across the panel coverplates, and across the insulation (neglecting contact resistances) to the overall thermal resistance ( $1/U$ ):

$$\begin{aligned} (Q/A) &= U(T_H - T_C) \\ &= \eta_{OH} h_H (T_H - T_{WH1}) \\ &= (k_a/a) (A_w/A_H) (T_{WH1} - T_{WH2}) \\ &= (k/t)_I (A_w/A_H) (T_{WH2} - T_{WC2}) \\ &= (k_b/b) (A_w/A_H) (T_{WC2} - T_{WC1}) \\ &= \eta_{OC} (h_C + h_B) (T_{WC1} - T_C) \end{aligned}$$

Eliminating temperatures from the above equations yields

$$1/U = 1/\eta_{OH} h_H + 1/(k_a/a) (A_w/A_H) + 1/(k/t)_I A_w/A_H + 1/(k_b/b) A_w/A_H + 1/\eta_{OC} (h_C + h_B) A_c/A_H \quad (7)$$

Where

- $h_H$  = average hydrogen-side convective film coefficient
- $h_C$  = average oxygen-side convective film coefficient
- $h_B$  = oxygen pool boiling film coefficient
- $\eta_{OH}$  = area-weighted fin effectiveness on hydrogen side
- $\eta_{OC}$  = area-weighted fin effectiveness on oxygen side
- $A_c/A_H$  = ratio of cold-side heat transfer area to hot-side area (=1.0)
- $A_w/A_H$  = ratio of plate area to hot-side area (=0.18)
- $k_a/a$  = thermal conductance across hot-side plate
- $k_b/b$  = thermal conductance across cold-side plate
- $k/t_I$  = insulation thermal conductance

Equation (17) is then used to calculate the required insulation thermal conductance,  $(k/t)_I$ , needed to limit the heat flux between the hydrogen and oxygen panels to the assumed value. (See figure III-5.)

### (1) Forced Convection Film Coefficients

Heat transfer data for the breadboard heat exchanger core geometry selected (figure III-10) were used to predict forced convection film coefficients for the hydrogen (figure III-11) and the oxygen (figure III-12). Hydrogen transport properties were evaluated at the bulk temperatures indicated in figure III-13, since for most heat flux levels of interest, the difference between the hydrogen bulk temperature and the hydrogen-side wall temperature will be small.

For two-phase oxygen flow, transport properties were evaluated at both saturated liquid and saturated vapor conditions and a homogeneous flow model (Reference 7) used to define transport properties for the two-phase mixture. While the homogeneous flow model was generally restricted to use with low vapor qualities, it was used here for the entire two-phase flow regime for consistency. Test results may dictate a modification of this technique or substitution of a separate flow model.

### (2) Oxygen Pool Boiling Heat Transfer

Saturated oxygen boiling heat transfer predictions are shown in figure III-13. In the nucleate boiling regime ( $\Delta T < 50^\circ\text{R}$  [ $27.8^\circ\text{K}$ ]) the correlation of Kutateladze for  $P=1.5$  atm, from Reference 10, has been used. In the film boiling regime ( $\Delta T > 50^\circ\text{R}$  [ $27.8^\circ\text{K}$ ]) the correlation of Breen and Westwater for  $P=1.0$  atm ( $101,352$  N/m<sup>2</sup>; Reference 10) was used. Film boiling is generally undesirable due to significantly reduced heat transfer rates and is expected to be present only for heat fluxes greater than  $0.8$  Btu/ft<sup>2</sup>-sec ( $9079.14$  w/m<sup>2</sup>).

### (3) Area-weighted Fin Effectivenesses

Area-weighted fin effectivenesses are shown in figure III-14 as functions of the local fluid film coefficient.

## b. Fluid Analysis

Fluid pressure loss estimates through the hydrogen and oxygen panels and their manifolds were required to select a heat exchanger geometry that will meet the established cycle  $\Delta P$  requirements (Reference 4). The following paragraphs discuss the techniques employed in evaluating fluid pressure losses in the breadboard heat exchanger core. Parametric analyses were undertaken to determine the effects of various geometric combinations on fluid pressure losses.

### (1) Hydrogen-Side Core $\Delta P$

Hydrogen frictional pressure losses through the heat exchanger core were evaluated parametrically using

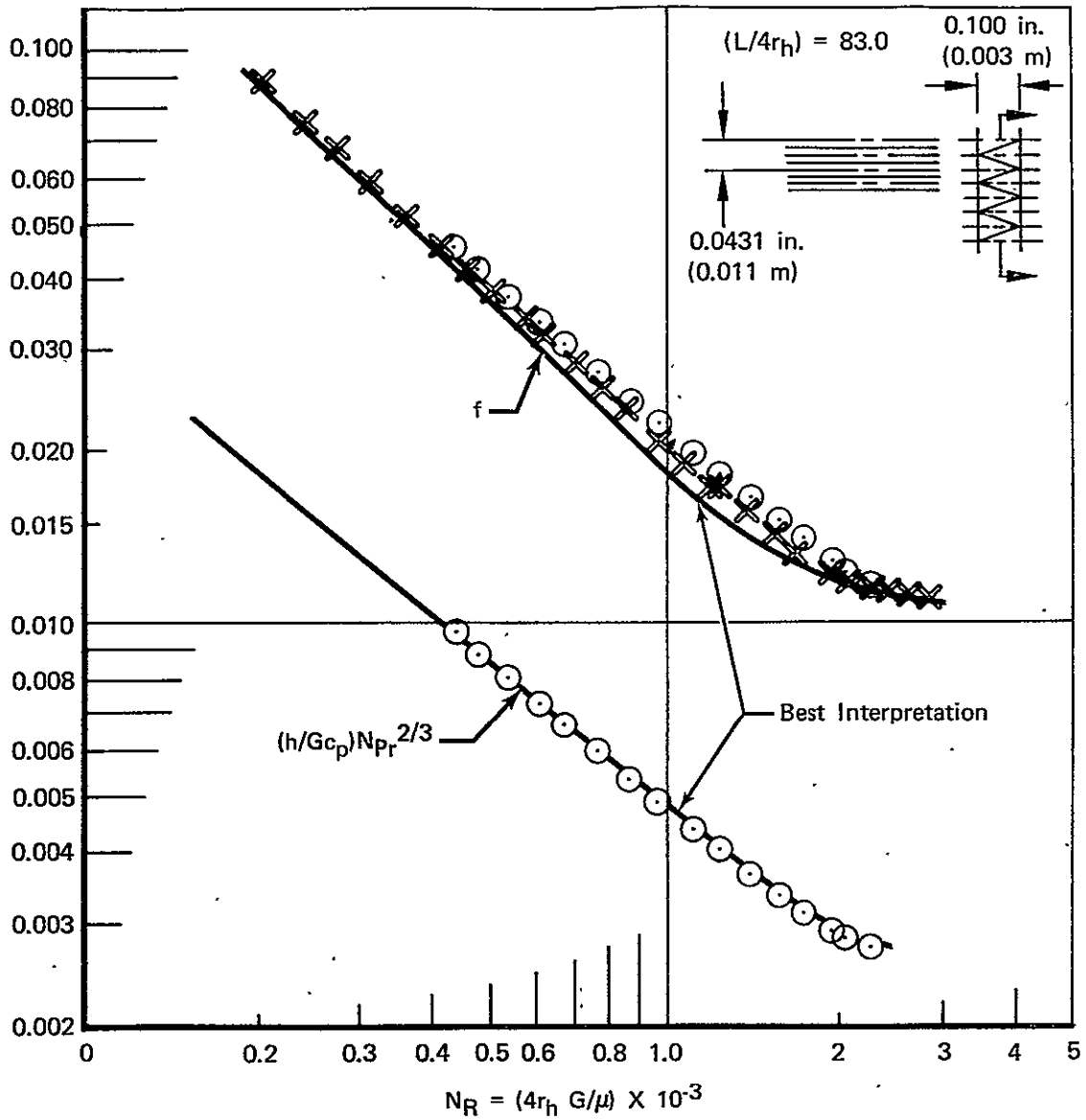
$$\Delta P_f/L = G^2/2g_c f/\Gamma_h 1/P_m \quad (8)$$

from Reference 8 and friction data from figure III-10. Contraction, expansion, and fluid acceleration losses were similarly evaluated using the following equation from Reference 8:

$$\Delta P_m = G^2/2g_c [K_c + 1 - \sigma_o^2/P_{IN} + 2(1/P_{IN} - 1/P_{EX}) - 1 - \sigma_o^2 - K_e/P_{EX}] \quad (9)$$

with  $\sigma_o = 0.635$  (free flow area/frontal area).

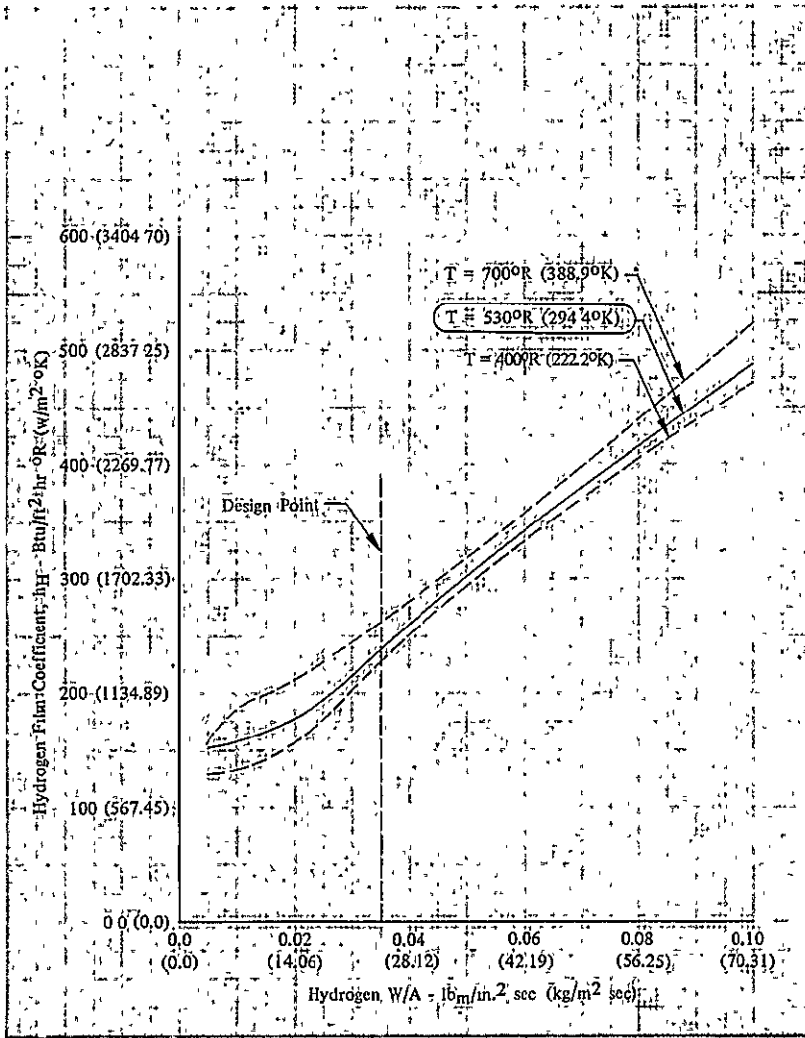
The results of the hydrogen core  $\Delta P$  calculations are given in figure III-15.



Fin Pitch = 46.45 per in. (1828.74 per m)  
 Plate Spacing,  $b = 0.100$  in. (0.00254 m)  
 Fin Length Flow Direction = 2.63 in. (0.0668 m)  
 Flow Passage Hydraulic Diameter,  $4r_h = 0.002643$  ft (0.000806 m)  
 Fin Metal Thickness = 0.002 in. (0.0000508 m) Stainless Steel  
 Total Heat Transfer Area/Volume Between Plates,  $\beta = 1332.45$  ft<sup>2</sup>/ft<sup>3</sup> (4371.555 m<sup>2</sup>/m<sup>3</sup>)  
 Fin Area/Total Area = 0.837

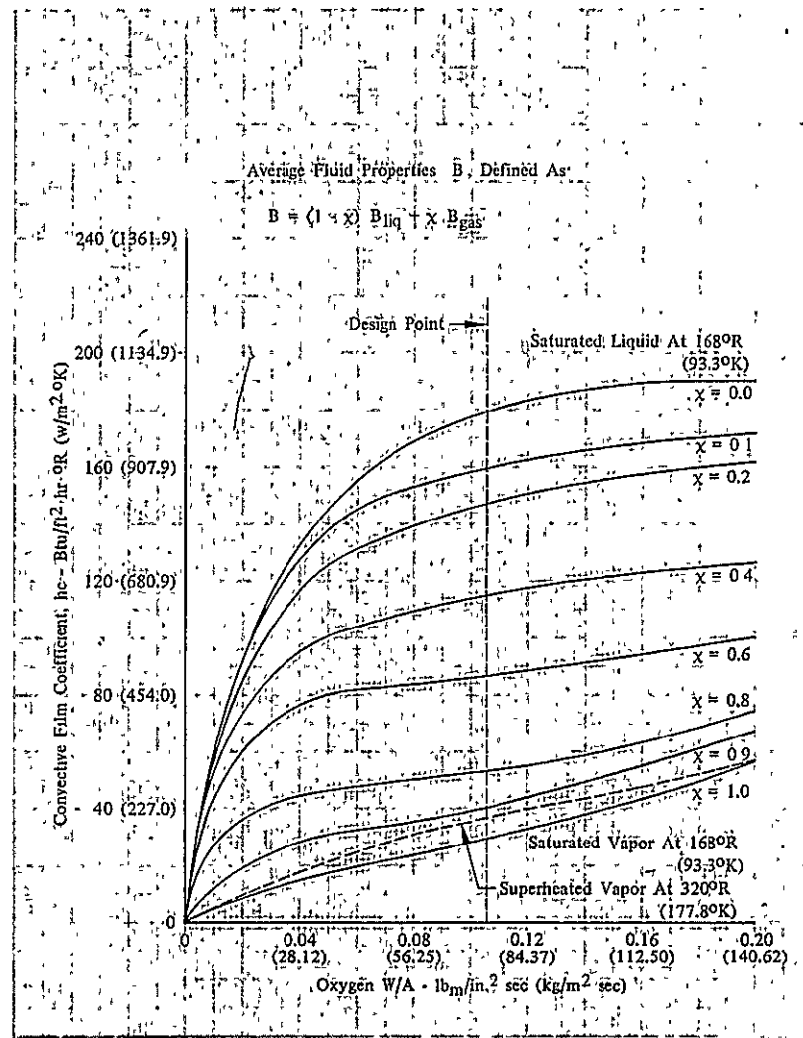
FD 95855

Figure III-10. Heat Transfer and Friction Data for Heat Exchanger Core (Reference 8)



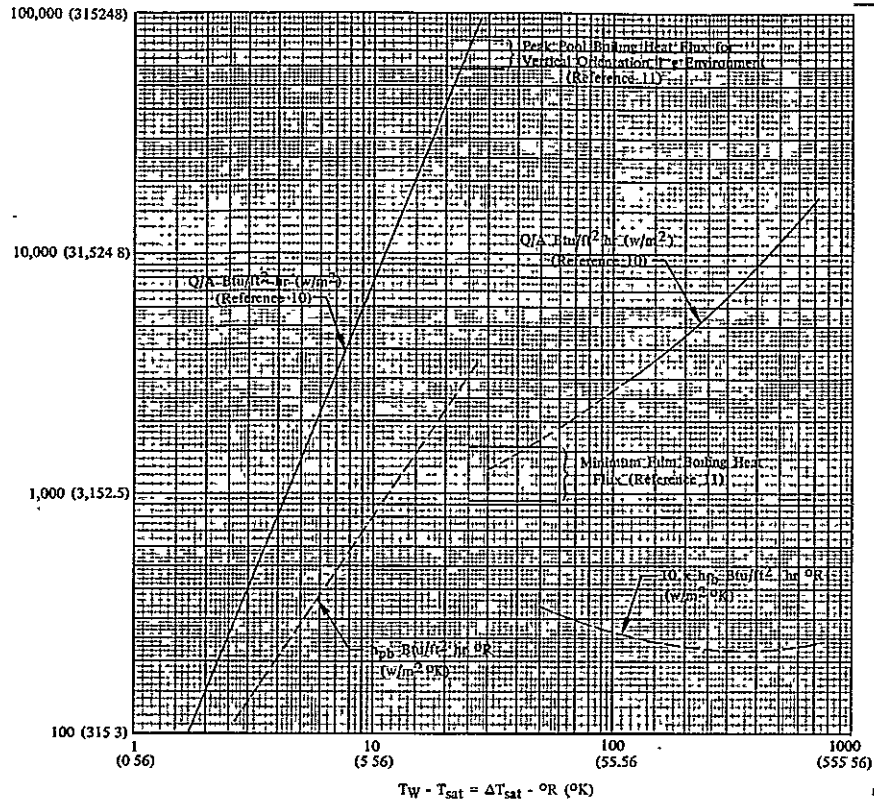
DF 101985

Figure III-11. Hydrogen-Forced Convection Film Coefficients  $10 < P < 20$  psia ( $68,948 < P < 137,895$  N/m<sup>2</sup>)



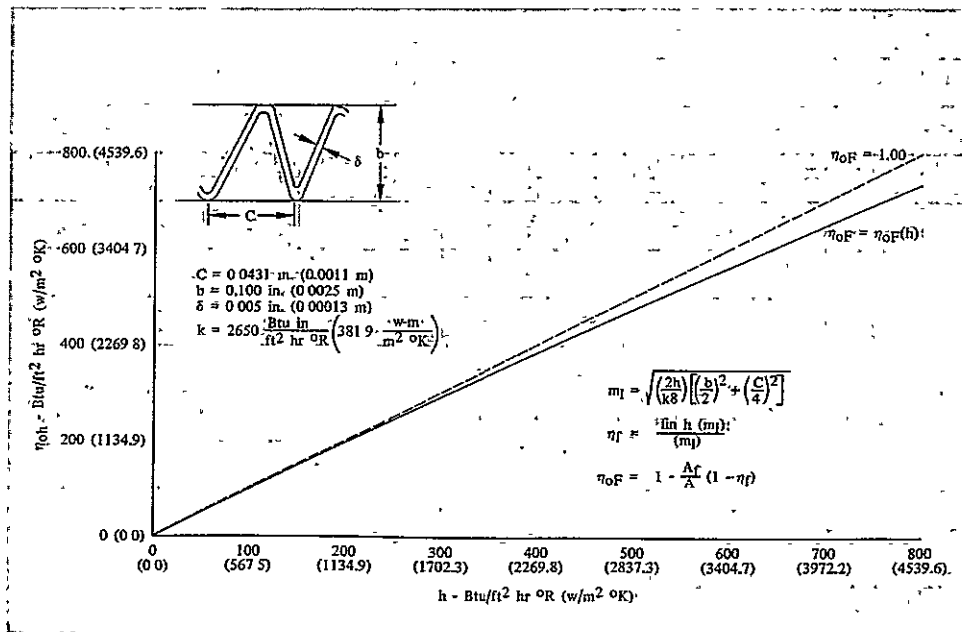
DF 101976

Figure III-12. Oxygen-Forced Convection Film Coefficients ( $P \approx 15$  psia [ $103,421$  N/m<sup>2</sup>])



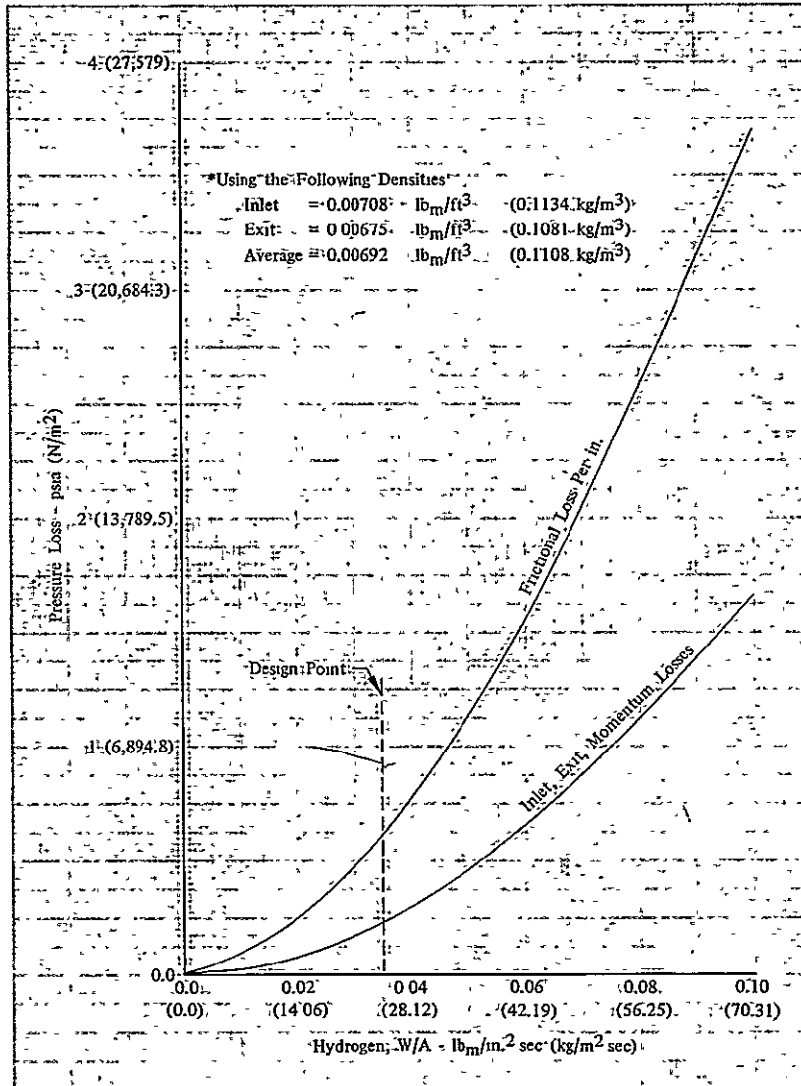
DF 101977

Figure III-13. Boiling Heat Transfer to 20 psia (137,895 N/m<sup>2</sup>) Saturated Oxygen



DF 101978

Figure III-14. Area-Weighted Effectiveness of Copper Fins



DF 101979

Figure III-15. Gaseous Hydrogen Pressure Losses Through Heat Exchanger Plate

(2) Oxygen-Side  $\Delta P$

Two techniques are available for evaluating pressure losses for the two-phase (boiling) oxygen, the homogeneous model from Reference 7 and the separated flow model from Reference 12. In general, the homogeneous model is restricted to use with low vapor qualities where the fluid behaves as a uniform mixture of vapor and liquid and the separated flow model is restricted to use with high vapor qualities and in particular, for the annular flow regime (for which it was developed). The separated flow model yields higher calculated pressure losses than does the homogeneous model; hence, it was employed in this analysis.

Total oxygen mass flux is given by

$$G_T = \dot{w}_{O_2}/A_c = \dot{w}_t/A_c \quad (10)$$

so that by using the definition of vapor quality

$$\chi = \dot{w}_g/\dot{w}_T \quad (11)$$

the liquid phase mass flux,  $G_r$ , and the vapor phase mass flux,  $G_g$ , can be defined as

$$G_g = \chi G_T \quad (12)$$

$$G_r = (1 - \chi) G_T \quad (13)$$

Now, using the heat exchanger core friction data from figure III-10, the single-phase local pressure gradients can be determined from

$$dP/dL)_r = 1/2 g_c P_r G_r^2 f/r_h \quad (14)$$

$$dP/dL)_g = 1/2 g_c P_g G_g^2 f/r_h \quad (15)$$

The Lockhart-Martinelli correlating parameter,  $X$ , is defined as follows

$$X^2 = (dP/dL)_r / (dP/dL)_g \quad (16)$$

The resulting two-phase local pressure gradients, shown in figure III-16, were then calculated from

$$dP/dX)_{TPF} = \phi^2_{XX} (dp/dL)_r \quad (17)$$

where

$\phi_{XX}$  is a unique function of  $X$ . (See Reference 12.)

Oxygen momentum pressure losses can be determined also from a separated flow model. (See Reference 7.)

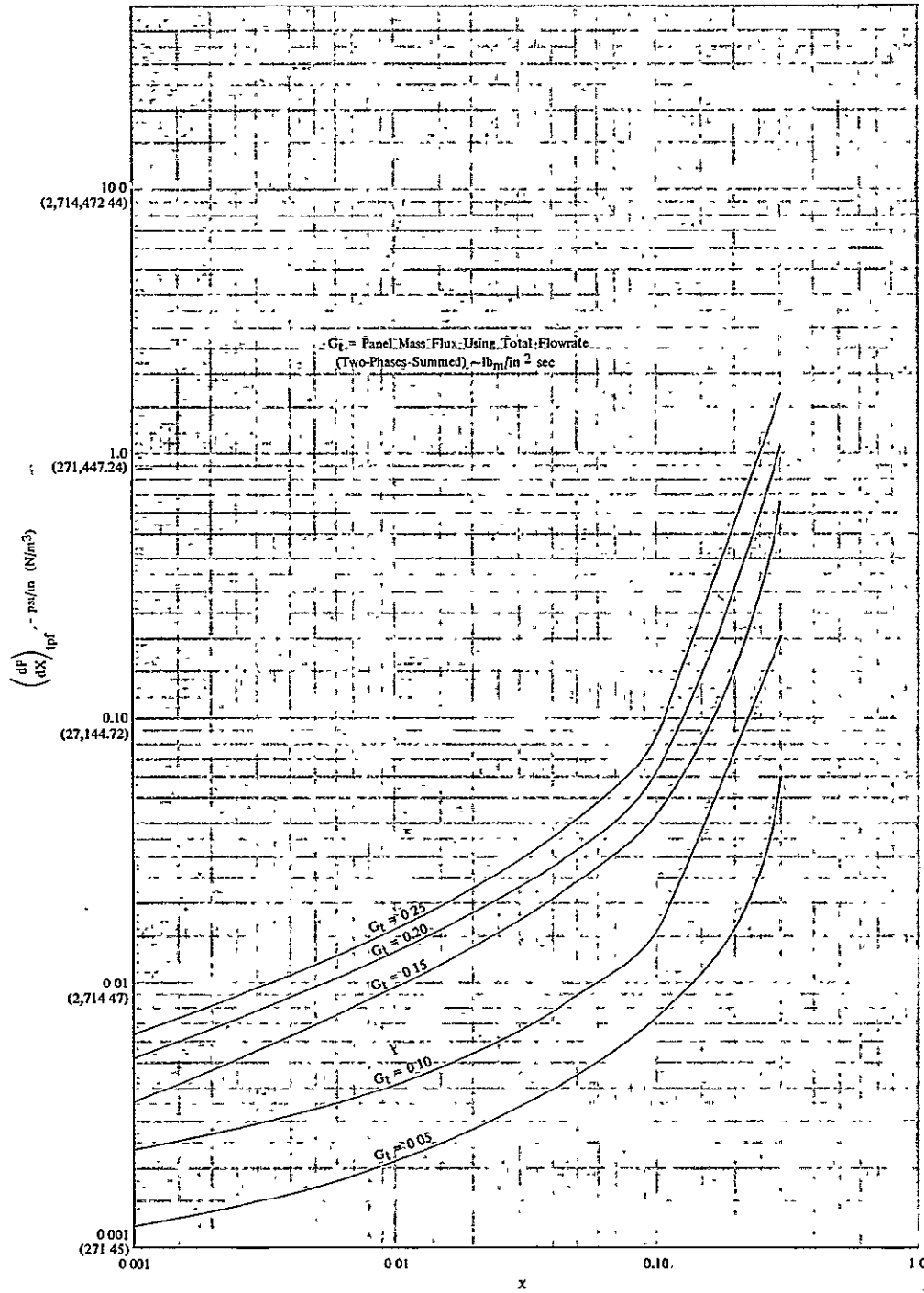
$$\Delta P_m = \gamma G_T^2 / P_{fgc} \text{ momentum } \Delta P \text{ from } \chi=0 \text{ to } \chi \quad (18)$$

where

$$\gamma = (1 - \chi)^2 / (1 - a)^2 + \chi^2 / a^2 (P_r / P_g)_{sat}^{-1} \quad (19)$$

and  $a = a(\chi)$  from Reference 12.

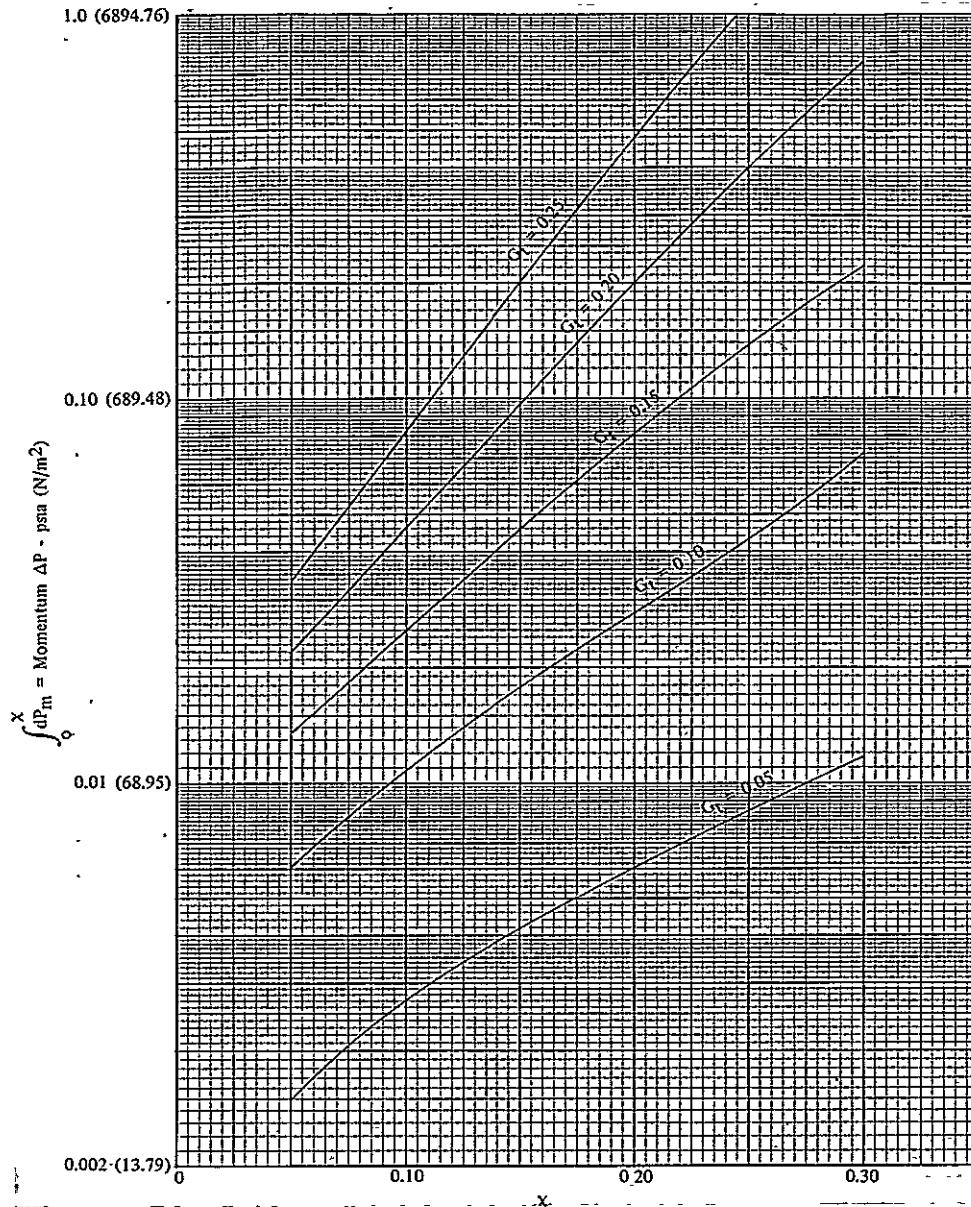
Calculated oxygen momentum pressure losses are presented in figure III-17.



DF 101980

Figure III-16. Two-Phase Frictional Pressure Gradients for Atmospheric Boiling Oxygen Flowing Through Heat Exchanger Plates (Martinelli-Lockhart Separated Flow Model)





DF 101981

Figure III-17. Two-Phase Momentum  $\Delta P$  Atmospheric Boiling Oxygen Flowing Through Heat Exchanger Panels (Martinelli-Lockhart Separated Flow Model, Reference 12)

**c. Stability Analysis**

To achieve the design of a compact heat exchanger, the hydrogen and oxygen plate-fin panel dimensions were selected to maximize the heat transfer rate between the warm and cold fluids consistent with the cycle  $\Delta P$  constraints. This involves iterations using the parametric results of the fluid and thermal analyses, previously discussed. The oxygen boiling stability criteria of Reference 5, however, indicates that a unique relationship exists between the heat transfer rate ( $Q/A$ ) and the oxygen mass flux ( $G_T$ ) for the inception of pressure oscillations (boiling instabilities). While the prime objective of the breadboard heat exchanger program is to confirm (or alter, if required) this stability criteria, it is desirable to use this criteria to predict regions of unstable operation in the breadboard heat exchanger prior to testing.

The stability criteria of Reference 5 relates the inception of pressure oscillations in the heat exchanger to the specific volume characteristics of the fluid being heated and the heat transfer characteristics of the heat exchanger. The specific volume characteristics are described by a specific volume number.

$$N_{sv} = V_{fg}/V \quad (20)$$

where

$V_{fg}$  is the specific volume change from liquid to vapor

$V$  is the specific volume of fluid (two-phase)

The heat exchanger characteristics are described by a boiling number

$$N_{BO} = (Q/A)/\lambda G_T \quad (21)$$

where

$Q/A$  is the local heat flux

$G_T$  is the local fluid mass flux

$\lambda$  is the heat of vaporization

For a given specific volume number, there is a minimum boiling number above which pressure oscillations occur, given by

$$N_{BO} = 0.005/N_{sv} \quad (22)$$

Figure III-18 presents predicted critical heat fluxes for oxygen boiling stability as functions of oxygen mass flux ( $W/A$ ) and quality ( $\chi$ ). Note the rapid increase in critical heat flux with oxygen quality at constant mass flux. The maximum possible heat transfer rates for the breadboard heat exchanger (no insulation) are estimated to be approximately 1.4 Btu/ft<sup>2</sup>sec (15,888.5 w/m<sup>2</sup>). This implies that no insulation (to limit heat fluxes to less than critical values) will be required in regions where the oxygen quality is greater than 15%.

#### 4. Thermal Test Data Analysis and Instrumentation Requirements

This section presents the instrumentation requirements for the heat exchanger and shows the mathematical formulations used to reduce the measured parameters into heat transfer terms.

Instrumentation requirements for the fluid supply and discharge lines, illustrated in figure III-19, are intended to establish overall heat exchanger performance parameters,  $\Delta T$ 's,  $\Delta P$ 's, and flowrates. Oxygen temperature and pressure are required immediately upstream of the quality meters, since the quality meters actually measure fluid density (which is related to quality by temperature and pressure).

Figure III-20 presents requirements for the center hydrogen panel and figure III-21 presents requirements for *one* outer hydrogen panel. The skin thermocouples in the heat transfer zone (referenced 10 in. by 20 in. [0.254 m by 0.508 m] area) must be located opposite corresponding oxygen panel thermocouples shown in figure III-22. Hydrogen fluid temperature measurements (skin thermocouples outside the heat transfer zone) are intended to define the nature of hydrogen

fluid temperature stratification within the heat exchanger core. Since the outer hydrogen panels transfer heat through one side only, fluid discharge temperatures should be higher than those of the center panel

Static pressure measurements within the oxygen panel manifolds are intended to define the oxygen panel core  $\Delta P$  as well as to indicate flowpath in the supply manifold. The lone skin thermocouple located on the oxygen supply manifold will be used to estimate heat transfer rates to the oxygen due to manifold chilldown.

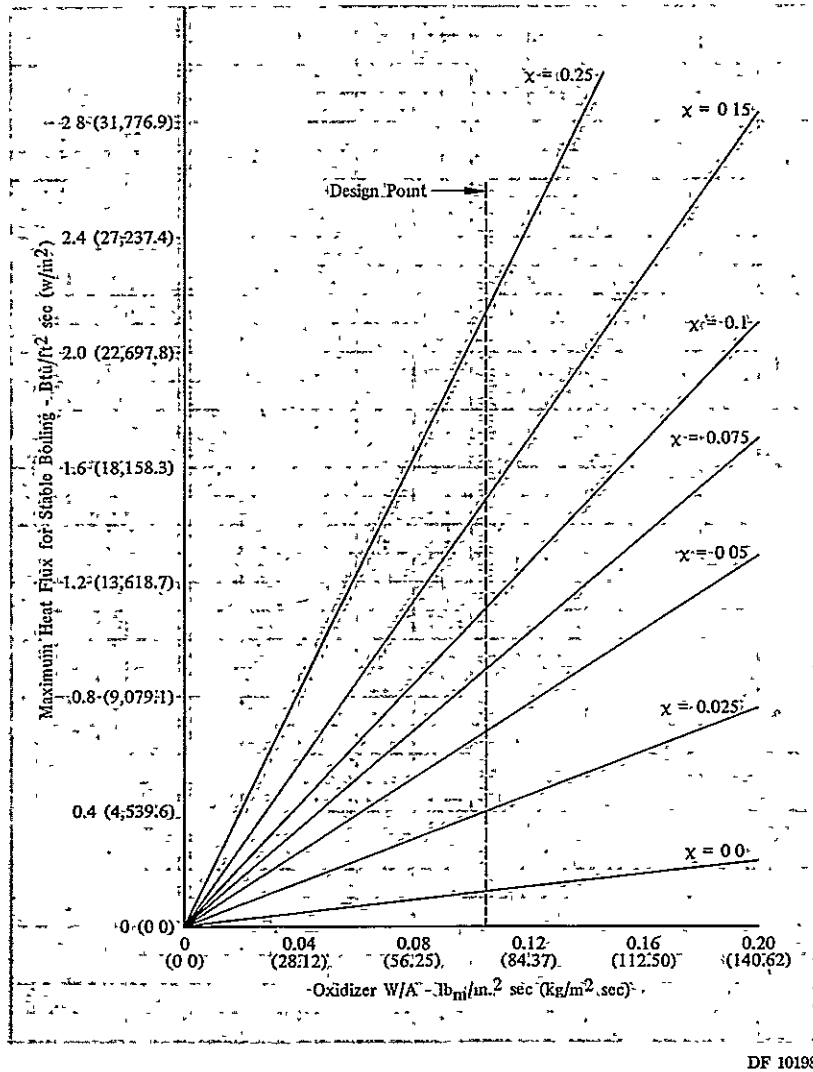
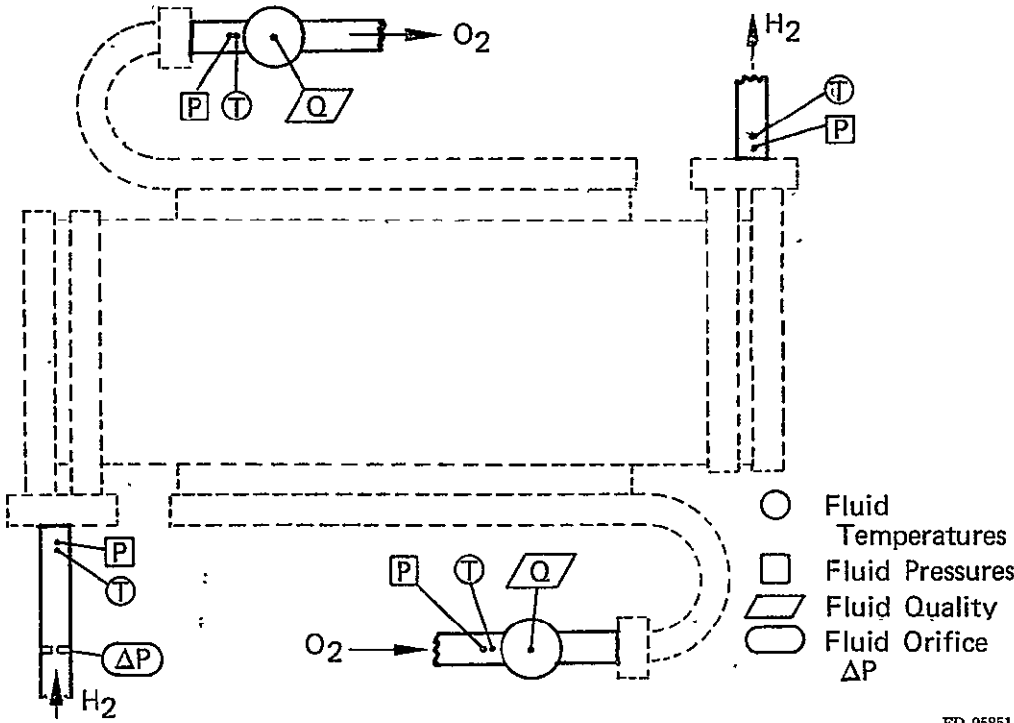
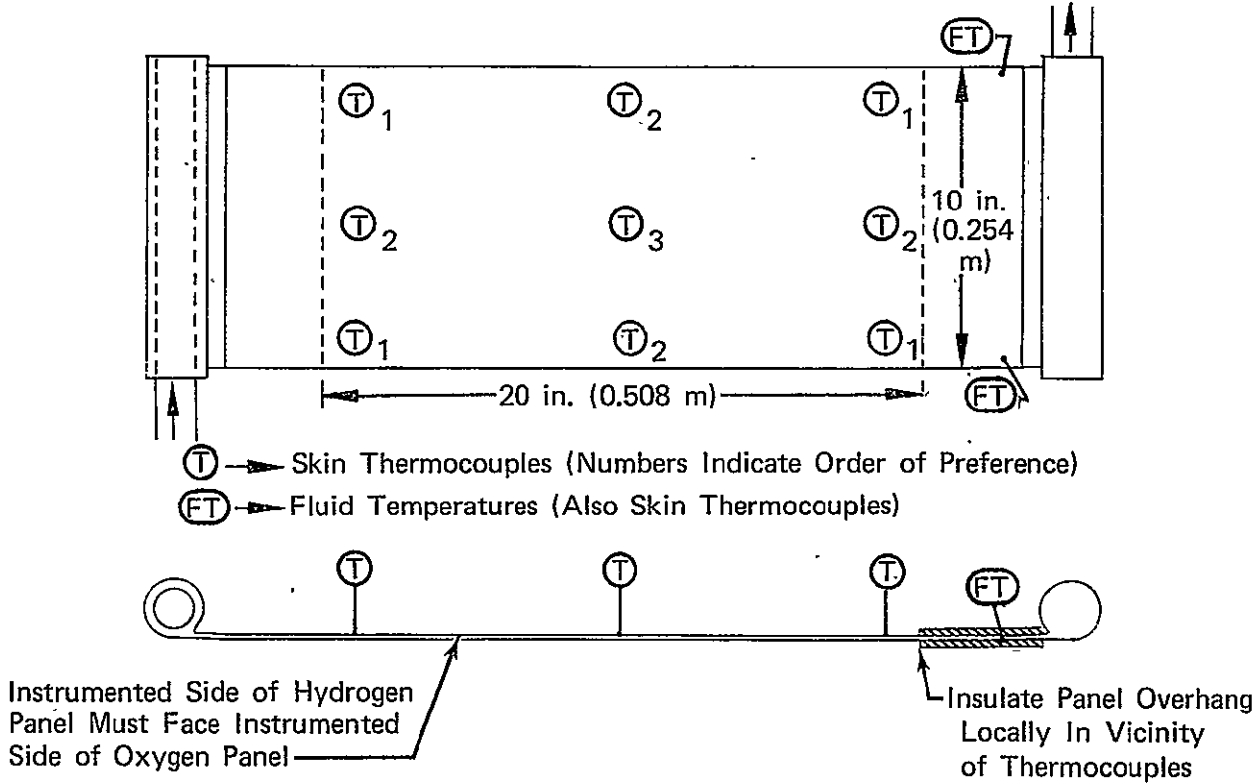


Figure III-18. Critical Heat Flux for Stable Boiling of Oxygen at 1 atm (51.01 N/m²)



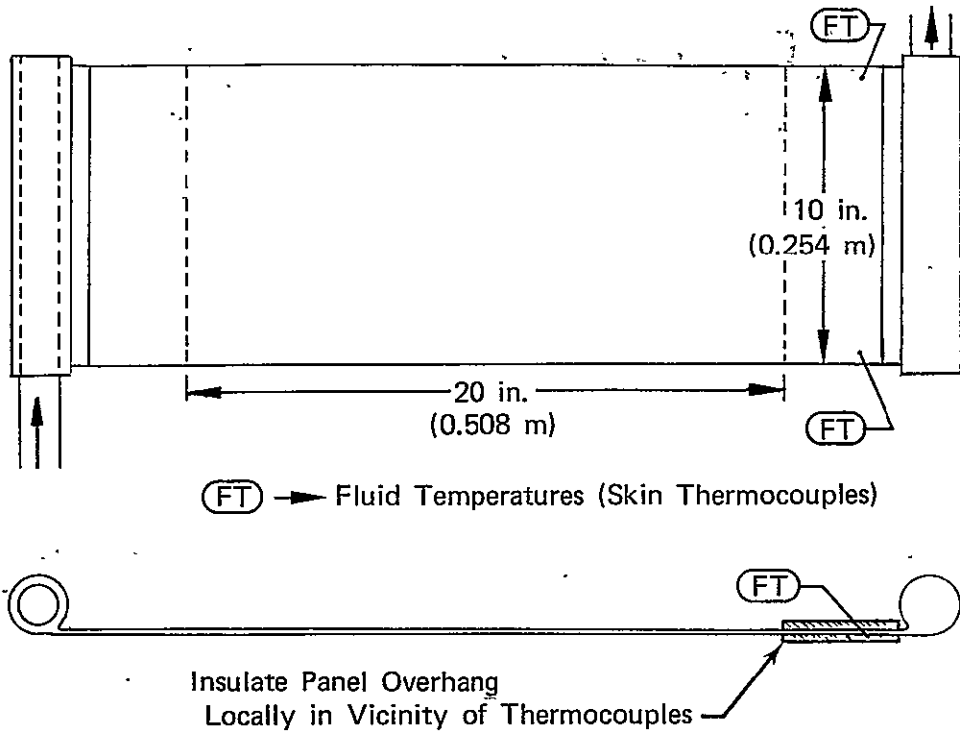
FD 95851

Figure III-19. Instrumentation Requirements for Fluid Supply/Discharge Lines



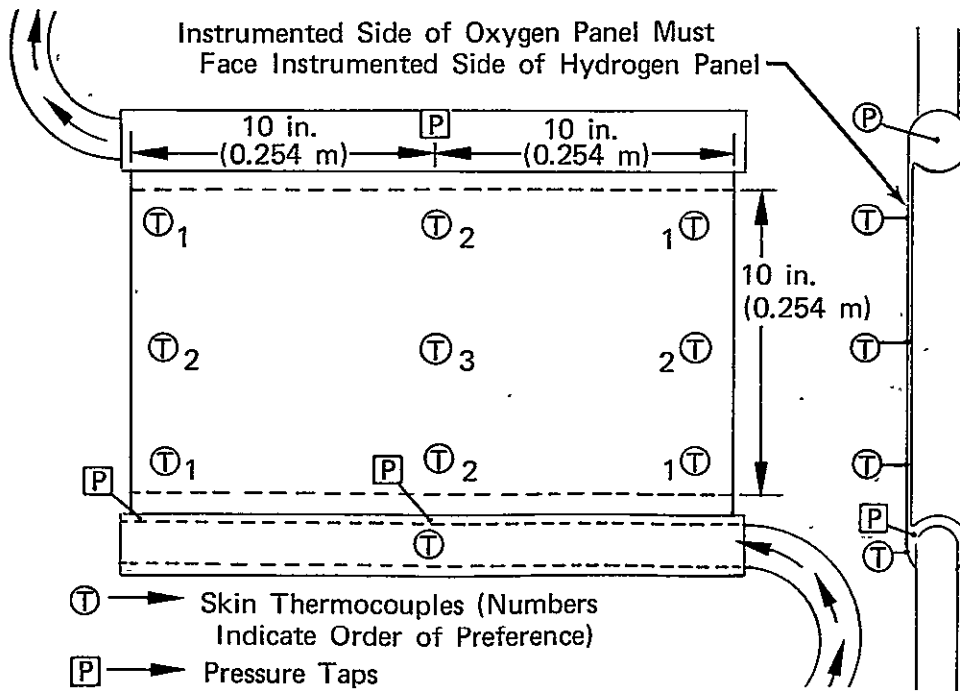
FD 95852

Figure III-20. Instrumentation Requirements for Center Hydrogen Panel



FD 95853

Figure III-21. Instrumentation Requirements for One Outer Hydrogen Panel



FD 95854

Figure III-22. Instrumentation Requirements for One Oxygen Panel (No Requirements for Other Panel)

Measured parameters include the following:

Parameter	Hydrogen-Side	Oxygen-Side
w, flowrate	X	X
T <sub>IN</sub> , inlet fluid temperature	X	X
T <sub>EX</sub> , exit fluid temperature	X	X
X <sub>IN</sub> , inlet fluid quality		X
X <sub>EX</sub> , exit fluid quality		X
P <sub>IN</sub> , inlet fluid pressure	X	X
P <sub>EX</sub> , exit fluid pressure	X	X
T <sub>WH</sub> 's, hydrogen plate temperatures (9)	X	
T <sub>WC</sub> 's, oxygen plate temperatures (9)		X

Total heat transferred -

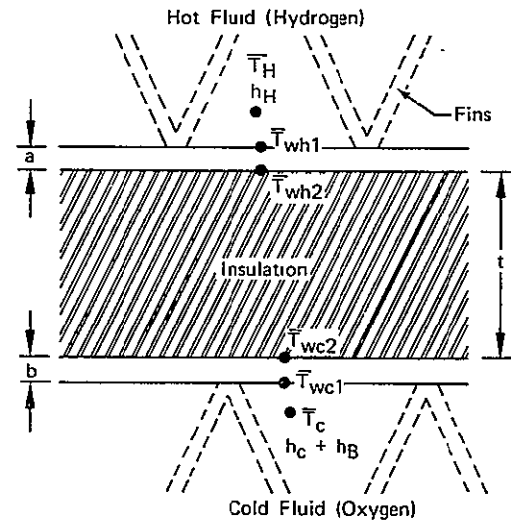
$$Q_T = \dot{w}_{H_2} C_{p_{H_2}} (T_{EX} - T_{IN}) H_2 = \dot{w}_{O_2} \lambda (X_{EX} - X_{IN}) O_2 \quad (23)$$

Average heat flux -

$$(Q/A) = Q_T / A_{HT}$$

One-dimensional heat balance -

$$\begin{aligned} (Q/A) &= U(T_H - T_C) \\ &= \eta_{OH} h_H (T_H - T_{WH1}) \\ &= (k_a/a)(A_w/A_H)(T_{WH1} - T_{WH2}) \\ &= (k/t)_I (A_w/A_H)(T_{WH2} - T_{WC2}) \\ &= (k_b/b)(A_w/A_H)(T_{WC2} - T_{WC1}) \\ &= \eta_{OC}(h_C + h_B)(T_{WC1} - T_C) \end{aligned}$$



Now, for all practical purposes

$$T_{WH1} = T_{WH2} = T_{WH}$$

$$T_{WC1} = T_{WC2} = T_{WC}$$

therefore,

$$\begin{aligned} (Q/A) &= U(T_H - T_C) = \eta_{OH} h_H (T_H - T_{WH}) \\ &= (A_w/A_H)(k/t)_I (T_{WH} - T_{WC}) \\ &= \eta_{OC}(h_C + h_B)(T_{WC} - T_C) \end{aligned}$$

Since, temperature gradient across cover plates is very small

where  $A_w/A_H$  is known geometric parameter

$$T_C = T_{\text{sat LOX}} \text{ for } X_{\text{EX}} \leq 1$$

$$T_H = (T_{\text{IN}} + T_{\text{EX}})_{\text{H}_2} / 2$$

$T_{\text{WH}}$  is average hydrogen plate temperature (from thermocouple readings)

$T_{\text{WO}}$  is average oxygen plate temperature (from thermocouple readings)

Insulation effective conductance -

$$(k/t)_I = (Q/A) / (A_w/A_H) (T_{\text{WH}} - T_{\text{WC}})$$

$T_{\text{WO}}$  is average oxygen plate temperature (from thermocouple readings)

Insulation effective conductance

$$(k/t)_I = (Q/A) / (A_w/A_H) (T_{\text{WH}} - T_{\text{WC}}) \quad (26)$$

Oxygen effective heat transfer coefficient

$$\eta_{\text{OC}}(h_B + h_C) = (Q/A) T_{\text{WC}} - T_C \quad (27)$$

Hydrogen effective heat transfer coefficient

$$\eta_{\text{OH}} h_H = (Q/A) / (T_H - T_{\text{WH}}) \quad (28)$$

Overall heat transfer coefficient

$$U = (Q/A) T_H - T_C \quad (29)$$

Overall heat exchanger effectiveness

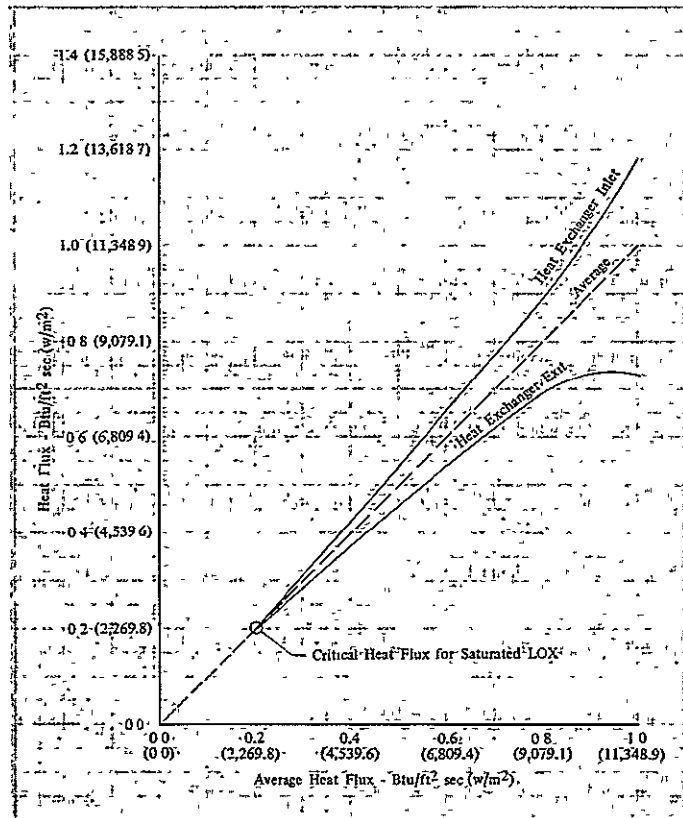
$$E = (T_{\text{EX}} - T_{\text{IN}})_{\text{H}_2} / (T_{\text{IN}})_{\text{H}_2} - (T_{\text{IN}})_{\text{O}_2} \quad (30)$$

Heat exchanger effective size ( $N_{\text{TU}}$ )

$$N_{\text{TU}} = UA_{\text{HT}} / \dot{w}_{\text{H}_2} C_{p_{\text{H}_2}} \quad (31)$$

$$\epsilon = e^{-N_{\text{TU}}} \quad (32)$$

These one-dimensional heat transfer formulations are predicated on the assumption that the heat flux is constant at all locations in the heat exchanger. Figure III-23 shows that this is a good assumption for moderate (0.5 Btu/ft<sup>2</sup>[5674.47 N/m<sup>2</sup>]) to low heat flux levels. At high heat fluxes, there is a considerable difference in local heat flux from the heat exchanger inlet to exit. This is caused by variations in fluid temperatures and film coefficients in the coolant passages. Significant departures from the constant heat flux case would be evidenced by variations in measured hot and cold plate temperatures.



DF 101976

Figure III-23. Breadboard Heat Exchanger Heat Flux Variation for Constant Conductance Insulation Configuration

## B. MECHANICAL AND STRUCTURAL DESIGN

The heat exchanger design was based on preliminary drawing L-230273, and this design was closely adhered to. The design is of a plate-type cross-flow heat exchanger of variable configuration with provision for incorporating insulation of different thickness between the heat exchanger plates.

The oxygen heat exchanger is composed of five panels, two oxygen panels surrounded by three hydrogen panels. Each panel is a corrugated type of construction that uses 0.005-in. (0.000127-m) thick copper sheet with approximately 20 corrugations to the inch, encased by outer sheets of 0.010-in. (0.000254-m) thick SS 347. The overall panel thickness is 0.120 in. (0.00305 m). Oxygen and hydrogen flow through their respective individual panels, which transfers heat from the hydrogen panels to the oxygen panels. The amount of heat that is transferred from panel to panel can be controlled by inserting insulation material between the panels. The heat exchanger has the capability of varying the distance between panels by loosening all the tube coupling nuts and then rotating the manifold in the direction indicated in drawing L-230991, and retightening the nuts.

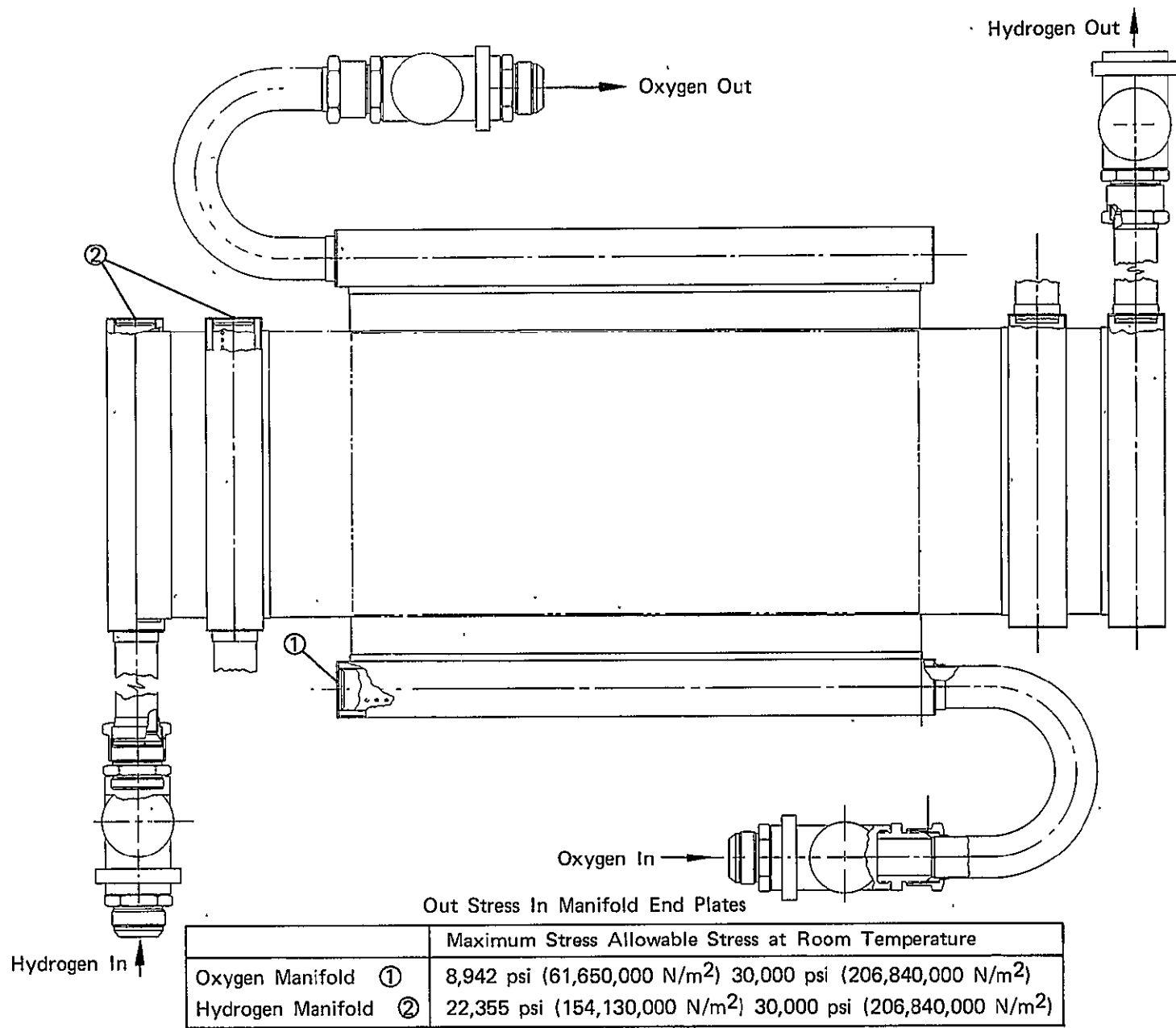
Maximum inlet pressures at the oxygen and hydrogen manifolds are 30 psi (206,843 N/m<sup>2</sup>) and 50 psi (344,738 N/m<sup>2</sup>), respectively. The approximate operating pressures at these points are 15 psi (103,421 N/m<sup>2</sup>) and 35 psi (241,317 N/m<sup>2</sup>).



The thermocouple instrumentation was installed with the using ribbon thermocouple wire. Thermocouples were placed on the oxygen and hydrogen panels at locations determined during the thermal analysis of the heat exchanger.

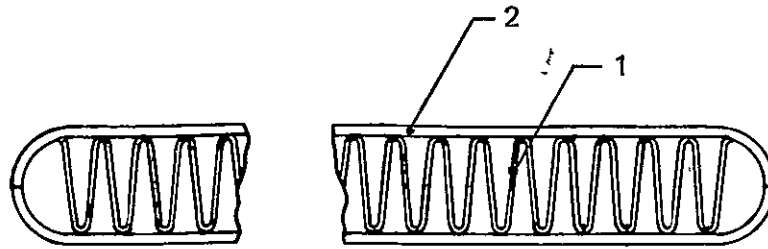
The following figures provide calculated stresses and safety factors for critical areas of the heat exchanger. Stresses were based on test operating pressures (oxygen = 30 psi [206,843 N/m<sup>2</sup>]; hydrogen = 50 psi [344,738 N/m<sup>2</sup>]).

1. Figure III-24 provides stresses in the manifold end caps. Note that the hydrogen manifold end cap is the area having the largest stresses on the heat exchanger.
2. Figure III-25 summarizes the stresses in the corrugated heat exchanger panels. Stresses shown are for the hydrogen panel only, which is higher stressed than the oxygen panel.
3. Figure III-26 provides the stresses in the outer manifold and panel /manifold adapter. The stress at point (1) shows the stress at three localized ribs. These ribs help maintain the structural integrity of a pressurized tube, while having a slot cut lengthwise along the tube.
4. Figure III-27 summarizes the stresses of the oxygen inner manifold tube. The stress shown was calculated between the 0.125-in. (0.00318-m) diameter holes, with a stress concentration factor of 3.0 included.
5. Figure III-28 summarizes the stresses of the hydrogen inner manifold tube. The stress shown was calculated between the 0.125-in. (0.00318-m) diameter holes, with a stress concentration factor of 3.0 included.



FD 95856

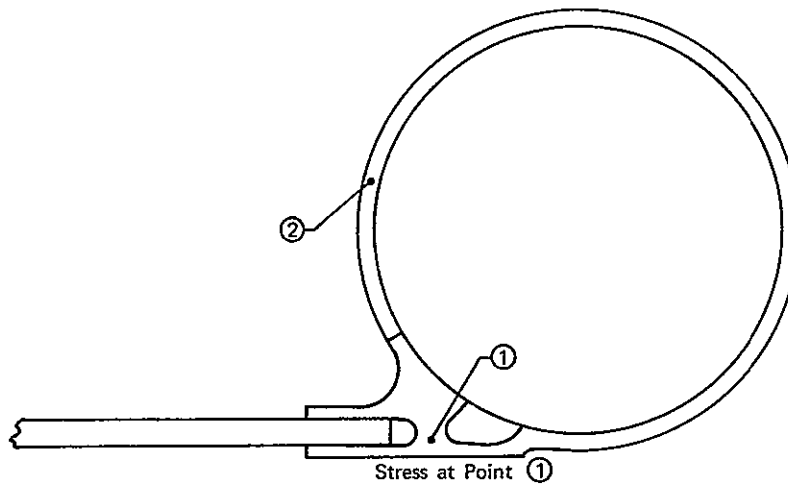
Figure III-24. Manifold End Cap Stresses



\*Stress in Copper Fins (Point ① ) Is 240 psi (1,655,000 N/m<sup>2</sup>)  
 Allowable Stress at Room Temperature = 30,000 psi (206,840,000 N/m<sup>2</sup>)  
 \*Maximum Stress in Outer Sheet (Point ② ) = 80 psi (55,158,000 N/m<sup>2</sup>)  
 Allowable Stress at Room Temperature = 30,000 psi (206,840,000 N/m<sup>2</sup>)

FD 95857

Figure III-25. Typical Heat Exchanger Panel



Stress at Point ①

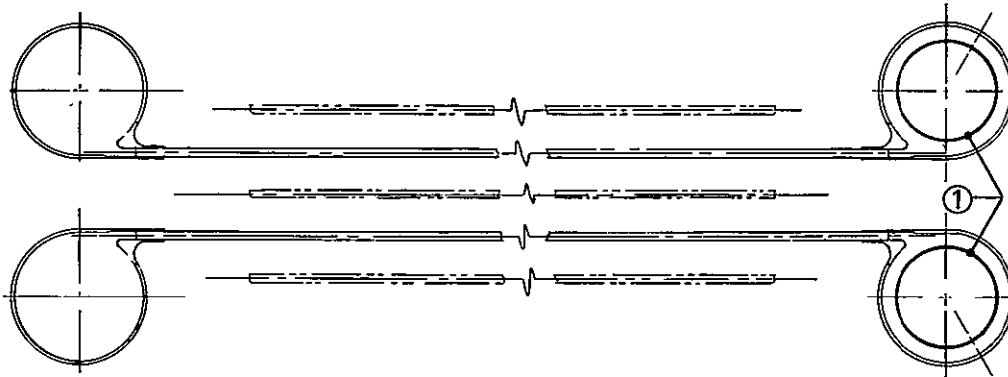
	Maximum Stress	Allowable Stress at Room Temperature
Hydrogen Manifold	18,568 psi (128,020,000 N/m <sup>2</sup> )	30,000 psi (206,840,000 N/m <sup>2</sup> )
Oxygen Manifold	18,550 psi (127,900,000 N/m <sup>2</sup> )	30,000 psi (206,840,000 N/m <sup>2</sup> )

Stress at Point ②

	Maximum Stress	Allowable Stress at Room Temperature
Hydrogen Manifold	1,055 psi (7,270,000 N/m <sup>2</sup> )	30,000 psi (206,840,000 N/m <sup>2</sup> )
Oxygen Manifold	422 psi (2,910,000 N/m <sup>2</sup> )	30,000 psi (206,840,000 N/m <sup>2</sup> )

FD 95858

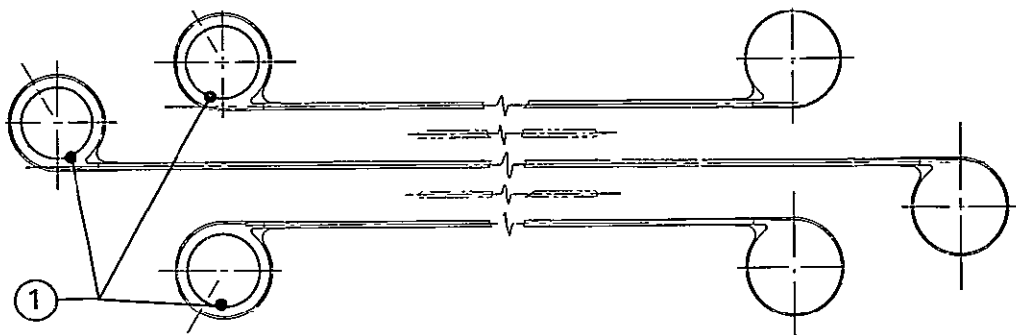
Figure III-26. Typical Manifold Cross Section



Maximum Stress at Point ① = 2,315 psi (15,960,000 N/m<sup>2</sup>)  
Allowable Stress at Room Temperature = 30,000 psi (206,840,000 N/m<sup>2</sup>)

FD 95859

Figure III-27. Oxygen Panel and Manifold



Maximum Stress at Point ① = 7,137 psi (49,210,000 N/m<sup>2</sup>)  
Allowable Stress at Room Temperature =  
30,000 psi (206,840,000 N/m<sup>2</sup>)

FD 95860

Figure III-28. Hydrogen Panel and Manifolds

## SECTION IV FABRICATION

### A. BASIC FABRICATION

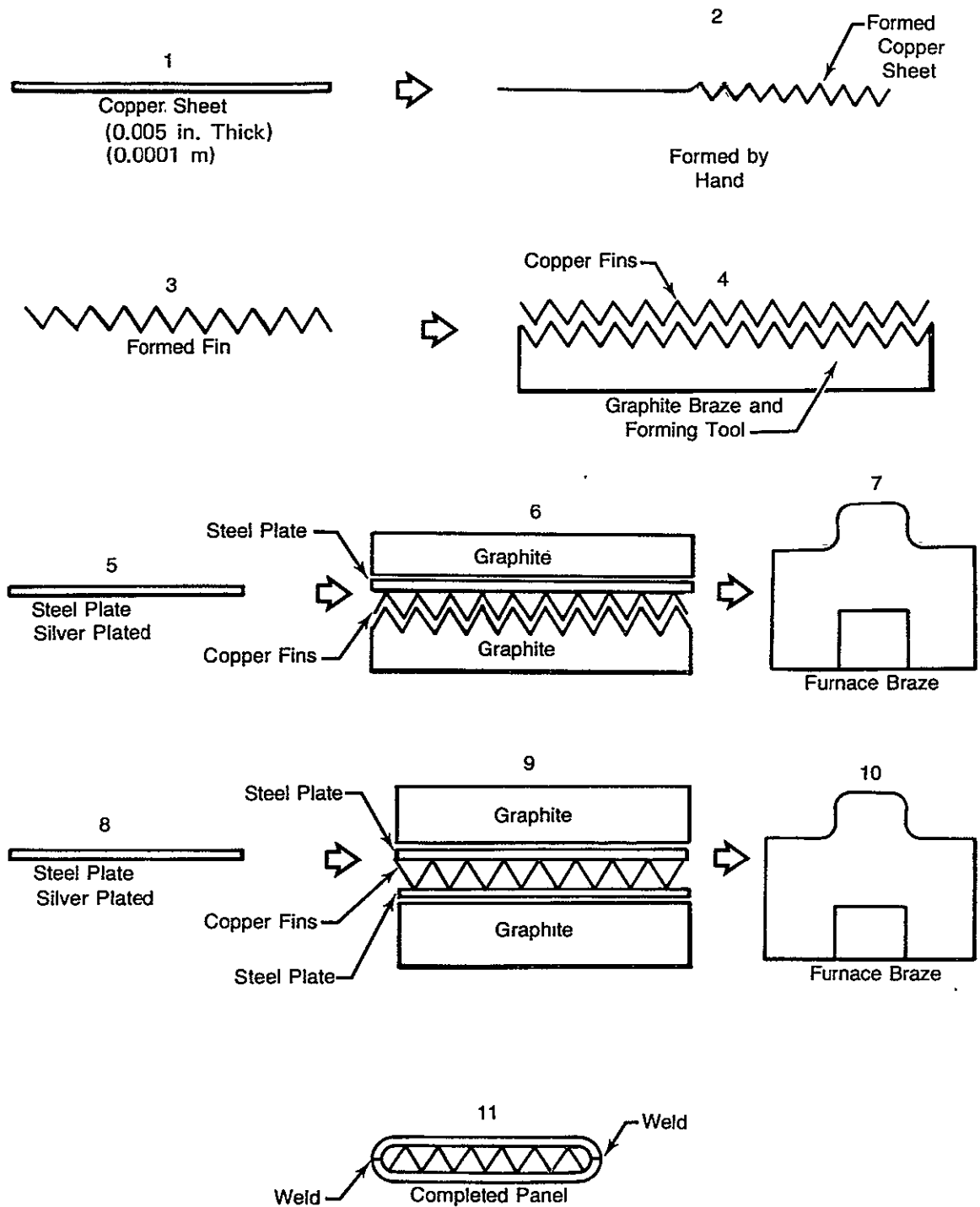
The breadboard heat exchanger was fabricated from drawing T-2177267 by the Saffran Engineering Company, 20225 East Nine Mile Road, St. Clair Shores, Michigan. The copper fin panels were fabricated using an 11-step method, as shown in figure IV-1. The first step was to form the copper sheet by hand (figure IV-1, steps 1 and 2) to provide the basic extended shape (figures IV-2 and IV-3). The formed fins were then form-gathered to an overcompressed form, and the overcompressed copper fin forms were extended to fit into slots in a graphite forming and braze holding fixture, as shown in figure IV-1, steps 3 and 4. This compressed copper fin form and one silver and copper-plated stainless steel side panel were assembled into a graphite holding fixture. The assembly was then furnace brazed at a temperature of 1550°F (1115°K) using the silver and copper plating as the braze filler. The sequence 4 operation is shown in figure IV-1, steps 5, 6 and 7. The other silver and copper-plated steel side panel was then furnace brazed at 1550°F (1115°K) to the copper fins using another graphite holding fixture. This sequence of operations is shown in figure IV-1, steps 8, 9, and 10. The brazed panel end closure operation was then completed by a welding operation using AMS 5786 weld rod and conventional welding methods, as shown in step 11. The tubular manifolds and other detail parts that made up the remainder of the heat exchanger assembly were constructed using conventional rolling and forming shop fabrication methods. (A fabricated panel assembly is shown in figure IV-4.)

The fabrication of the breadboard heat exchanger was completed by Saffran Engineering in accordance with drawing T-2177267 and the assembly received at FRDC on 1 November 1975. The fabricated breadboard heat exchanger rig assembly is shown in figure IV-5.

### B. ASSEMBLY

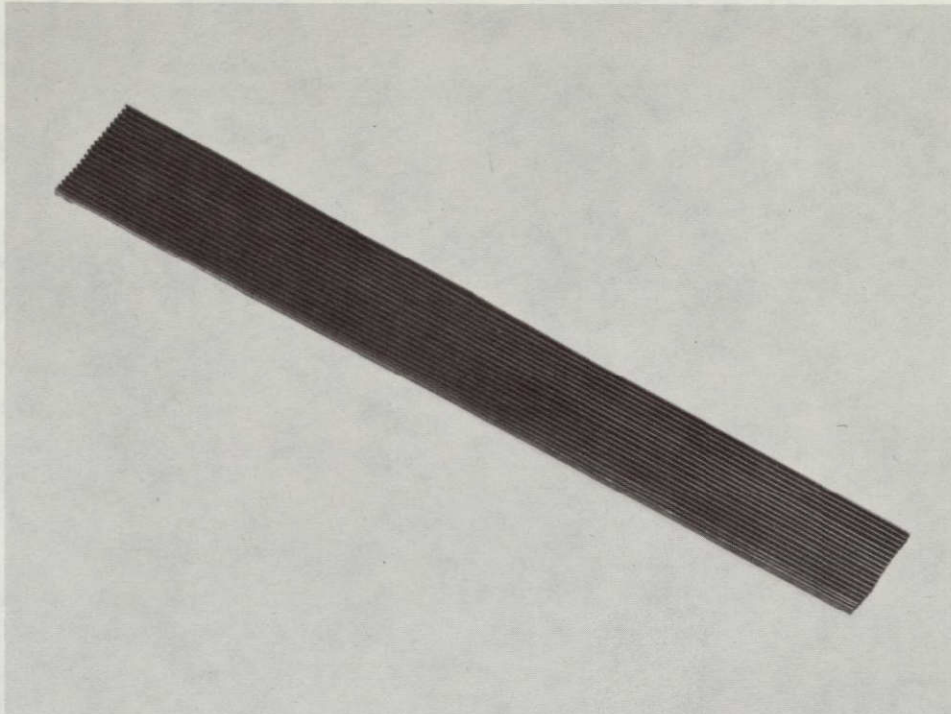
Upon receipt from the vendor, the heat exchanger assembly was disassembled so that the oxygen panels and fuel panels could be cleaned. The fabricated panels were flushed with trichlorethylene under pressure to remove any residue or non-oxygen-compatible material from the panel flow passages. Some leaks were discovered in the panel to manifold joints during this operation. Attempts were made on the oxygen panels to hand braze repair the leaks, but these attempts were not successful in that they caused some panel warpage. Due to the fact that these were only pin hole leaks and the rig would only be subjected to a low pressure, it was decided to make the leak repairs using Dow-Corning 92-024 (PWA 617) RTV rubber. Twelve leaks were repaired in the two oxygen panels and four leaks were repaired in the three fuel panels using this method.

The breadboard heat exchanger rig was then assembled, pressure-tested satisfactorily, and delivered to the P&WA FRDC E-6 test stand.



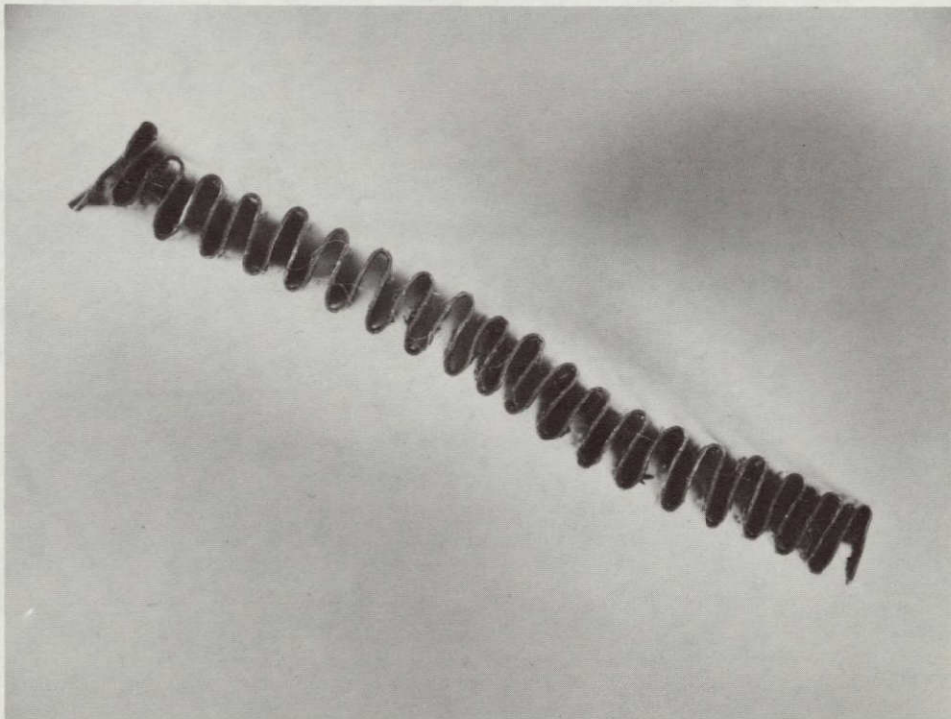
FD 92602A

Figure IV-1. Fabrication Flow Chart



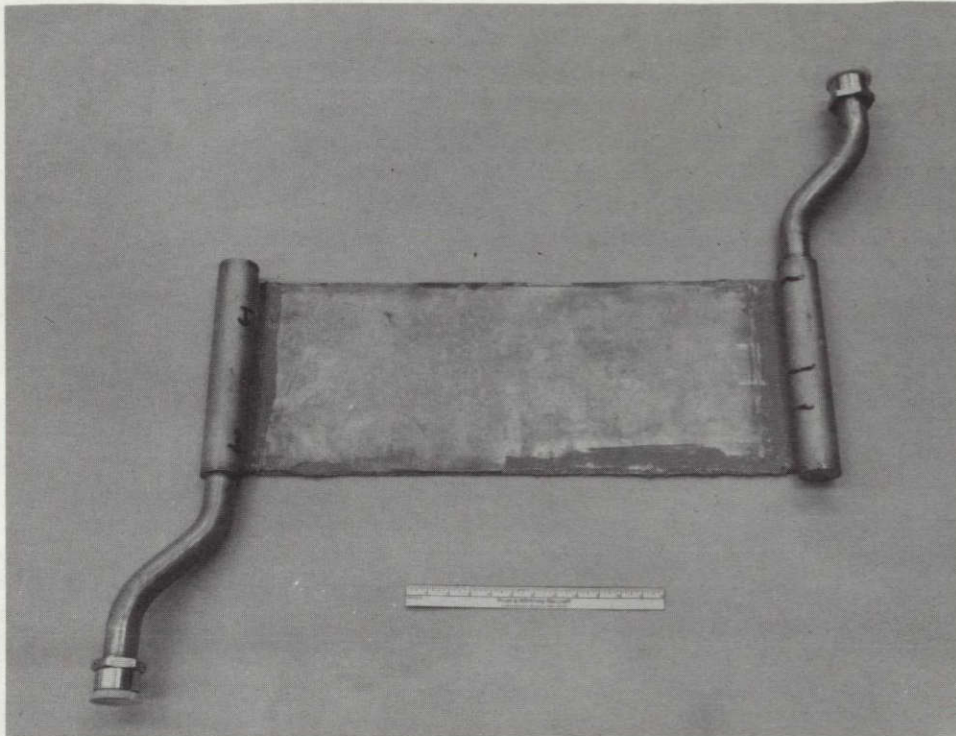
FE 147287

Figure IV-2. Hand-Formed Copper Sheet - Basic Extended Shape ( $\frac{3}{4}$  Plan View)



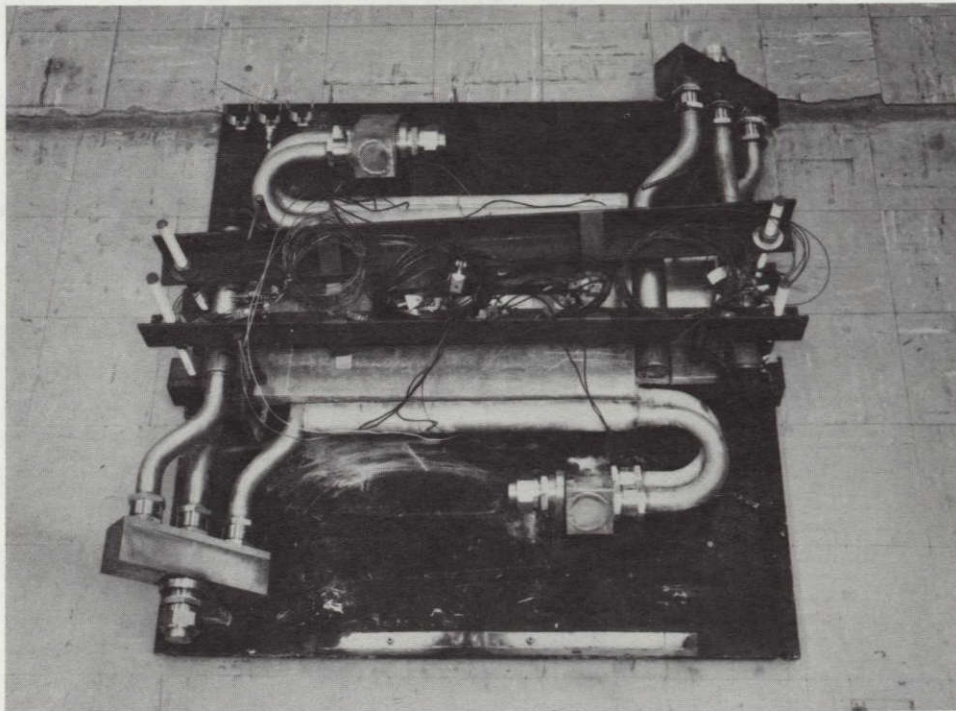
FE 147288

Figure IV-3. Hand-Formed Copper Sheet - Basic Extended Shape (End View)



FE 339225

*Figure IV-4. Fabricated Hydrogen Panel Assembly*



FE 339269

*Figure IV-5. Breadboard Heat Exchanger Rig Assembly*



The work accomplished at FRDC to prepare the breadboard heat exchanger rig and engine for testing is listed below in chronological order:

- 8 October 1975 - Opened work orders for breadboard heat exchanger rig (F33029) and engine P641915.
- 28 October 1975 - Started engine preparations for tests.
- 3 November 1975 - Engine delivered to test for mount and hydrogen side plumbing checkout.
- 3 November 1975 - Received breadboard heat exchanger rig F33029 at Rocket Assembly.
- 5 November 1975 - Disassembled rig. Sent mounting plate and collectors to E-6 stand for mockup. Started backflush cleaning operations on panels.
- 6 November 1975 - The rig mounting plate was installed in E-6 stand. Started oxygen side plumbing mockup.
- 7 November 1975 - Found leak on upper oxygen panel during backflush cleaning and sent panel to shop for braze repair.
- 11 November 1975 - Oxygen side plumbing was completed and sent to the rocket shop for installation of instrumentation bosses. The rig mounting plate was returned to assembly to obtain measurements for restraining plates.
- 12 November 1975 - Sent upper oxygen panel back to shop for second attempt at low-temperature silver braze repair. (Came back from first attempt with two leaks.) Second attempt opened up six leaks.
- 13 November 1975 - Attempted running continuous pass braze repair on upper oxygen panel. Leaks were sealed, but excessive warpage resulted. Made an attempt at hand braze repair by using decreased heat and argon backup. Local warpage of panel sheet became too severe to continue.
- 17 November 1975 - Built rig with aluminum backup plates for pressure test and cold shock. Pressure test showed leaks on upper oxygen panel and leaks at VOI-shan and Natorque plumbing seals.
- 18 November 1975 - Cold shocked rig with leaks. Flowed LN<sub>2</sub> through rig at 5 psig (34,474 N/m<sup>2</sup>) gauge for 5 min on both hydrogen and oxygen sides. Rig brought back to ambient between flows.
- 19 November 1975 - Disassembled rig and pressure-tested panels at 50-psig (344,738 N/m<sup>2</sup>) gauge fuel side and 30-psig (206,843 N/m<sup>2</sup>) gauge oxygen side. Oxygen panels had 12 leaks; fuel panels had 4 leaks. Leaks occurred at both braze and weld joints.
- 21 November 1975 - Panels were sealed with Dow-Corning 92-024, PWA 617, RTV. Natorque seals (AN adapter to collector manifold) were sealed with "T"-film and 150 ft-lb torque (204 j). Panel "B" nuts and the AN sides of the adapters were lubricated with PWA 585 lubricant. VOI-shans (Panel "B" nuts to AN side of adapters) sealed with 150 ft-lb torque (204 j). Rig assembly was completed.
- 24 November 1975 - Successful pressure tests and GN<sub>2</sub> purge were completed. Rig was delivered to test.

## SECTION V FACILITIES

### A. GENERAL

The breadboard heat exchanger was tested in the altitude chamber of P&WA FRDC E-6 stand. The heat exchanger was mounted in the altitude chamber and plumbed in-line between the oxidizer pump and injector on RL10 engine P641915.

### B. FACILITIES DESIGN

A schematic of the heat exchanger installation is shown on figure V-1. The design objective was to use as much of the existing E-6 stand equipment and piping as possible, so only minor stand modifications were required for testing the oxygen heat exchanger (HEX). An RL10 engine was mounted in the stand to allow maximum utilization of existing tanks, valves, and piping and to simulate engine conditions. The engine was mounted 6 in. (0.15 m) lower than normal to permit the insertion of a low-range flowmeter and cooldown piping between the facility LOX supply line and the engine LOX inlet valve. The HEX was mounted beside the engine and piped in-line between the oxidizer pump and the injector inlet. To facilitate the plumbing changes, the engine oxidizer flow control valve, which is located immediately downstream of the pump, was left in the system but its internal parts removed to eliminate it as a flow restriction.  $\text{GH}_2$  was supplied to the HEX from an existing stand source and was discharged to the facility vent and burnoff stack. All piping, tubing, fittings, valves, and other equipment were class 300 stainless steel, except for a bronze hydrogen relief valve. Stainless steel flex hose was used as the most economical choice for flexible connections between the test stand piping and rig.

#### 1. LOX System

The existing LOX tank was used to supply LOX to the rig. Some NPSH adjustment was obtained by varying the liquid level in the tank.

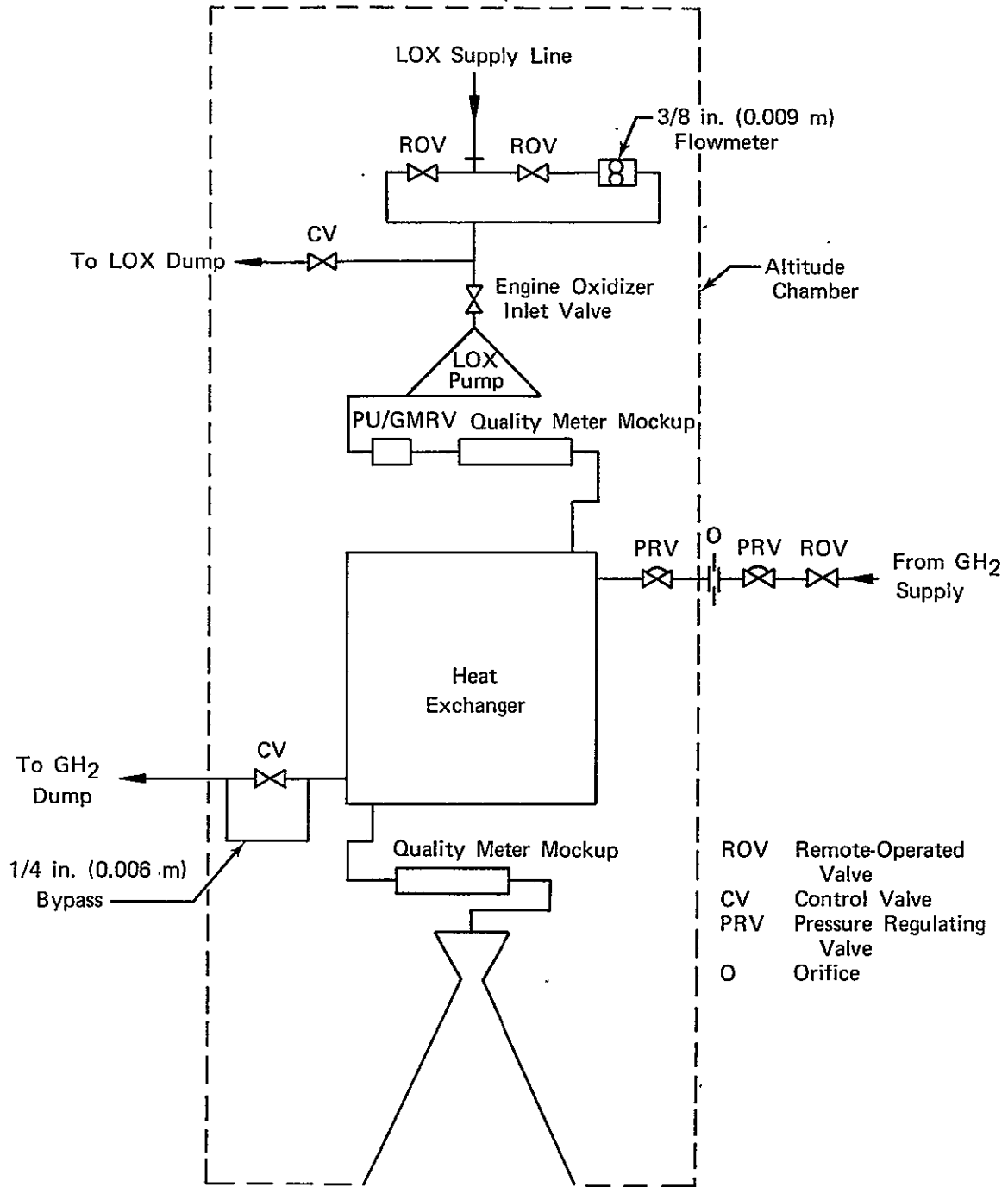
Cooldown of the small plumbing and the flowmeter in the LOX line was critical as the 0.375-in. (0.009-m) flowmeter could be damaged by LOX boiloff. (This meter was damaged during checkout tests.) A larger bypass line around the flowmeter was provided to assist the cooldown process. Cooldown flow passed through an existing remote-operated valve upstream of the flowmeter and a control valve downstream of the flowmeter.

Two quality meters (densitometers) were in the LOX system, one on the upstream side of the HEX and the other downstream. They were used to determine the liquid/gaseous phase of the propellant.

The altitude facility and engine were evacuated to about 1.0 psia (6895  $\text{N/m}^2$  abs) so that the flow across the injector would be choked.

#### 2. $\text{GH}_2$ System

Gaseous hydrogen was provided from the existing 750-psia (5,171,070  $\text{N/m}^2$  abs)  $\text{GH}_2$  supply through two pressure regulators to the HEX inlet. An orifice was located between the two regulators to measure gas flow. An existing control valve was installed downstream of the HEX to control the flow/back pressure. A 0.25 by 0.035 in. (0.006 by 0.0009 m) stainless steel line was connected across the control valve so pressure could not be trapped in the HEX. The burst pressure of the HEX was 75 psia (517,107  $\text{N/m}^2$  abs). An existing relief valve was reworked to relieve at 50 psig (344,738  $\text{N/m}^2$  gauge) and installed upstream of the HEX.



FD 95300

Figure V-1. Breadboard Heat Exchanger Test Configuration

### 3. Engine/HEX Mount

Space was provided for the small LOX flowmeter and associated plumbing between the facility LOX supply line and the engine LOX inlet. A 6-in. (0.5-m) spool piece was fabricated and installed between the facility mounting flange and the engine gimbal assembly. Longer gimbal rods were provided for mounting the engine.

## C. MODIFICATIONS

Using an RL10 engine to interface between the facility and the heat exchanger (HEX) kept stand modifications to a minimum.

### 1. Mount

No facility changes were required for mounting the HEX or engine. Mounting brackets were provided for the HEX.

### 2. LOX System

Facility changes required were associated with plumbing on the upstream of the HEX. Electrical control circuits for the two Remote-Operated Valves (ROV) in the flowmeter/cooldown plumbing were relocated. The circuits used are from ROV's in the fuel system, which was not used for HEX testing. A 2-in. (0.051-m) line, formerly used for nitrogen purge of the altitude chamber, was modified and used as a LOX cooldown dump line. The LOX dump line was piped to an existing fitting on the LOX dump system.

### 3. GH<sub>2</sub> System

Facility changes were made upstream of the HEX. Two Pressure Regulating Valves (PRV) and corresponding hand loaders, used in production RL10 testing, were used for this program. One of the PRV's was relocated to inside the altitude chamber. A nitrogen purge system was installed using an ROV from the existing fuel conditioning system. The control valve (CV) located on the discharge side of the HEX was also obtained from the fuel conditioning system.

## D. INSTALLATION

Installation of the test rig and associated work are listed below in chronological order. The installation of the engine and test rig in E-6 stand are shown in figure V-2.

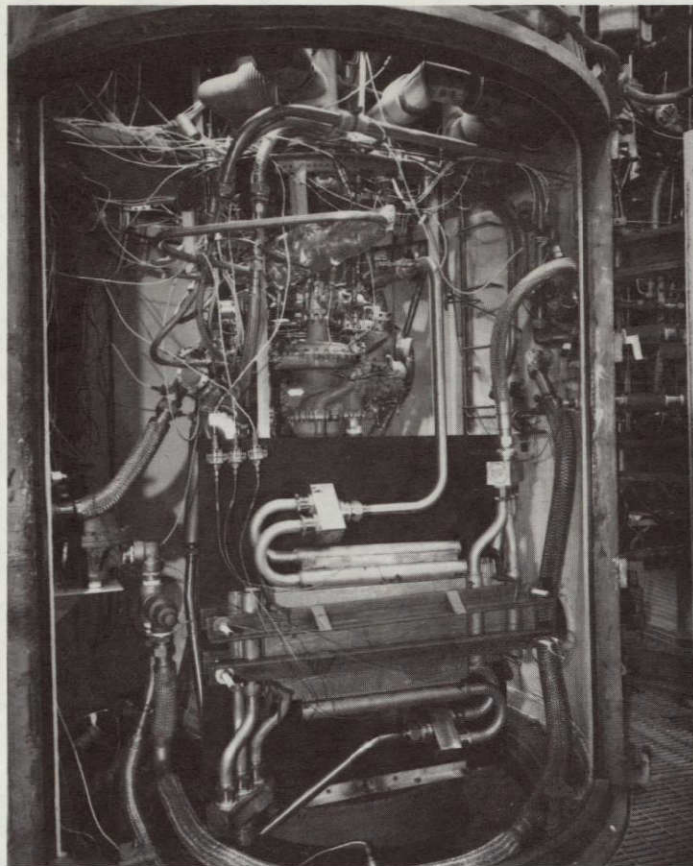
- 3 November 1975 - Engine P641915 arrived at E-6 stand and was mounted in the altitude chamber.
- 4 November 1975 - Field fit and installed piping, two ROV's and a 0.375-in. (0.009-m) flowmeter in LOX system upstream of the oxygen inlet valve. The bypass line was routed in close proximity to the flowmeter line for conductive cooling. Following pressure checks, the two lines were wrapped together with aluminum foil and insulated.
  - Started instrumenting engine/HEX.
- 5 November 1975 - Installed 0.75-in. (0.019-m) thick aluminum plate on which HEX was to be mounted. The HEX oxidizer and GH<sub>2</sub> inlet and discharge fittings were already mounted on the plate to enable field fitting of the respective supply and discharge lines.

- 5 November 1975 - Field fitted  $\text{GH}_2$  supply and discharge lines to HEX fittings. Installed mounting bracket inside altitude chamber for pressure relief valve.
- 6 November 1975 - Started field fitting oxidizer supply and discharge lines to HEX fittings.
- 7 November 1975 - Pressure-checked LOX system up to the engine inlet valve.
  - Wrapped foil and insulation around the flowmeter and cooldown plumbing upstream of the engine inlet.
- 11 November 1975 - Completed field fit/installation of the oxidizer piping to the HEX. The piping was removed and sent to Rocket Engine Assembly to add instrumentation taps for pressures and temperatures. Piping was LOX cleaned.
  - Removed HEX mount plate and returned it to Rocket Engine Assembly for mounting of HEX.
- 12 November 1975 - Quality meter shipping date slipped from 11-15-75 to 12-1-75.
- 11 November 1975 - Existing RL10 run procedures were modified for HEX testing.  
to
- 24 November 1975
- 24 November 1975 - HEX was returned to E-6 stand and was installed.
  - $\text{GH}_2$  supply ROV was added to the Abort Bus to fail closed on abort.
- 25 November 1975 - Closed circuit TV cameras and lighting were aligned and set up.
  - Mockup versions of the quality meters were installed in the system to enable checkout cold flow.
- 26 November 1975 - Leak checked the entire systems and found three leaks in LOX system and four on the  $\text{GH}_2$  system. These leaks were corrected.

#### **E. CHECKOUT**

A checkout test of the entire system was planned for 26 November. However, the test was not completed due to some minor stand problems.

The checkout test was made on 1 December 1975. The desired LOX conditions at the HEX inlet could not be met due to a system heat leak. On the following runs, the plumbing from the LOX pump discharge to the HEX inlet were insulated. The heat loss problem was compounded by the low rate of oxidizer flow. At the start of the test, when the oxygen inlet valve was opened, the cooldown valves upstream of the oxygen inlet valve were closed. The low flowrates in the supply line were unable to keep the line cold. A low LOX level in the run tank prevented the opening of the cooldown lines to increase flow to the engine inlet. The LOX tank level was kept to a minimum to reduce head pressure. In addition, the small LOX flowmeter did not indicate flow, because it was damaged during the stand system purge. Hence, pressure drop across the injector was used to determine oxidizer flowrate.



FAE 339210

*Figure V-2. Engine and Test Rig Installation*

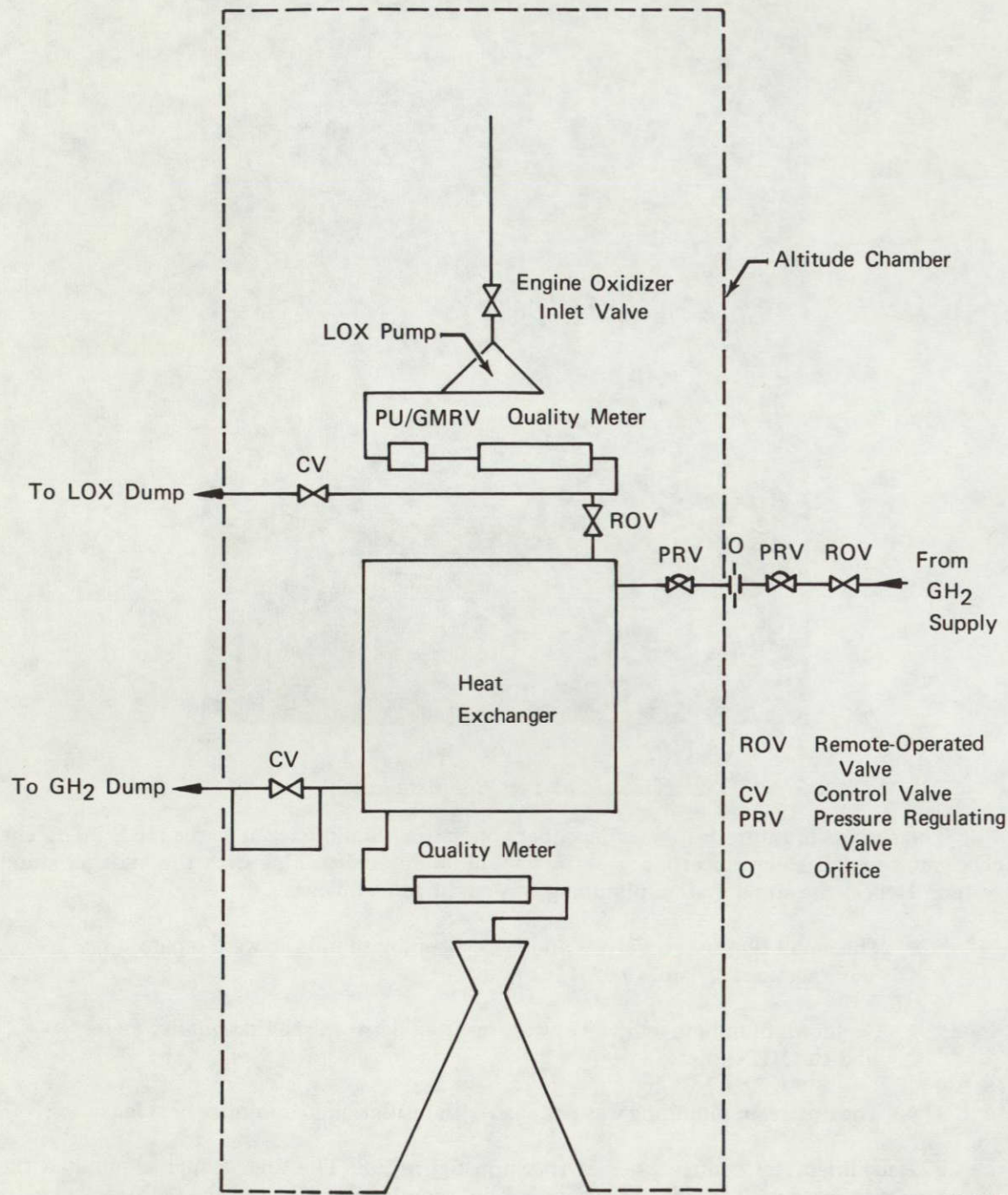
The success of future tests was dependent on getting liquid oxygen at the HEX inlet. The checkout test left some uncertainty as to the ability to achieve this with the existing stand system. Hence, the stand system plumbing was modified as follows:

- The small flowmeter, valves, and corresponding plumbing were replaced by short sections of 1-in. (0.0254-m) pipe.
- Cooldown plumbing and valves were inserted between the first quality meter and the HEX inlet.
- The upstream plumbing was wrapped with insulation to minimize heat leaks.

The modified test configuration is shown in figure V-3. The first change eliminated the plumbing associated with the small flowmeter. The second change allowed the LOX system to be prechilled up to the HEX. Also, the control valve in the new cooldown line provided some control over HEX inlet pressure. In addition, all plumbing in the oxidizer system upstream of the HEX was insulated.

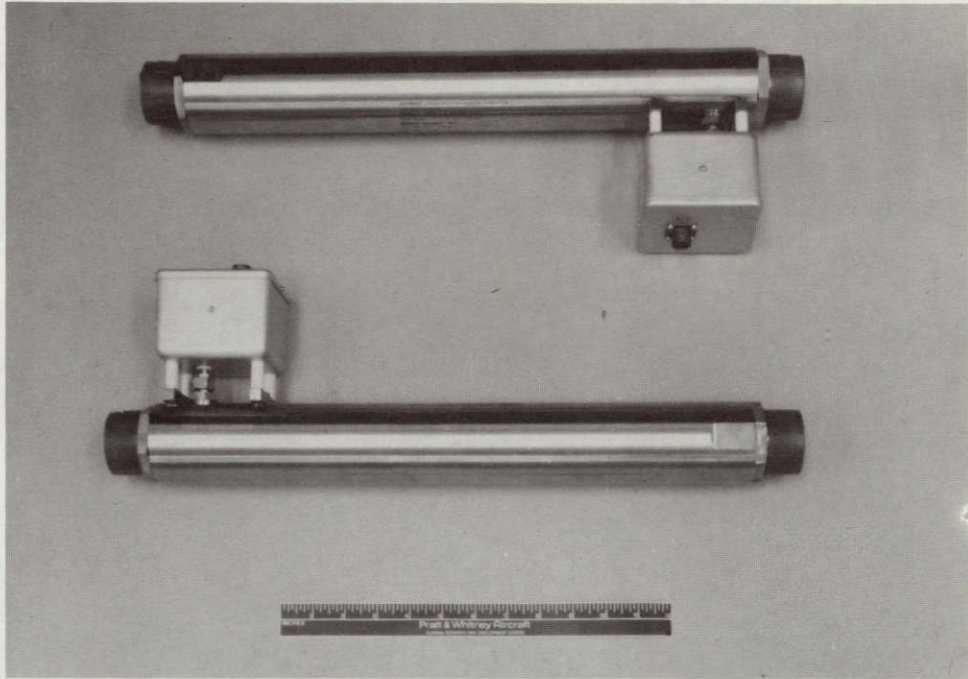
The quality meters were installed in the stand plumbing after the checkout test as shown in figure V-3. The quality meters are shown in figure V-4.

The modifications to the test configuration enabled the facility to provide the desired HEX oxidizer conditions. The test program was completed with the modified test stand configuration shown in figure V-3.



FD 95847

Figure V-3. Modified Test Configuration



FE 39236

*Figure V-4. Quality Meters*



## SECTION VI TEST

### A. GENERAL

A checkout test and two evaluation tests were conducted with the breadboard heat exchanger rig. The checkout test was planned to test out the rig setup and provide heat exchanger characteristics with no insulation between the panels. The second test was conducted with 30% dense feltmetal insulation between the panels and was made to provide heat exchanger characteristics with an intermediate heat flux level. The third test was run with no insulation and aluminum powder between the panels to obtain heat exchanger characteristics with a high heat flux in the heat exchanger.

Data from the checkout test indicated that the heat flux with no insulation between the panels was not as high as expected. This was believed to be due to warpage of the panels (poor contact) that resulted from attempts to braze repair panel leaks. Therefore, for the third test, powdered aluminum was placed between the panels to fill in the cavities, thus improve contact, in hopes of obtaining a higher heat flux level than was available during the checkout test. The instrumentation and symbol definition is shown in table VI-1.

### B. CHECKOUT TEST (TEST 1.01)

The checkout test was completed on 1 December 1975. A schematic of the breadboard heat exchanger rig setup and location of instrumentation used for this test is shown in figure VI-1. The quality meters were not received from the manufacturer in time for the checkout test. Thus test was made with sections of line that simulated the quality meter size (mockup quality meters). To keep head to a minimum and provide a low oxidizer inlet pressure, only 600-gal (2.27 m<sup>3</sup>) of liquid oxygen were tanked in the run tank for this test. With the tank vented to ambient this gave an oxidizer inlet pressure of approximately 23 psia (158,579 N/m<sup>2</sup> abs). The test was started by cooling down the oxidizer inlet lines by dumping liquid oxygen through valves ROV 185 and CV3. After liquid oxygen conditions were obtained at the engine inlet, as indicated by temperature measurement LFT, cell pressure (HS-P31) was reduced to below 1 psia (6895 N/m<sup>2</sup> abs), and hydrogen flow was set to a nominal flowrate ( $\approx 0.75$  lb/sec [0.34 kg/sec]). Cooldown of the oxidizer side of the rig was then initiated by opening the engine oxygen inlet valve and flowing oxygen through the heat exchanger and injector. Cooldown of the oxidizer system was attempted for approximately 600 sec, but liquid oxygen conditions could not be obtained at the heat exchanger inlet. The test was terminated. The lowest temperature obtained was 250°R (139°K).

The incomplete cooldown of the system was due to higher-than-expected heat leaks in the oxidizer plumbing upstream of the heat exchanger, an insufficient quantity of oxygen in the run tank to maintain liquid at the pump inlet throughout the cooldown period, and an excessive pressure loss (10 psi [68,948 N/m<sup>2</sup>]) due to a section of small plumbing between the large vacuum-jacketed test stand propellant line and the engine inlet valve. During this test, liquid oxygen flowmeter FM107 did not work properly and post-test inspection showed it to be inoperative. Superheated gas was present at the injector, and it was choked throughout the test. Therefore, oxygen flows were calculated from the injector measurements using compressible flow equations.

The data obtained during this test indicated a lower heat flux level than had been predicted for the heat exchanger with no insulation between the panels. The lower heat transfer level was believed to be due to the warpage of the panels, which resulted in poor contact between the plates.

Table VI-1. Breadboard Heat Exchanger Rig Instrumentation

Symbol Definition	Range	Strip Chart	Digital	Oscillograph
Liquid Oxygen Flowmeter (LFLOW)	0.05 to 0.5 lb/sec (0.023 to 0.227 kg/sec)	X	X	X
LOX Flowmeter Temperature (LFT)	160 to 200°R (89 to 111°K)	X	X	X
LOX Flowmeter Upstream Pressure (LFUP)	15 to 40 psia (103,421 to 275,790 N/m <sup>2</sup> abs)	X	X	
LOX Flowmeter Downstream Pressure (LFDP)	15 to 40 psia (103,421 to 275,790 N/m <sup>2</sup> abs)		X	
Oxidizer Heat Exchanger Inlet Temperature (OHEIT)	160 to 600°R (89 to 333°K)	X	X	X
Oxidizer Heat Exchanger Inlet Temperature Rosemount (OHEITR)	160 to 200°R (89 to 111°K)	X	X	
Oxidizer Heat Exchanger Inlet Pressure (OHEIP)	5 to 35 psia (34,474 to 241,317 N/m <sup>2</sup> abs)	X	X	X
Oxidizer Heat Exchanger Discharge Temperature (OHEDT)	160 to 600°R (89 to 333°K)	X	X	X
Oxidizer Heat Exchanger Discharge Pressure (OHEDP)	5 to 35 psia (34,474 to 241,317 N/m <sup>2</sup> abs)		X	X
Oxidizer Injector Temperature (OIT1R)	160 to 200°R (89 to 111°K)		X	
Oxidizer Injector Pressure (OIMP11)	5 to 35 psia (34,474 to 241,317 N/m <sup>2</sup> abs)	X	X	X
Ejector Pressure (HS-P31)	0 to 15 psia (0 to 103,421 N/m <sup>2</sup> abs)	X	X	X
Upstream Quality Meter (UDM)	-	X	X	X
Downstream Quality Meter (DDM)	-	X	X	
Oxidizer Pump Inlet Pressure (OPIP31)	15 to 40 psia (103,421 to 275,790 N/m <sup>2</sup> abs)	X	X	
Oxidizer Pump Housing Temperature (OPHT1R)	100 to 672°R (56 to 373°K)		X	
Oxidizer Pump Impeller Temperature (OPIPTI)	160 to 600°R (89 to 333°K)		X	
Fuel Heat Exchanger Inlet Temperature (FHEIT)	300 to 600°R (167 to 333°K)	X	X	
Fuel Heat Exchanger Inlet Pressure (FHEIP)	10 to 50 psia (68,948 to 344,738 N/m <sup>2</sup> abs)	X	X	
Fuel Heat Exchanger Discharge Temperature (FHEDT)	300 to 600°R (167 to 333°K)		X	X
Fuel Heat Exchanger Discharge Pressure (FHEDP)	10 to 50 psia (68,948 to 344,738 N/m <sup>2</sup> abs)	X	X	
Fuel Flow Orifice Pressure (FFOP)	To Be Defined By Facilities	X	X	X
Fuel Flow Orifice Temperature (FFOT)	To Be Defined By Facilities		X	
Fuel Flow Orifice Delta Pressure (FFODP)	To Be Defined By Facilities	X	X	
Oxidizer Heat Exchanger Inlet Manifold Pressure No. 1 (OEIMP1)	5 to 30 psia (34,474 to 206,843 N/m <sup>2</sup> abs)	X	X	X
Oxidizer Heat Exchanger Inlet Manifold Pressure No. 2 (OEIMP2)	5 to 30 psia (34,474 to 206,843 N/m <sup>2</sup> abs)		X	
Oxidizer Heat Exchanger Inlet Manifold Temperature (OHEIMT)	160 to 600°R (89 to 333°K)	X	X	
Oxidizer Heat Exchanger Discharge Manifold Pressure (OEDMP)	5 to 30 psia (34,474 to 206,843 N/m <sup>2</sup> abs)		X	X

Table VI-1. Breadboard Heat Exchanger Rig Instrumentation (Continued)

<i>Symbol Definition</i>	<i>Range</i>	<i>Strip Chart</i>	<i>Digital</i>	<i>Oscillograph</i>
Heat Exchanger Oxidizer Plate Metal Temperature No. 1 (HEOP1)	160 to 600°R (89 to 333°K)		X	
Heat Exchanger Oxidizer Plate Metal Temperature No. 2 (HEOP2)	160 to 600°R (89 to 333°K)		X	
Heat Exchanger Oxidizer Plate Metal Temperature No. 3 (HEOP3)	160 to 600°R (89 to 333°K)		X	
Heat Exchanger Oxidizer Plate Metal Temperature No. 4 (HEOP4)	160 to 600°R (89 to 333°K)		X	
Heat Exchanger Oxidizer Plate Metal Temperature No. 5 (HEOP5)	160 to 600°R (89 to 333°K)		X	
Heat Exchanger Oxidizer Plate Metal Temperature No. 6 (HEOP6)	160 to 600°R (89 to 333°K)		X	
Heat Exchanger Oxidizer Plate Metal Temperature No. 7 (HEOP7)	160 to 600°R (89 to 333°K)		X	
Heat Exchanger Oxidizer Plate Metal Temperature No. 8 (HEOP8)	160 to 600°R (89 to 333°K)		X	
Heat Exchanger Oxidizer Plate Metal Temperature No. 9 (HEOP9)	160 to 600°R (89 to 333°K)		X	
Oxidizer Inlet Line Temperature (OPIT1R)	160 to 200°R (89 to 111°K)	X	X	
Oxidizer Inlet Line Pressure (OPIP11)	15 to 40 psia (103,421 to 275,790 N/m <sup>2</sup> abs)	X	X	
Heat Exchanger Fuel Plate Metal Temperature No. 1 (HEFP1)	160 to 600°R (89 to 333°K)		X	
Heat Exchanger Fuel Plate Metal Temperature No. 2 (HEFP2)	160 to 600°R (89 to 333°K)		X	
Heat Exchanger Fuel Plate Metal Temperature No. 3 (HEFP3)	160 to 600°R (89 to 333°K)		X	
Heat Exchanger Fuel Plate Metal Temperature No. 4 (HEFP4)	160 to 600°R (89 to 333°K)		X	
Heat Exchanger Fuel Plate Metal Temperature No. 5 (HEFP5)	160 to 600°R (89 to 333°K)		X	
Heat Exchanger Fuel Plate Metal Temperature No. 6 (HEFP6)	160 to 600°R (89 to 333°K)		X	
Heat Exchanger Fuel Plate Metal Temperature No. 7 (HEFP7)	160 to 600°R (89 to 333°K)		X	
Heat Exchanger Fuel Plate Metal Temperature No. 8 (HEFP8)	160 to 600°R (89 to 333°K)		X	
Heat Exchanger Fuel Plate Metal Temperature No. 9 (HEFP9)	160 to 600°R (89 to 333°K)		X	
Heat Exchanger Fuel Center Panel Fluid Discharge Temperature No. 1 (HCPDT1)	300 to 600°R (167 to 333°K)		X	
Heat Exchanger Fuel Center Panel Fluid Discharge Temperature No. 2 (HCPDT2)	300 to 600°R (167 to 333°K)		X	
Heat Exchanger Fuel Outer Panel Fluid Discharge Temperature No. 1 (HOPDT1)	300 to 600°R (167 to 333°K)		X	
Heat Exchanger Fuel Outer Panel Fluid Discharge Temperature No. 2 (HOPDT2)	300 to 600°R (167 to 333°K)		X	



### C. SECOND TEST (TEST 2.01)

The second test was completed on 30 December 1975. For this test, 30% dense feltmetal insulation was used between the heat exchanger panels. Several changes were made to the rig set up to correct the problems encountered during the checkout test. These changes are described in Section V, paragraph E. The rig setup used for this second test is shown in figure VI-2.

Several instrumentation items that were not available during the checkout test were installed prior to this run. The density meters purchased from Quantum Dynamics, Inc., were installed in the heat exchanger inlet and exit lines. Also, nine thermocouples were installed in opposing locations on one hydrogen and one oxygen panel of the heat exchanger. The oxidizer flow meter, which was inoperative during the checkout test, was removed from the system and injector measurements used for the subsequent tests to calculate flows.

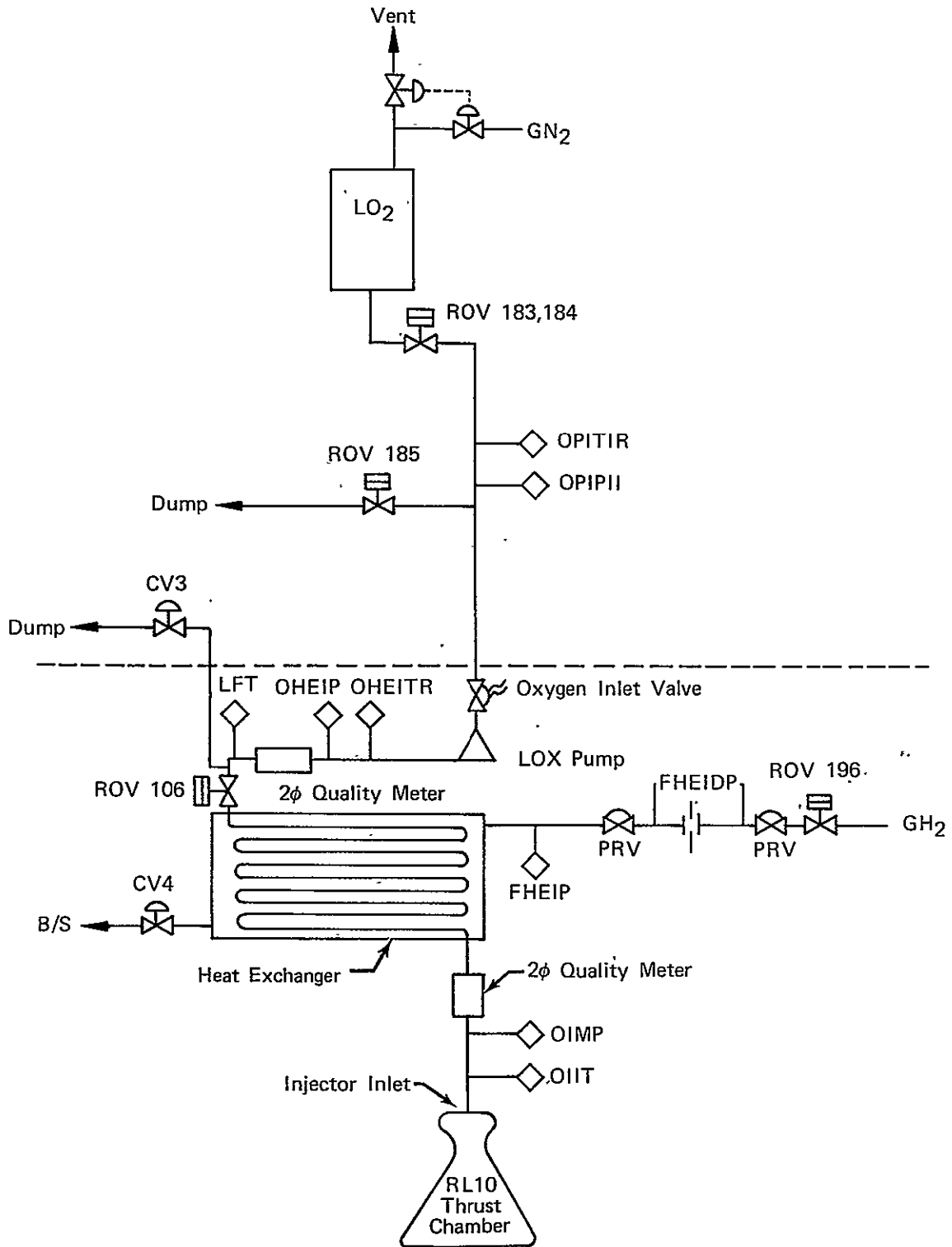
Prior to starting the test, the oxygen system was cooled down until liquid was obtained at the heat exchanger inlet (liquid at LFT). Then hydrogen flow was set at the nominal value ( $\approx 0.075$  lb/sec [0.34 kg/sec]), cell pressure was reduced to below 1 psia (6895 N/m<sup>2</sup> abs) and ROV 106 was opened to allow oxygen flow through the heat exchanger. Steady-state data was obtained at two different heat exchanger oxygen inlet pressures (25 psia [172,369 N/m<sup>2</sup> abs] and 22 psia [151,684 N/m<sup>2</sup> abs]) with nominal hydrogen flowrates. Hydrogen flow was then reduced to 0.035 lb/sec (0.016 kg/sec), while maintaining oxygen inlet pressure at 22 psia (151,684 N/m<sup>2</sup> abs) and another steady-state data point was taken. At the end of this test, to obtain data at oxygen pressures lower than 22 psia (151,684 N/m<sup>2</sup> abs) and determine inlet quality effects on heat exchanger stability, ROV 183 was closed to allow the oxygen pressure to decay down to  $\approx 3$  psi (20,684 N/m<sup>2</sup>) over a 170-sec period. Two-phase fluid conditions existed at the heat exchanger inlet during the last 100 sec of the run when the pressures were below the saturation pressure.

Oxygen flowrates during this test were higher than planned because of lower-than-expected heat addition to the oxygen downstream of the heat exchanger. The lower heat addition resulted in two-phase conditions at the injector and higher-than-expected flowrates through the injector. Another problem occurred with the density meter readings. When liquid conditions were present the density meter readings did not agree with the densities calculated from temperature and pressure measurements. Adjustments to the meter readings required to bring the two into agreement were determined and these corrections applied to the meter readings whenever two-phase conditions were present to determine heat exchanger inlet quality. Instability was present during most of the steady-state points and most of the blow down transient; however, in all cases, the amplitudes of the pressure oscillations were less than the  $\pm 0.5$  mixture ratio limit.

### D. THIRD TEST (TEST 3.01)

The third test was completed on 9 January 1976. The setup for this test was the same as for the second run. Prior to this test, the feltmetal insulation was removed and powdered aluminum placed between the heat exchanger panels to fill the cavities resulting from panel warpage. This was done in an attempt to improve contact and to get higher heat transfer rates than had been obtained during the checkout test.

The test was run in three parts. The first consisted of cooling down the oxygen system to the engine inlet and then opening the oxidizer inlet valve to allow oxygen to flow through the heat exchanger and CV3. Heat exchanger inlet pressure was maintained at 26-psia (179,263 N/m<sup>2</sup> abs), and hydrogen flowrates were reduced over a series of steady-state points. Hydrogen flows of 0.08 (0.036), 0.045 (0.020), and 0.02 (0.009) lb/sec (kg/sec) were run. This part of the test was then terminated by closing ROV 106, which stopped oxygen flow through the heat exchanger.



FD 95849

Figure VI-2. GOX Heat Exchanger Rig Schematic of Configuration Used for Tests 2.01 and 3.01

The second and third parts of the test consisted of oxidizer system blowdowns, and they were both run in the same manner. The heat exchanger was warmed to near ambient temperatures by continuing hydrogen flow through it. ROV 106 was then opened allowing oxidizer to flow through the heat exchanger. As soon as oxygen flow was established, ROV 183 was closed and the oxygen system was allowed to bleed down through the heat exchanger. The same three hydrogen flowrates, as in part one of the test, were run during each of the blowdowns.

Heat flux for this test was higher than during the checkout test, but it was still only 33% of the level predicted for the heat exchanger with no insulation. The lower heat transfer level was attributed to poor contact between the plates, which apparently still existed even with the aluminum powder in the cavities. Since heat transfer was lower, oxygen flowrates were again higher than expected.

Instability was present during all of the steady-state points and most of the blowdown transients; however, in all cases the amplitudes of the pressure oscillations were less than the  $\pm 0.5$  mixture ratio limit.

## SECTION VII ANALYSIS

### A. CHECKOUT TEST (TEST NO. 1.01)

This test was made with no insulation between the heat exchanger panels. Its purpose was to check out the test rig setup and provide heat exchanger characteristics with no insulation between the panels. Liquid conditions at the heat exchanger oxygen inlet, which are necessary for stability evaluation, were not obtained during this test. Evaluation of the data indicated that this was due to excessive pressure losses and heat leaks in the oxygen plumbing upstream of the heat exchanger. Figures VII-1 through VII-3 show the measured and calculated data obtained during this test. The large change in conditions between 130 and 265 sec was due to the oxygen inlet valve being closed during this time. The oxygen flowmeter was inoperative during this test so oxygen flowrates were calculated using the measured engine injector parameters and compressible flow equations.

The test was successful in defining the rig modifications required to obtain the desired oxygen conditions at the heat exchanger inlet; however, the characteristics and stability criteria for the heat exchanger with no insulation between the panels were not fully defined.

#### 1. Heat Transfer

Heat transfer during this test, based on hydrogen side heat loss, was only about 20% of predicted. This was presumably due to poor contact between the heat exchanger panels because of warpage resulting from the attempts to braze-repair the panel leaks.

#### 2. Pressure Losses

Figures VII-4 and VII-5 show the gaseous hydrogen and gaseous oxygen heat exchanger pressure losses and compare them with predicted levels. They show that the rig pressure losses were near predicted levels. Actually the gaseous oxygen pressure losses were less than predicted, because the measured values included the loss of approximately 6 ft (1.83 m) of 1.5-in. (0.038-m) diameter flex line tubing in addition to the heat exchanger.

#### 3. Stability

No instability occurred during this run because only gaseous oxygen was present at the heat exchanger inlet.

### B. TEST WITH 30% DENSE FELTMETAL INSULATION (TEST NO. 2.01)

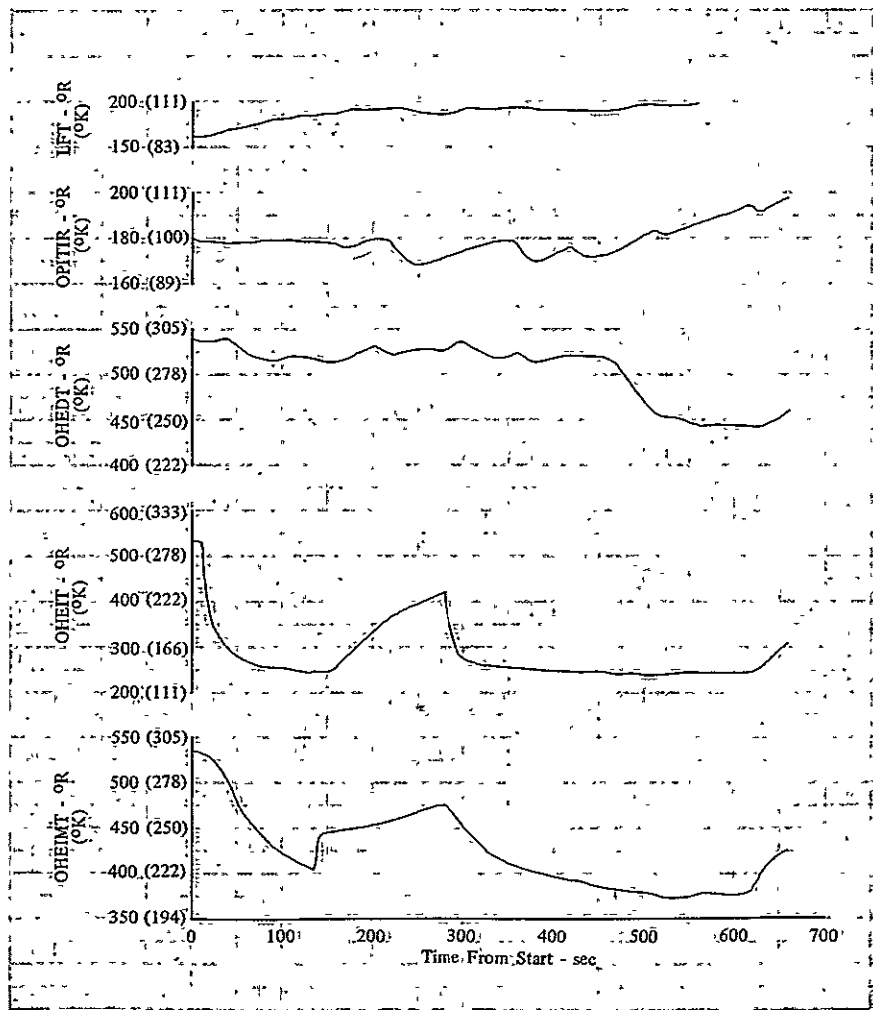
This test had 30% dense feltmetal insulation between the heat exchanger panels and was used to determine heat exchanger characteristics at an intermediate heat flux level. Nine thermocouples were installed on one hydrogen panel and one oxygen panel in opposing locations prior to this test to provide additional heat flux information. The rig was also modified prior to the test to be sure of obtaining liquid oxygen at the heat exchanger inlet during the test. (See Section VI, Test.) Figures VII-6 through VII-10 show measured data throughout the test. Oxygen flowrates were higher than planned because of lower heat addition upstream of the injector than expected. Oxygen flowrates were calculated at specific steady-state points using iterative two-phase flow calculations. These calculations were made by assuming an oxygen flowrate, adding the heat addition from the hydrogen side to the heat exchanger oxygen inlet conditions to obtain an exit quality, then calculating oxygen flowrate using engine injector characteristics and two-phase flow routines. The iteration was continued until a flow balance was achieved. The density



meters purchased from Quantum Dynamics, Inc., indicated densities that were inconsistent with densities calculated from measured temperatures and pressures when liquid conditions were present. Corrections necessary to make the two agree were determined and these corrections applied to the meter readings whenever two-phase conditions were present. (Refer to Section VI, paragraph C.) The upstream meter was used to determine inlet quality to the heat exchanger, and as mentioned above exit quality was calculated as a part of the oxidizer flow calculations.

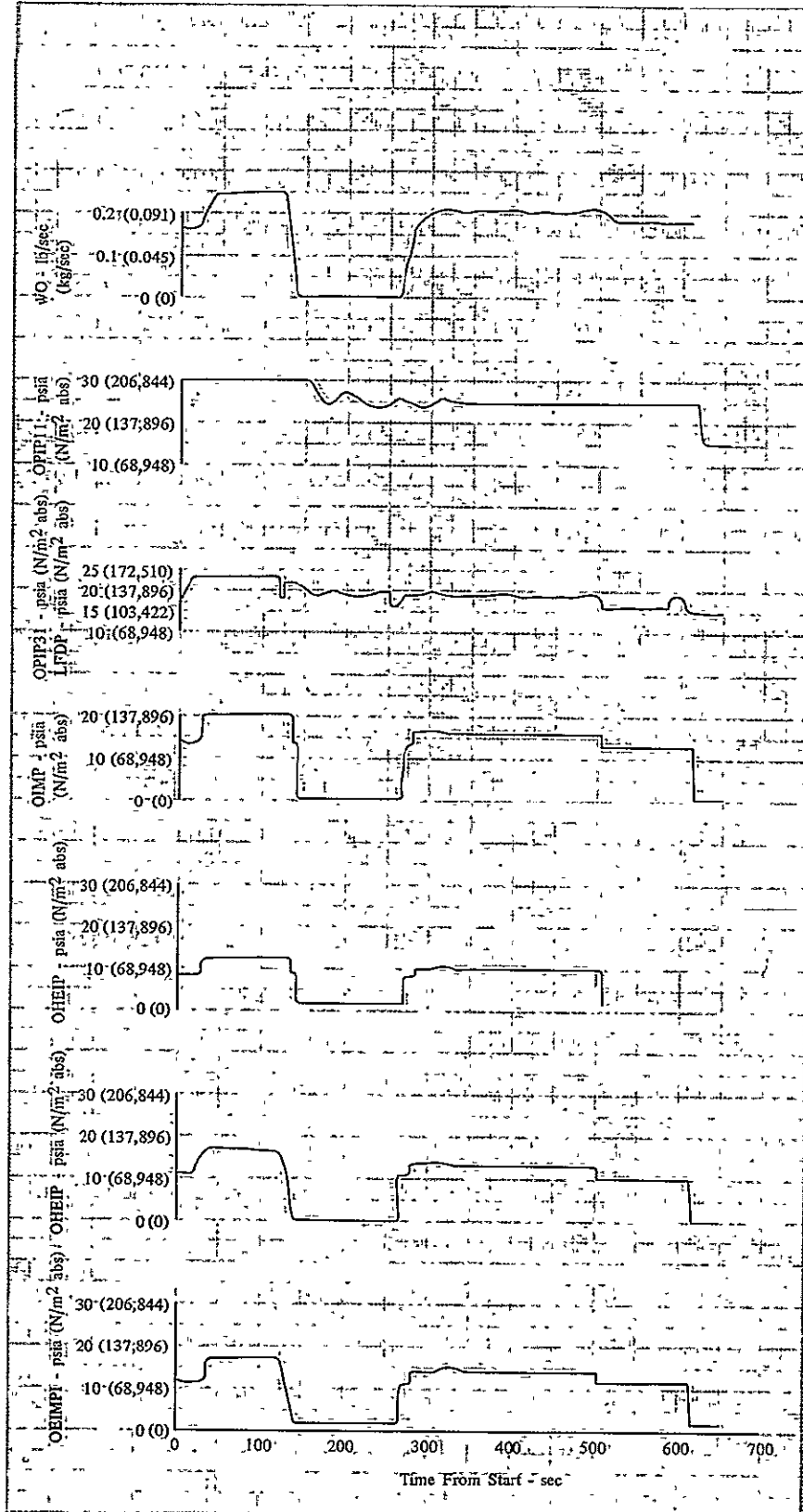
**1. Heat Transfer**

Steady-state heat flux for this test was approximately 70% of predicted. This lower heat transfer level is attributed to contact resistance between the insulation and the panels, and probable poor bonding between the copper fins and panels. The panel thermocouple measurements indicated much lower heat flux levels than those indicated by the fluid temperature measurements, and they were not used in the final analysis.



DF 101942

*Figure VII-1. Measured Oxygen Data Characteristics of Breadboard Heat Exchanger Checkout Test*

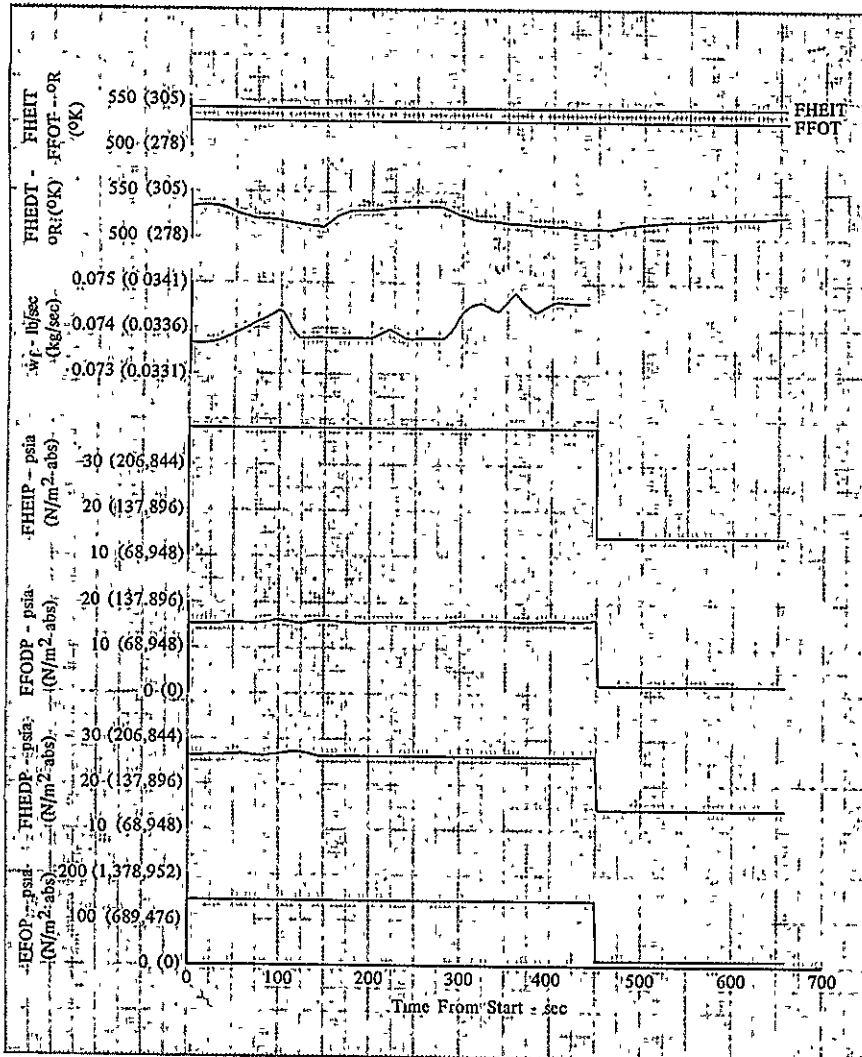


DF 101943

Figure VII-2. Measured and Calculated Oxygen Data Characteristics of Breadboard Heat Exchanger Checkout Test

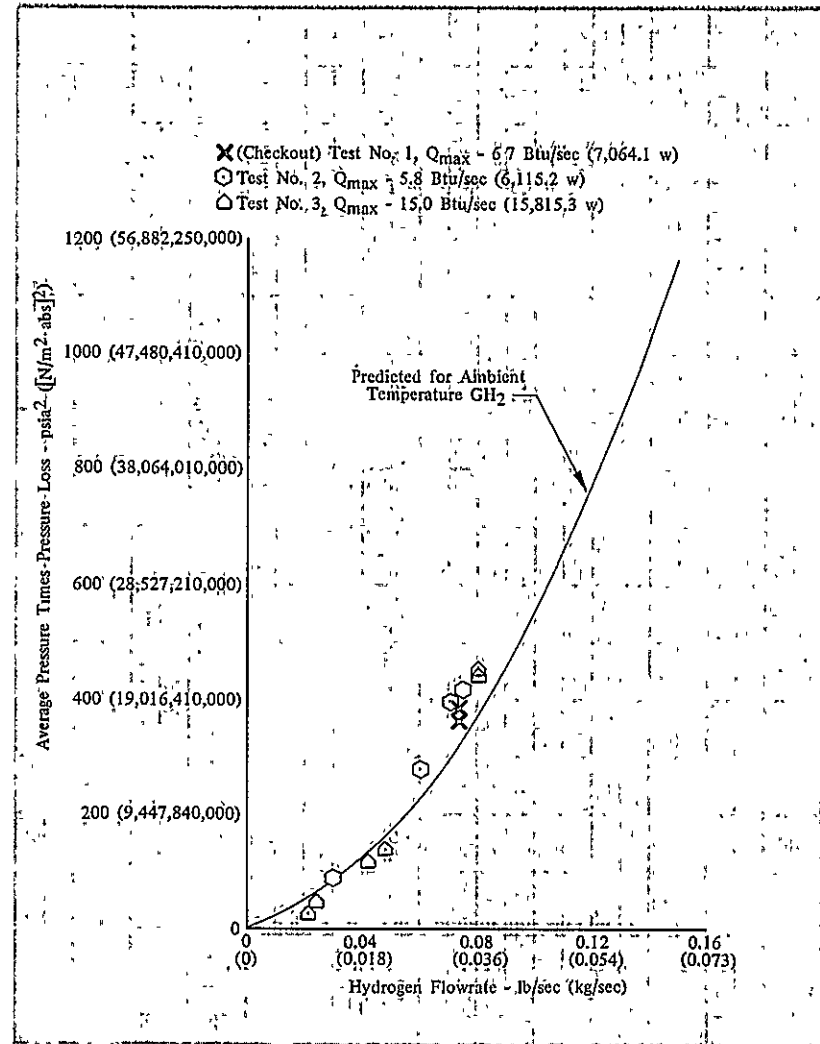
REPRODUCIBILITY OF THE ORIGINAL PAGE IS POOR

VII-4



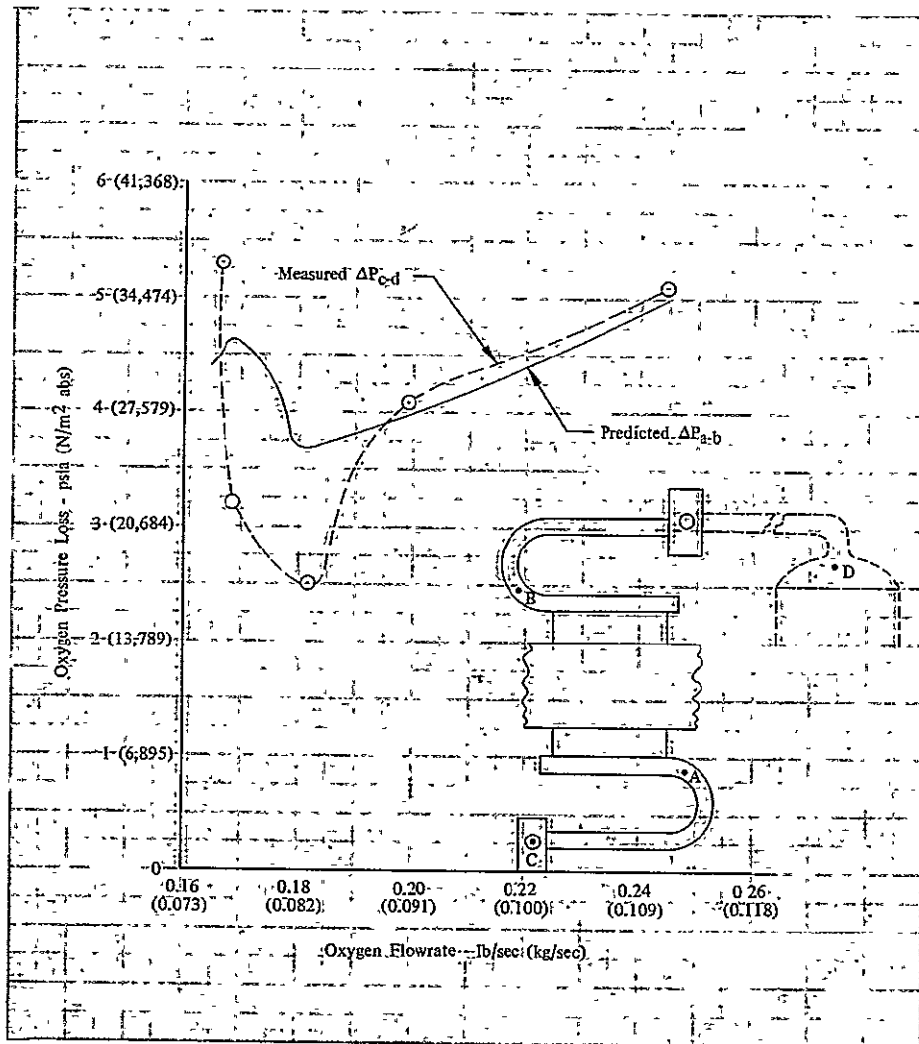
DF 101944

Figure VII-3. Measured and Calculated Hydrogen Data Characteristics of Breadboard Heat Exchanger Checkout Test



DF 101945

Figure VII-4. Hydrogen Pressure Loss Characteristics from Breadboard Heat Exchanger Tests



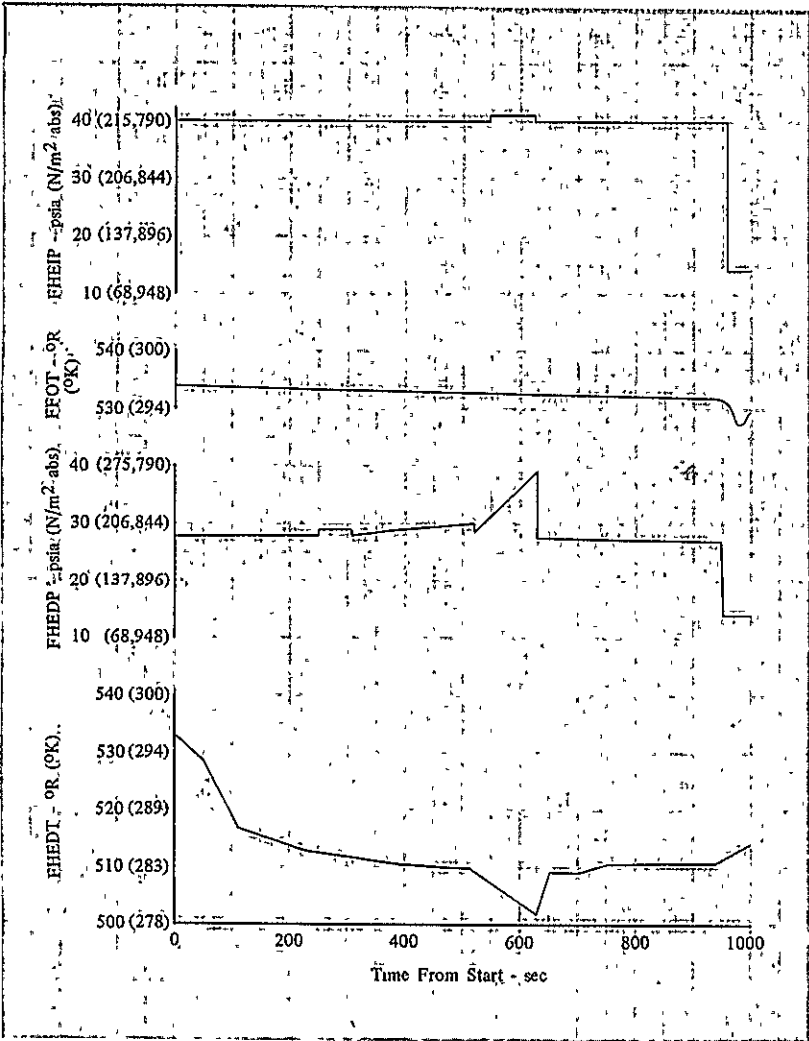
DF 101946

Figure VII-5. Gaseous Oxygen Pressure Loss Characteristics from Breadboard Heat Exchanger Run 1.01 Checkout Test

Table VII-1 contains steady-state measured and calculated heat exchanger parameters. Figure VII-11 compares predicted and calculated heat exchanger exit conditions. The calculated values are based on the measured heat flux levels and design oxygen flowrates and they are the conditions that would be expected had the oxygen flowrates been at the design levels. Figure VII-12 compares predicted and calculated heat exchanger effective conductance, and figure VII-13 shows the effect of hydrogen flowrate on heat transfer.

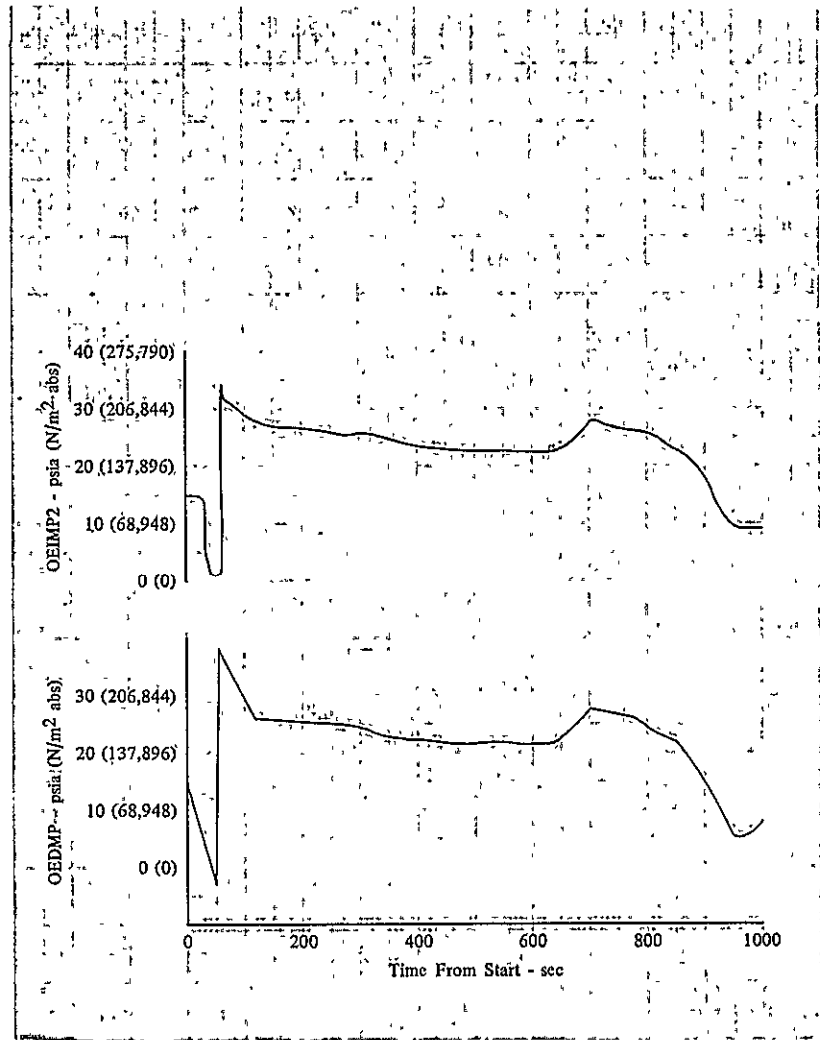
## 2. Pressure Losses

Hydrogen pressure losses again were close to predicted as shown by figure VII-4. Figures VII-14 and VII-15 show oxygen side core pressure losses and exit quality vs flowrate. The measured oxidizer pressure losses were also near predicted levels; however, the accuracies of the transducers used were approximately 0.25 psia (1724 N/m<sup>2</sup> abs), making the absolute level of measurement differences under 1 psid (6895 N/m<sup>2</sup> diff) questionable.



DF 101947

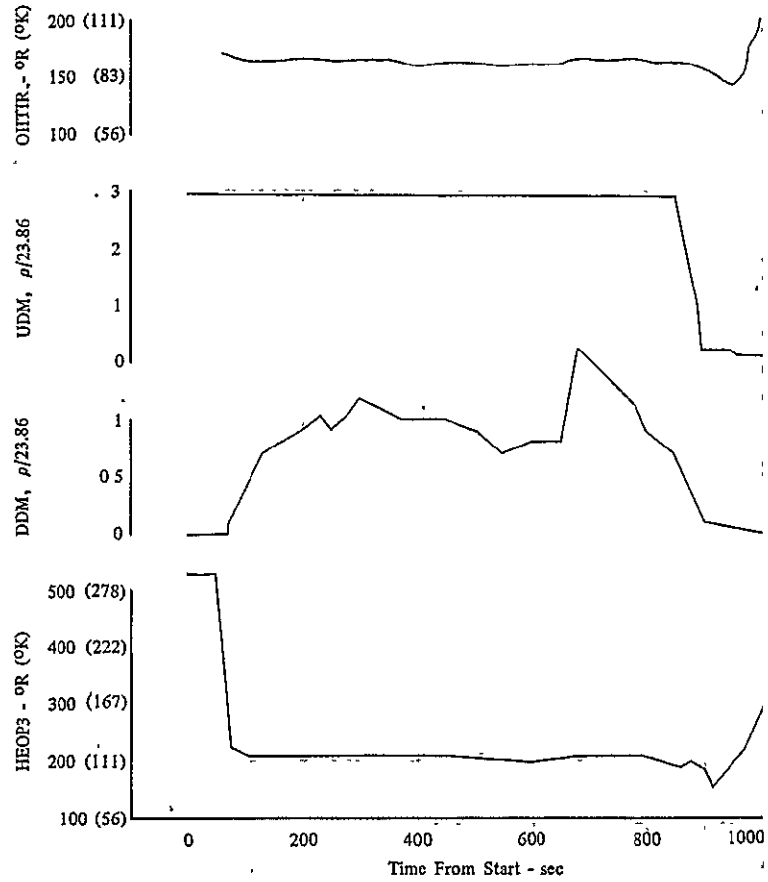
Figure VII-6. 30% Dense Feltmetal Insulation Data Characteristics for Breadboard Heat Exchanger Test No. 2.01



DF 101948

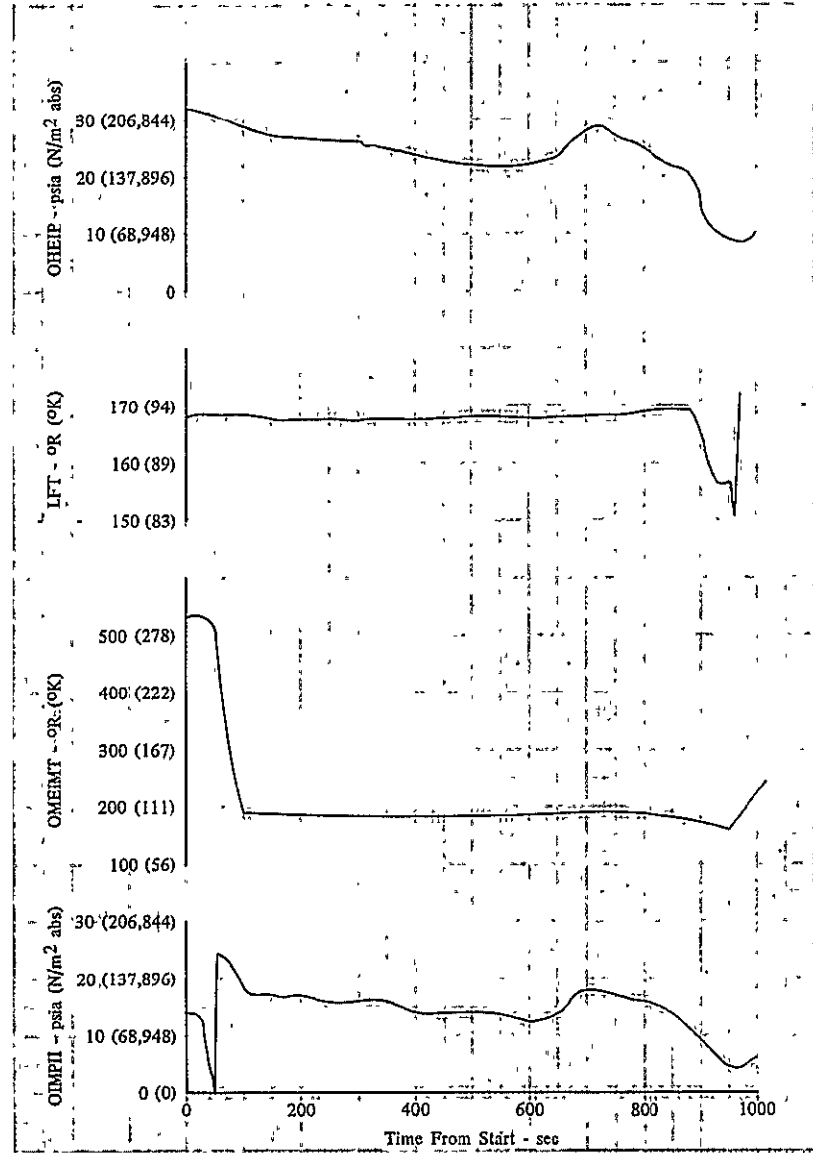
Figure VII-7. 30% Dense Feltmetal Insulation Data Characteristics for Breadboard Heat Exchanger Test No. 2.01

VII-7



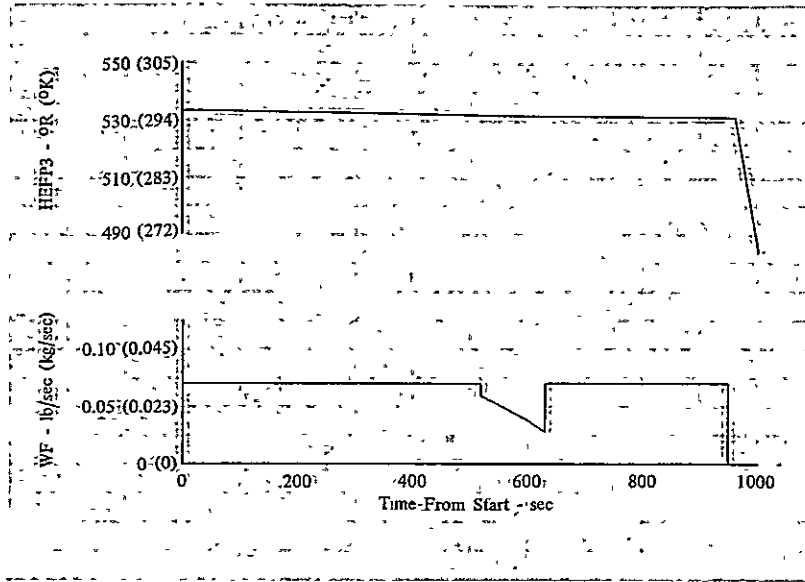
DF 101949

Figure VII-8. 30% Dense Feltmetal Insulation Data Characteristics for Breadboard Heat Exchanger Test No. 2.01



DF 101950

Figure VII-9. 30% Dense Feltmetal Insulation Data Characteristics for Breadboard Heat Exchanger Test No. 2.01

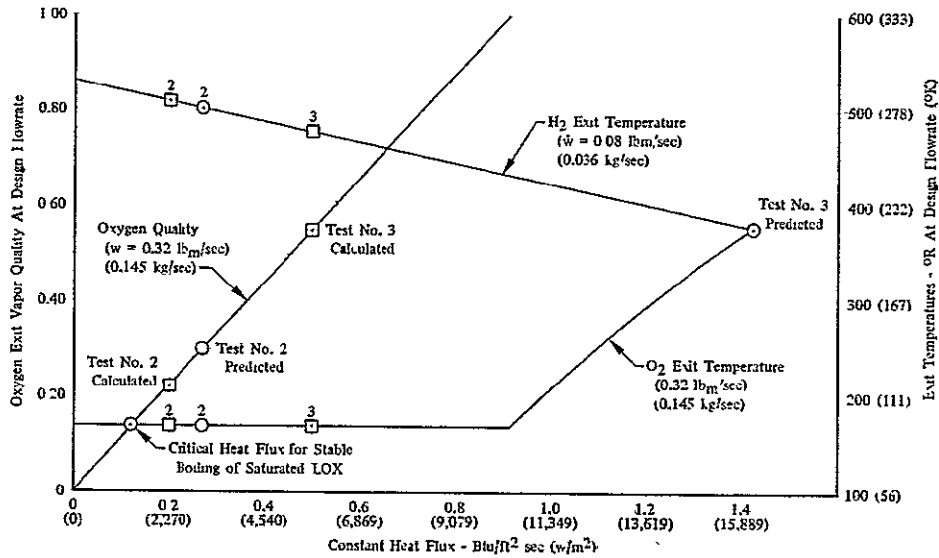


DF 101951

Figure VII-10. 30% Dense Feltmetal Insulation Data Characteristics for Breadboard Heat Exchanger Test No. 2.01

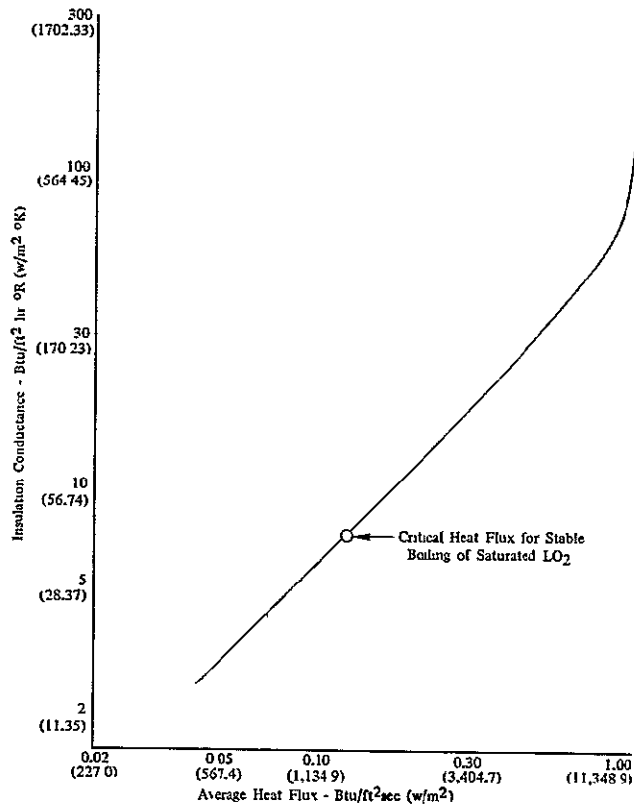
Table VII-1. Breadboard Heat Exchanger Steady-State Operating Characteristics

	Run No. 2.01	Run No. 3.01
Time	855	1950
Heat Transfer, Btu/sec (w)	5.9 (6,219)	14.7 (15,494)
Oxygen Flowrate, lb/sec (kg/sec)	2.27 (1.03)	1.28 (0.58)
Exit Quality, %	3.6	13.4
Hydrogen Flowrate, lb/sec (kg/sec)	0.074 (0.034)	0.081 (0.037)
Heat Exchanger Oxygen Inlet Pressure, psia (N/m <sup>2</sup> abs)	21.6 (148,927)	19.0 (131,000)
Oxygen Inlet Manifold Pressure, psia (N/m <sup>2</sup> abs)	22.45 (154,787)	20.05 (138,240)
Oxygen Discharge Manifold Pressure, psia (N/m <sup>2</sup> abs)	21.69 (149,547)	19.30 (133,069)
Oxygen Injector Manifold Pressure, psia (N/m <sup>2</sup> abs)	12.2 (84,116)	10.85 (74,808)
Heat Exchanger Oxygen Inlet Temperature, °R (°K)	169.0 (93.8)	166.9 (92.6)
Oxygen Injector Manifold Temperature, °R (°K)	160.5 (89.1)	158.8 (88.1)
Measured Inlet Density, lb/ft <sup>3</sup> (kg/m <sup>3</sup> )	69.1 (1,106.8)	66.0 (1,057.2)
Measured Exit Density, lb/ft <sup>3</sup> (kg/m <sup>3</sup> )	17.6 (281.9)	7.1 (113.7)
Heat Exchanger Fuel Inlet Pressure, psia (N/m <sup>2</sup> abs)	40.1 (276,480)	41.4 (285,443)
Heat Exchanger Fuel Discharge Pressure, psia (N/m <sup>2</sup> abs)	27.3 (188,227)	28.3 (195,122)
Heat Exchanger Fuel Inlet Temperature, °R (°K)	532.4 (295.5)	507.4 (281.6)
Heat Exchanger Fuel Discharge Temperature, °R (°K)	510.4 (283.3)	457.2 (253.8)



DF 101952

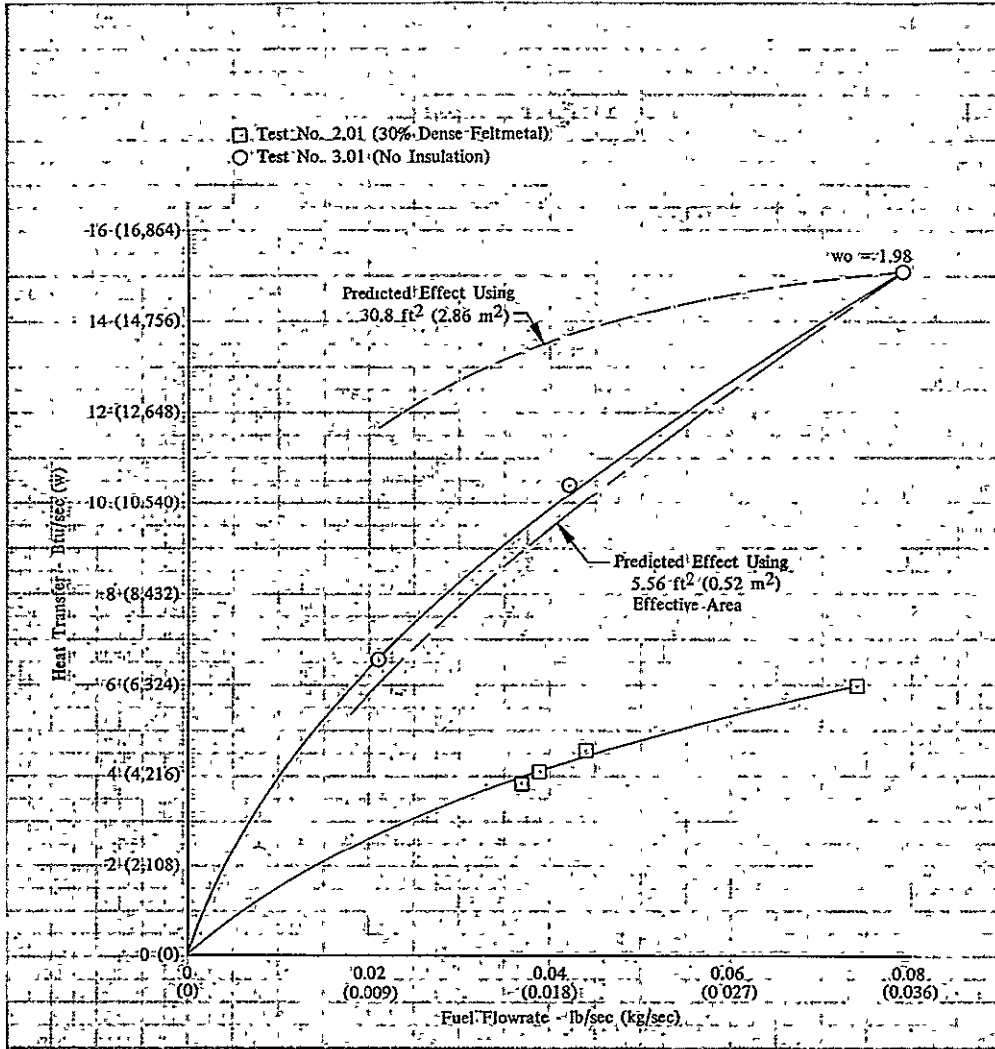
Figure VII-11. Estimated Performance at Constant Heat Fluxes for Breadboard Hydrogen/Oxygen Heat Exchanger



DF 101953

Figure VII-12. Insulation Conductance Requirements of Breadboard Hydrogen/Oxygen Heat Exchanger



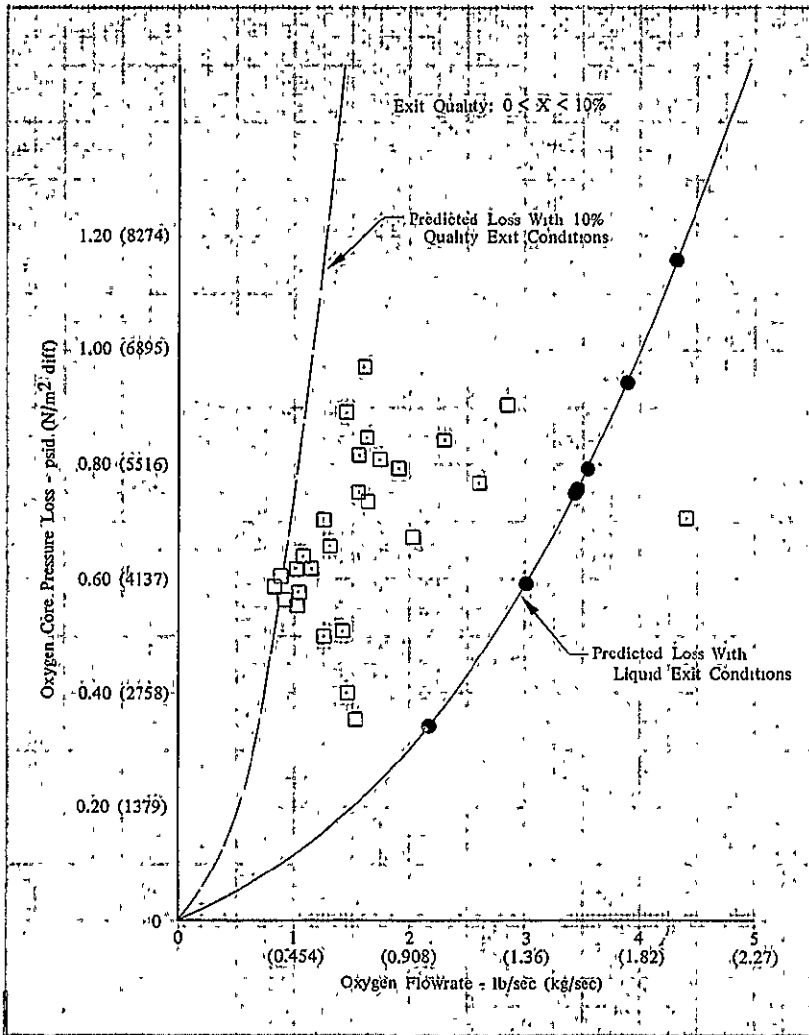


DF 101954

Figure VII-13. Fuel Flow Effects on Heat Transfer of Breadboard Heat Exchanger

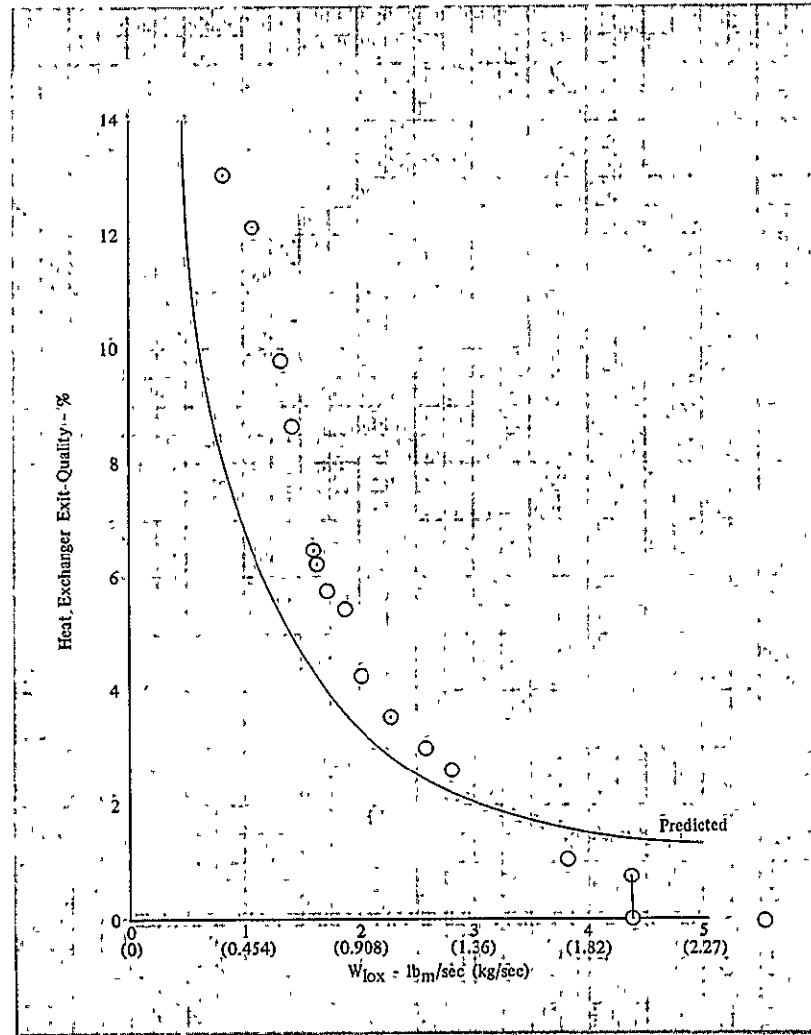
### 3. Stability

Instability was experienced throughout the test; however, the maximum steady-state pressure oscillation amplitude (peak-to-peak) was less than 10%, well under the allowable 25% corresponding to  $\pm 0.5$  mixture ratio. Figure VII-16 shows the steady-state instability characteristics and compares them to the predicted oscillation inception line. Because of the poor bonding of the copper fins to the panel walls and possible poor contact between the panels, even with the insulation material, the effective heat transfer area of the heat exchanger was undefined, making the comparison inconclusive. As can be seen from the figure, the heat exchanger became stable when oxygen inlet quality to the heat exchanger was above 4.4%. As expected, the heat exchanger was also stable when liquid conditions existed throughout the heat exchanger.



DF 101956

Figure VII-14. Oxygen Core Pressure Loss for Breadboard Heat Exchanger Test No. 2.01



DF 101956

Figure VII-15. Exit Quality Flowrate for Breadboard Heat Exchanger Test No. 2.01

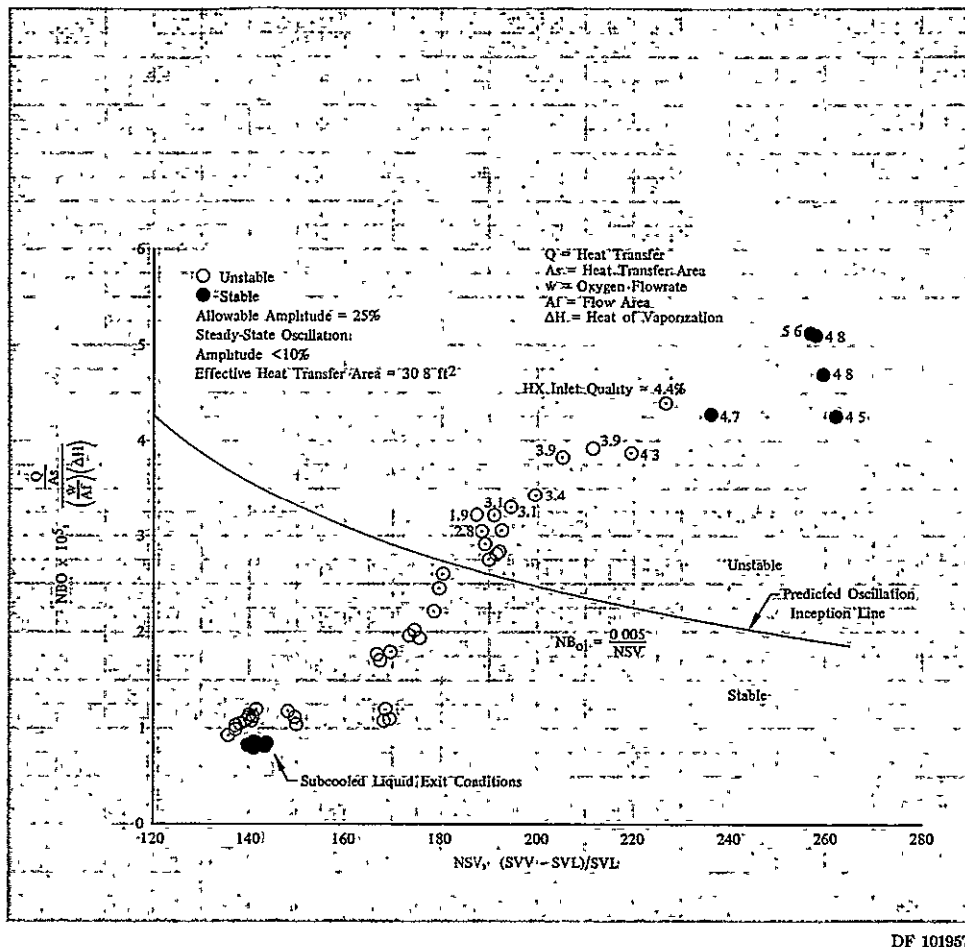


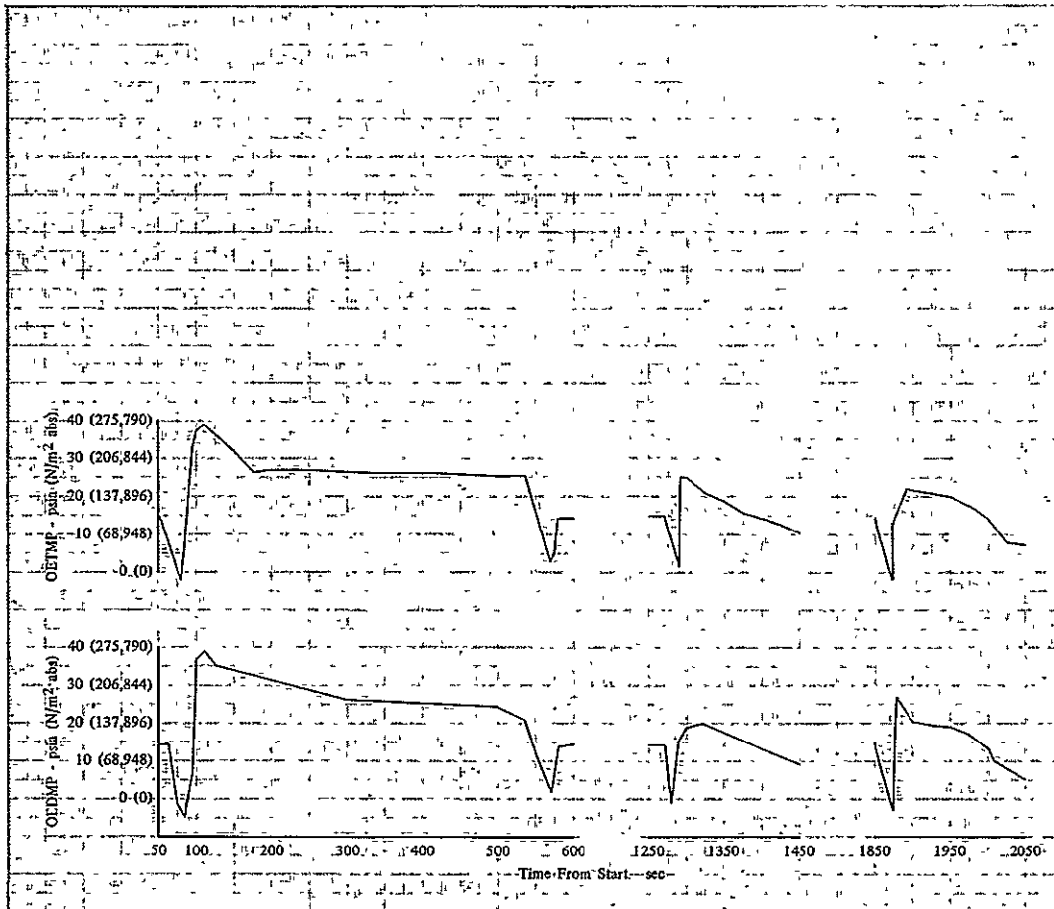
Figure VII-16. Steady-State Instability Characteristics of 30% Dense Feltmetal Insulation for GOX Heat Exchanger Test No. 2.01

**C. TEST WITH POWDERED ALUMINUM BETWEEN THE PANELS (TEST NO. 3.01)**

This test had powdered aluminum between the heat exchanger panels to fill the voids resulting from warpage due to attempts to braze-repair leaks. This configuration was used in an attempt to obtain higher heat transfer rates than those obtained on the checkout test. Analysis of the data from the second test indicated that the amplitude of the instability was less than the maximum allowable, making higher heat transfer rates desirable for the final test to further define stability criteria. Oxygen flowrates were again higher than expected because of lower-than-predicted heat transfer. The flowrates were again only calculated for selected steady-state points using the iterative procedure discussed in paragraph B of this section. Data characteristics from this test are shown in figures VII-17 through VII-19.

**1. Heat Transfer**

Steady-state heat flux for this test was only approximately 33% of the heat flux predicted for the heat exchanger design. Figures VII-11 and VII-12 show the heat exchanger characteristics for the tested configuration. The effect of hydrogen flowrate on heat flux is shown in figure VII-13. It indicates that the effective heat transfer area was only about 20% of predicted, even with the powdered aluminum between the panels. Table VII-1 contains measured and calculated steady-state parameters for the test.



DF 101968

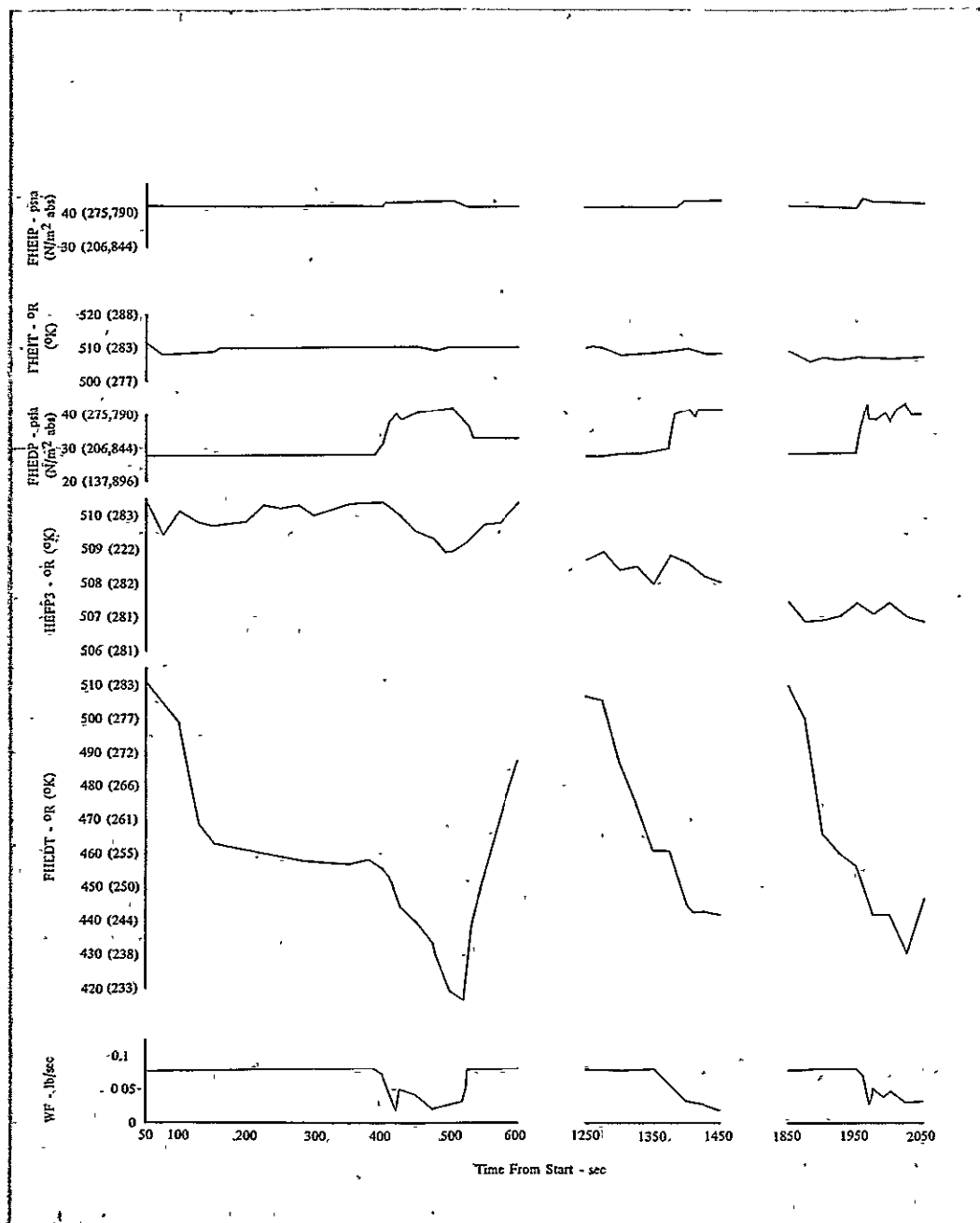
Figure VII-17. Data Characteristics of Breadboard Heat Exchanger Test No. 3.01

## 2. Pressure Losses

Hydrogen pressure losses were again close to predicted, as shown by figure VII-4. Figure VII-20 shows that the measured oxygen core pressure losses were also again near predicted levels.

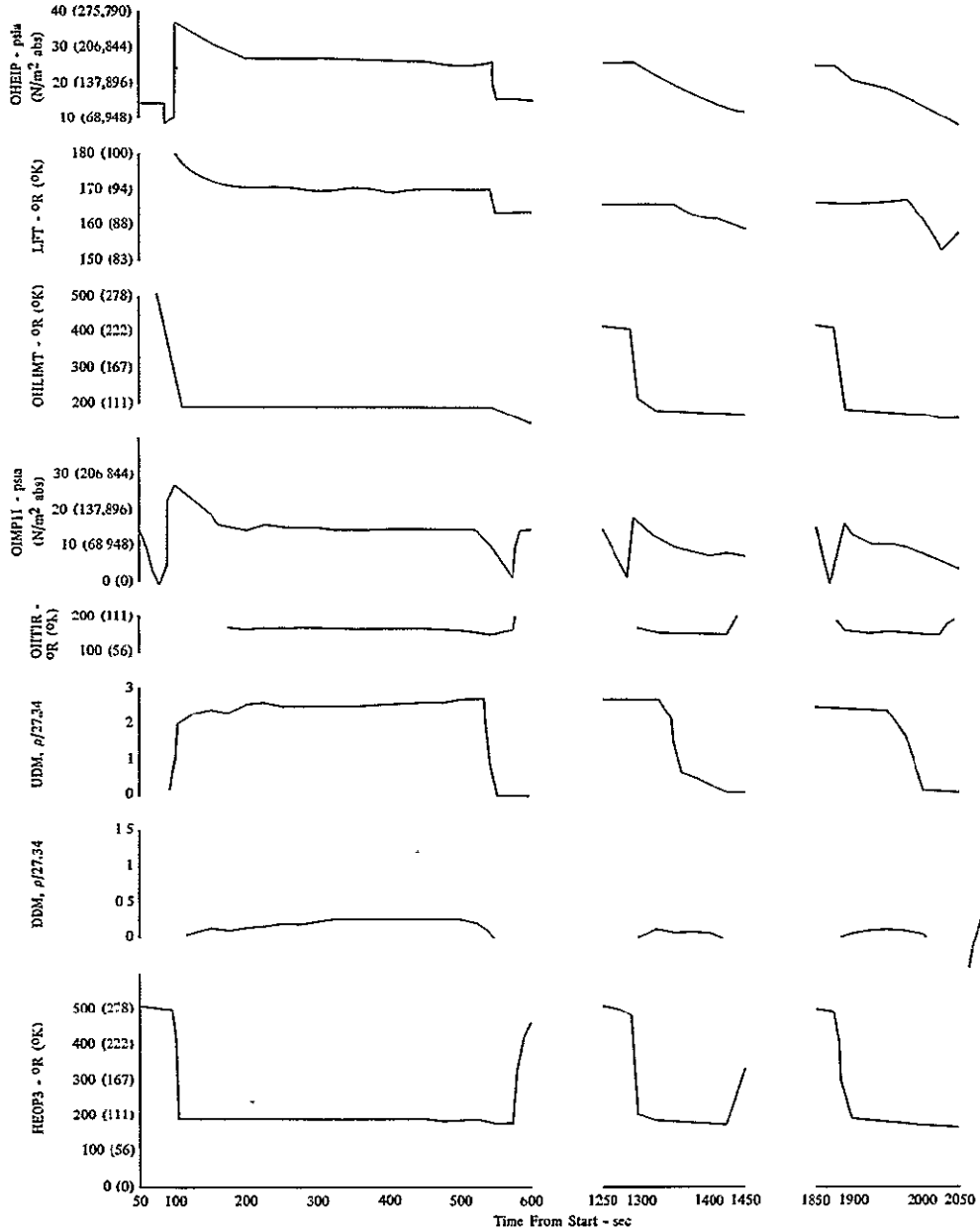
## 3. Stability

As expected, instability was experienced throughout the test. However, the steady-state oscillation amplitudes were less than 11%. Figure VII-21 shows the instability characteristics for this configuration and compares them with the predicted oscillation inception line. The two do not agree, probably because of the lower effective heat transfer area due to the poor contact between panels. During the cooldown transients, because of the heat stored in the heat exchanger at start, higher-than-design-point heat transfer was applied to the oxygen and near-design-point flowrates were obtained. Figures VII-22 and VII-23 show the oxygen parameter characteristics during these cooldowns. Figures VII-24 and VII-25 present the oxidizer injector manifold pressure during the tests and they show that instability amplitudes were acceptable even during the transients. Figure VII-26 presents oscillation amplitude as a function of heat transfer and oxygen flowrate. It includes both steady-state and transient data and shows that the amplitude of the instability was acceptable at heat exchanger design point conditions. The frequency of the oscillations appeared to be approximately 15 Hz with a 3-Hz modulation. During the third cooldown transient two cycles of 0.2-Hz modulation also occurred at a higher amplitude.



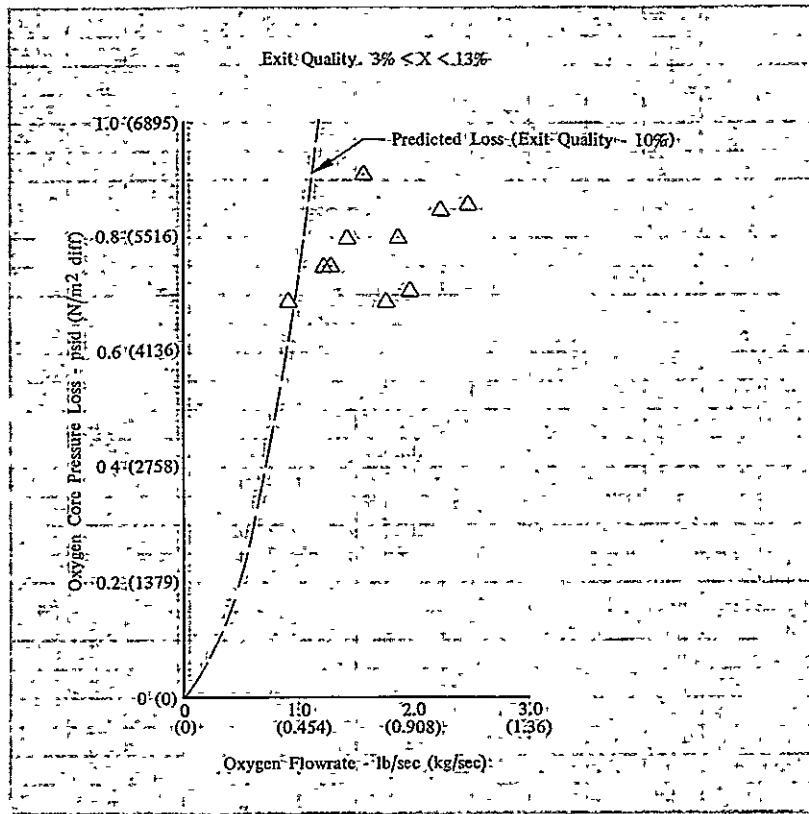
DF 101959

Figure VII-18. Data Characteristics of Breadboard Heat Exchanger Test No. 3.01



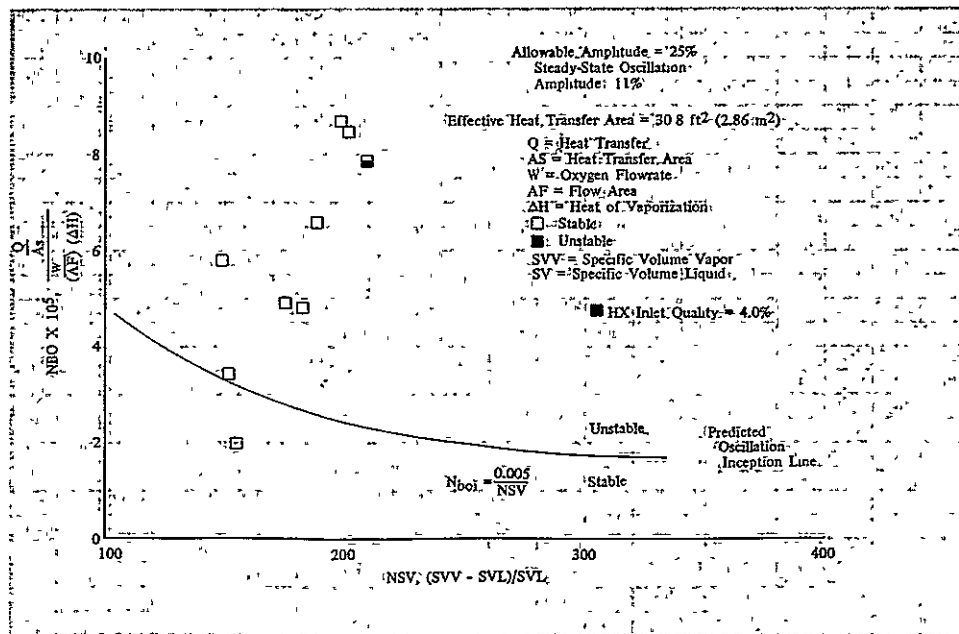
DF 101960

Figure VII-19. Data Characteristics of Breadboard Heat Exchanger Test No. 3.01



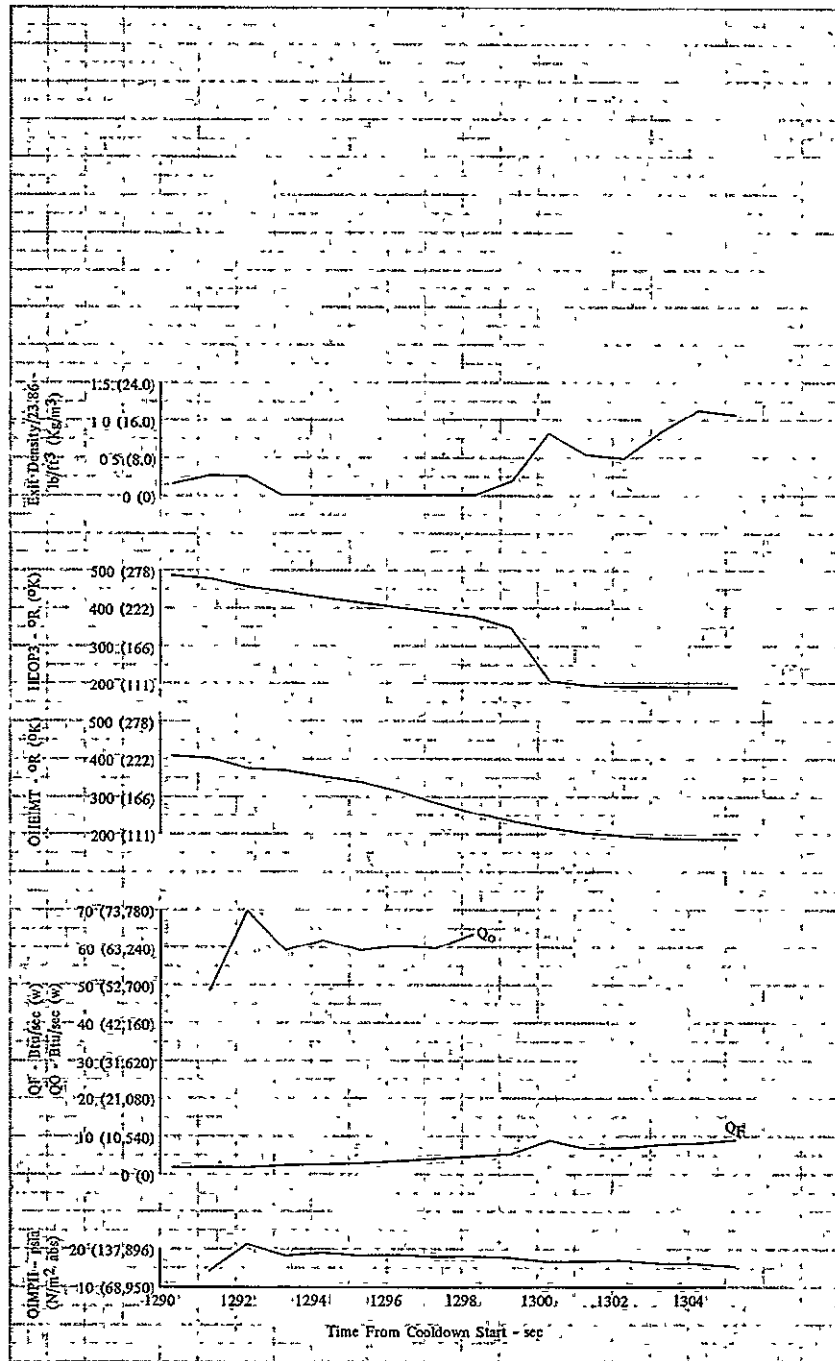
DF 101961

Figure VII-20. Oxygen Core Pressure Loss from GOX Heat Exchanger Test No. 3.01



DF 101962

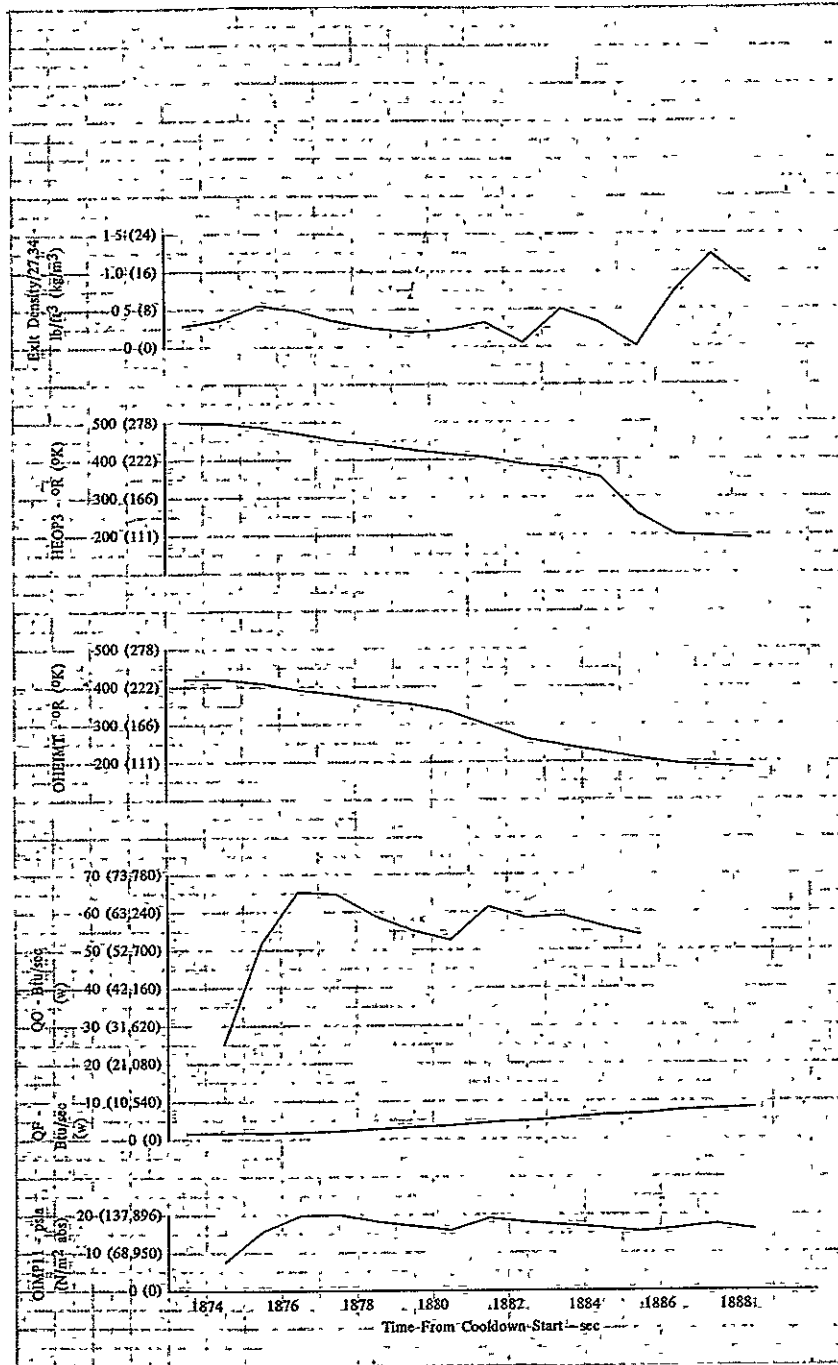
Figure VII-21. Steady-State Instability Characteristics of Powdered Aluminum Between Panels for GOX Heat Exchanger Test No. 3.01



DF 101963

Figure VII-22. Second Cooldown Transient Characteristics from Breadboard Heat Exchanger Test No. 3.01





DF 101964

Figure VII-23. Third Cooldown Transient Characteristics of Breadboard Heat Exchanger Test No. 3.01

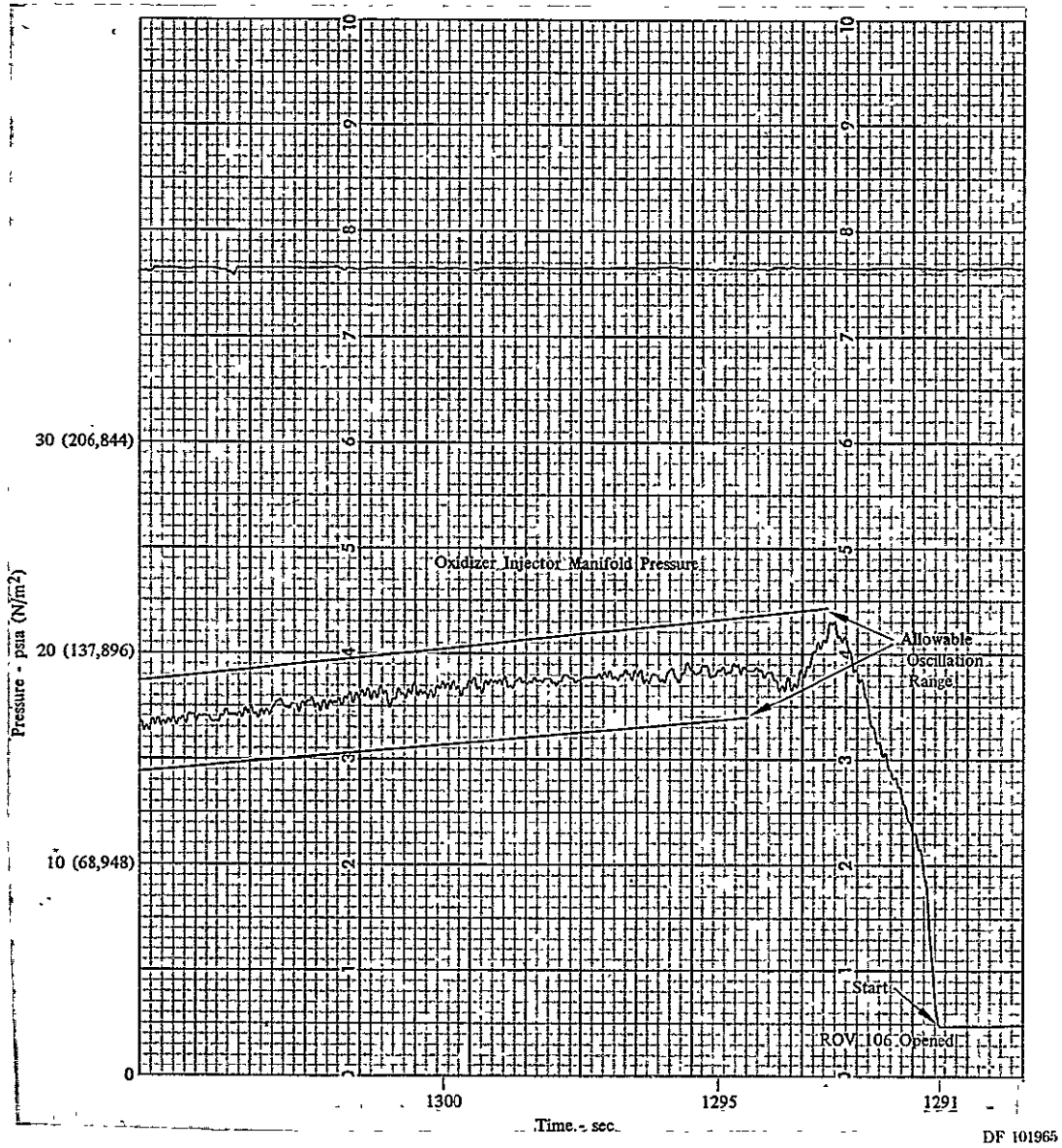
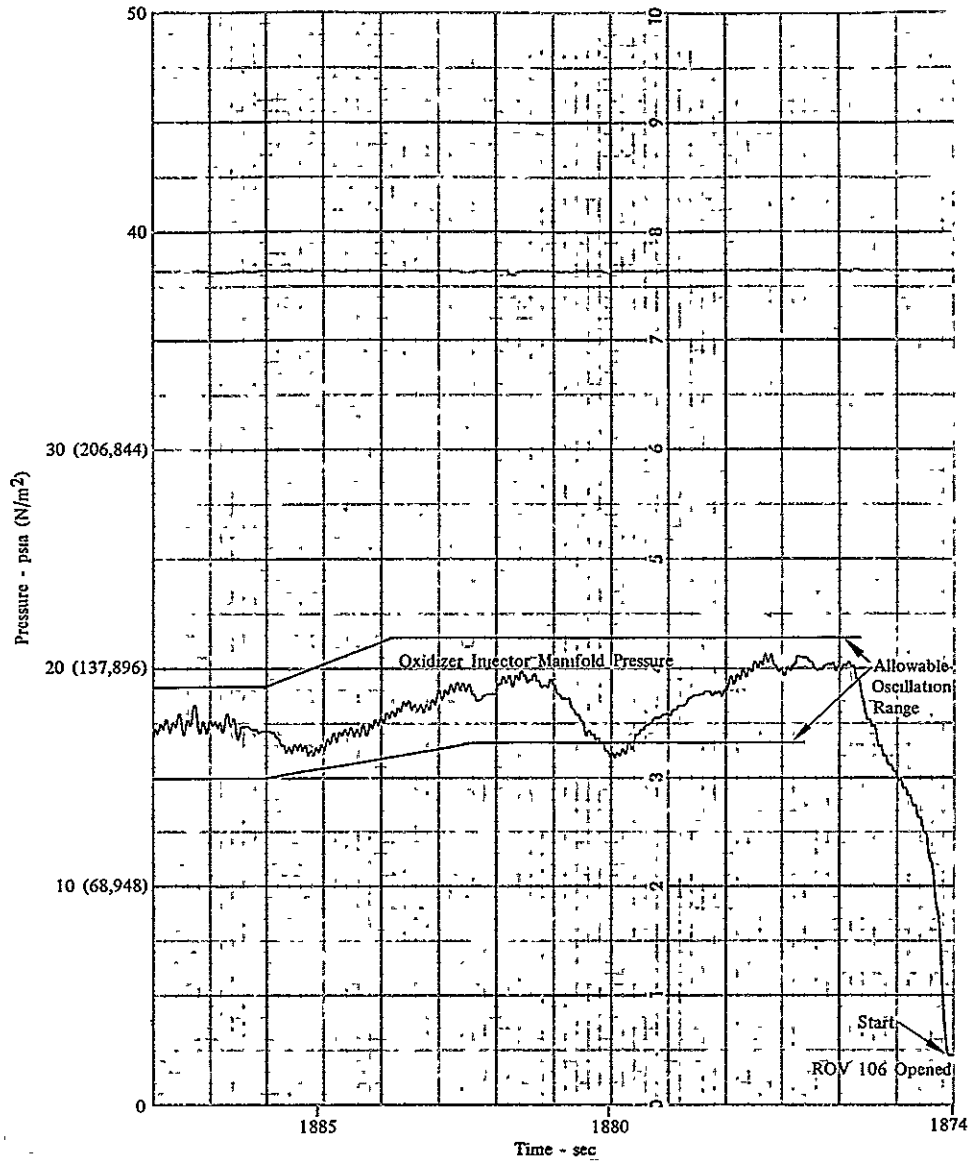


Figure VII-24. Second Transient Instability Characteristics of GOX Heat Exchanger  
Test No. 3.01



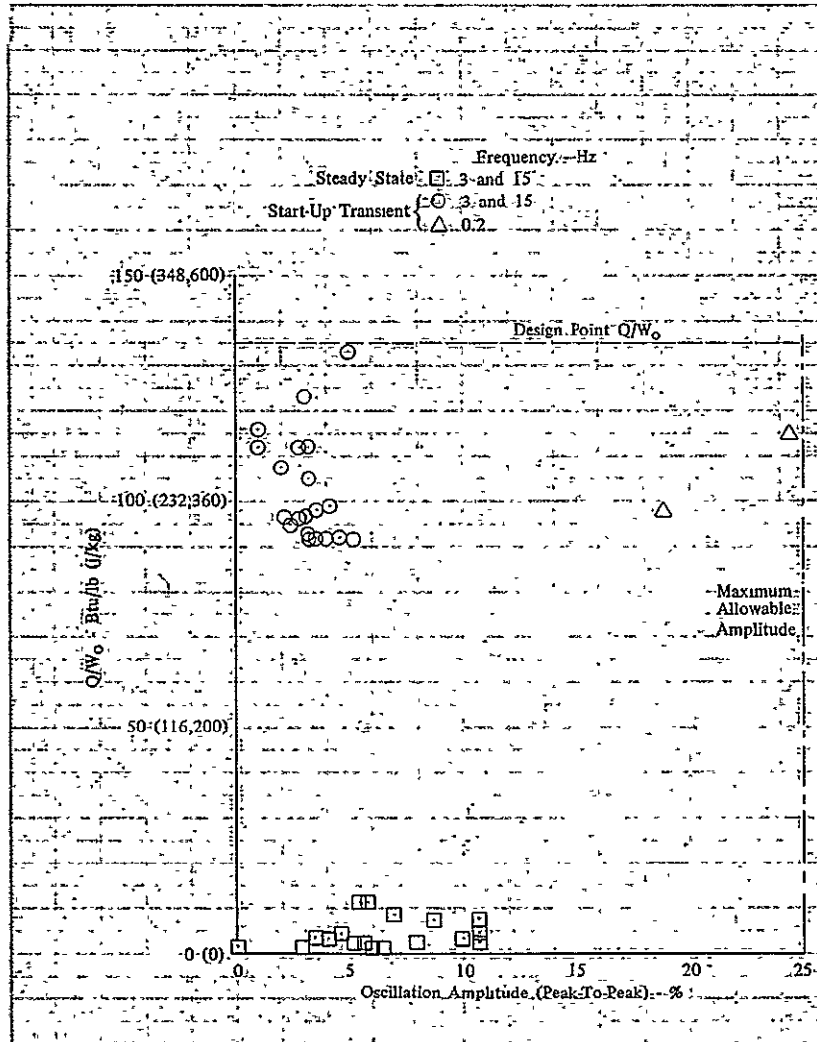
DF 101966

Figure VII-25. Third Transient Instability Characteristics of GOX Heat Exchanger Test No. 3.01

#### D. OVERALL TEST RESULTS

##### 1. Heat Transfer

Measured heat transfer was lower than predicted for all three tests. The test with insulation was 70% of predicted, compared to 33% or lower for the other two tests with no insulation. This indicated that the primary cause of the low heat transfer was the warpage of the plates, resulting from attempts to braze-repair panel leaks. Warpage would not be expected to occur during the fabrication of a flight-type heat exchanger, as the entire assembly would be brazed as a unit. If the panels had not been warped, it is expected that heat transfer would have been near predicted levels.



DF 101967

Figure VII-26. Oscillation Amplitude Characteristics of Breadboard GOX Heat Exchanger Tests No. 2.01 and 3.01

## 2. Pressure Loss

Pressure losses on all three tests were near predicted levels.

## 3. Stability

Stability requirements were met on all tests, even during heat exchanger cooldown transients. The heat exchanger was completely stable when oxygen inlet quality was greater than 5%. Instability amplitude was less than 50% of allowable at the highest steady-state heat flux tested (0.5 Btu/sec-ft<sup>2</sup> [5674 w/sec-m<sup>2</sup>]). Transient heat transfer rate was much higher than during steady-state, and stability limits were still not exceeded. Only steady-state data obtained during these tests would be used in designing a flight-type heat exchanger, however.

A flight-type heat exchanger could be designed using an insulation for the first pass that would give a heat flux of 0.5 Btu/sec-ft<sup>2</sup> (5674 w/sec-m<sup>2</sup>). This would result in exit quality for the first pass greater than 5%, eliminating the requirement for insulation in the second pass. A heat exchanger of this design, sized to provide superheated gaseous oxygen, would be approximately 1 ft<sup>2</sup> (0.093 m<sup>2</sup>) by 5 in. (0.13 m) thick.

## SECTION VIII CONCLUSIONS AND RECOMMENDATIONS

### A. CONCLUSIONS

Test data from this program indicate that a stable flight-type oxygen heat exchanger of acceptable size (approximately 1 ft<sup>2</sup> [0.305 m<sup>2</sup>] and 5 in. [0.13 m] deep) can be designed. The preliminary conceptual design of the flight-type heat exchanger is shown in figure VIII-1. The data indicate that a heat exchanger heat flux of 0.5 Btu/sec-ft<sup>2</sup> (5674 w/m<sup>2</sup>) will meet the stability requirements of  $\pm 0.5$  mixture ratio variation and that no instability will be present when the inlet quality of the oxygen is greater than 5%.

Insulation would be required between the panels of the flight-type heat exchanger for the first pass to give a heat flux of 0.5 Btu/sec ft<sup>2</sup> (5674 w/m<sup>2</sup>) and result in an exit oxygen quality of greater than 5%. The second pass in the flight-type heat exchanger would require no insulation between the panels.

### B. RECOMMENDATIONS

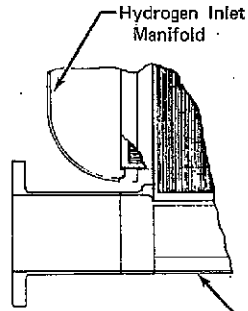
A program to design, package, fabricate, and characterize an engine flight-type oxygen/hydrogen heat exchanger should be accomplished as the logical next step in the design of a oxygen/hydrogen heat exchanger for an RL10 Derivative engine with a Tank Head Idle (THI) capability. The results from the "breadboard" tests indicate that a stable compact heat exchanger can be designed. The next program would provide for the refinement of the design, engine mounting, and plumbing provisions for engine-mounted testing.

This program would further provide more technical information to show that the pressure-fed THI mode of operation of the main engine for the Space Tug without an active control system is practical. This THI operation can be used for Space Tug vehicle thermal conditioning, propellant settling, and low  $\Delta V$  space maneuvers.

Plans for a follow-on program have been submitted to NASA MSFC as Proposal FP 75-252.

FOLDOUT FRAME

REPRODUCIBILITY OF THE ORIGINAL PAGE IS POOR



Section D-D  
Oxygen Inlet Manifold

Oxygen Flow Passages  
6 Required Material: 347SS

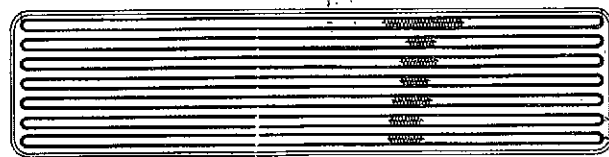
Oxygen Manifold  
Base Material: 347 SS

Oxygen Inlet Manifold

Section B-B

Hydrogen Flow Passages 7 Required  
Material: 347SS

Oxygen Outlet Manifold



Section C-C

H<sub>2</sub> Outlet Manifold

Hydrogen Flow Passages  
7 Required

Section A-A

H<sub>2</sub> Inlet Manifold

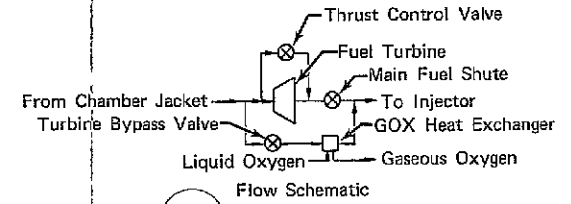
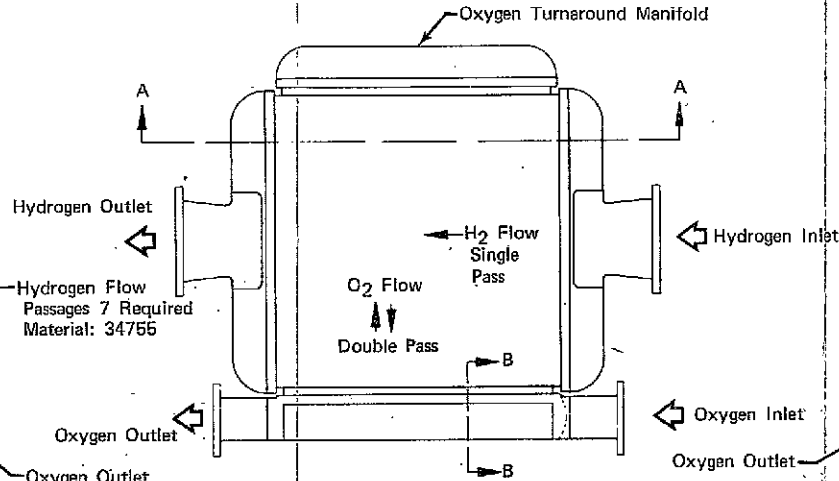
View E

0.100

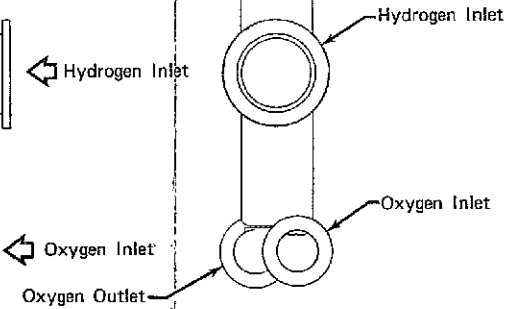
View E

Copper Fins Typical for All Tubes

Outer Sheet Thickness Increased for Handling Reasons Only



Flow Schematic



Hydrogen Inlet

Oxygen Inlet

Oxygen Inlet

Oxygen Outlet

Figure VIII-1. Compact Hydrogen/Oxygen Heat Exchanger - RL10 Derivative II

**SECTION IX  
REFERENCES**

1. Cuffe, J. P. B., P&WA Memorandum, *GOX Heat Exchanger Simulation Demonstration Program*, 13 August 1974.
2. Cuffe, J. P. B., P&WA Memorandum, *Program Operating Plan - Oxygen Heat Exchanger for RL10 Engine*, 31 March 1975.
3. Thompson, C. C., P&WA Memorandum, *Proposed RL10 GOX Heat Exchanger Configuration Meets Simulation Demonstration Program Objectives*, 28 August 1974.
4. Limerick, C. D., P&WA Memorandum, *Design Requirements for Breadboard Oxygen Heat Exchanger for RL10*, 14 April 1975.
5. Thurston, R. S., and J. D. Rogers, "Pressure Oscillations Induced by Forced Convection Heating of Dense Hydrogen," *Advances in Cryogenic Engineering*, Vol 12, Plenum Press, New York, pp 438, 1967.
6. Feltmetal Technical Bulletin No. M-5006 Brunswick Corporation, Technical Products Division, Skokie, Illinois, 1 November 1972.
7. Tong, L. S., *Boiling Heat Transfer and Two-Phase Flow*, John Wiley & Sons, Inc., New York, 1965.
8. Kays, W. M., and A. L. London, *Compact Heat Exchangers*, Second Edition, McGraw-Hill Book Company, New York, 1964.
9. Grootenhuis, P., R. W. Powell, and R. P. Tye, "Thermal and Electrical Conductivity of Porous Metals Made by Powder Metallurgy Methods," *Proceedings of London Physical Society*, Vol 65, No. 3918, pp 502-511, July 1952.
10. Brentari, E. G., and R. V. Smith, *Nucleate and Film Pool Boiling Design Correlations for O<sub>2</sub>, N<sub>2</sub>, H<sub>2</sub>, and He*, National Bureau of Standards, Boulder Colorado, Paper No. P-1, 1964.
11. Frost, W. and G. S. Dzakowic, *Manual of Boiling Heat-Transfer Design Correlations*, AEDC-TR-69-106, December 1969.
12. Lockhart, R. W. and R. C. Martinelli, "Proposed Correlation of Data for Isothermal Two-Phase, Two-Component Flow in Pipes," *Chemical Engineering Progress*, Vol 45, No. 1, 1949.
13. Quotation No. B1525, Brunswick Corporation, Technical Products Division, Skokie, Illinois, 16 June 1975. (In response to P&WA RFQ PEC 01801.)